Universität für Bodenkultur Wien
University of Natural Resources and Life Sciences, Vienna

Department für Wasser-Atmosphäre-Umwelt
Institut für Wasserwirtschaft, Hydrologie und konstruktiver Wasserbau (IWHW)

MASTER THESIS

Simulation of Discharge and Nitrate-Nitrogen Loads in the Raab Catchment with the hydrological model SWAT

Set-up and Verification of the hydrological model SWAT for the Watershed of river Raab in Austria

Master thesis submitted in fulfillment of the requirements for the degree of
Diplom-Ingenieur (Dipl.-Ing.) in Kulturtechnik und Wasserwirtschaft
by

Benedikt GRATH, BSc

Supervisor: Univ.Prof. Dipl.Geoökol. Dr.rer.nat. Karsten Schulz
Co-Supervisor: Bano Mehdi, MSc. Ph.D.
Co-Supervisor: Dipl.-Ing. Christoph Schürz

Vienna, June 2016

BOKU Matrikelnummer: 0746419

Acknowledgements

This Master thesis would not have been possible without the support of many people throughout the research for and writing of this thesis.

First, I want to thank my supervisor Karsten Schulz for providing me with the opportunity of the present Master thesis within the scope of the UnLoadC^3 project. Further I want to express my gratitude to Bano Mehdi who introduced me to the use of SWAT and guided me with her knowledge through my research. Special thanks go to Christoph Schürz who provided me with input data and essential information regarding the study area. Bano Mehdi and Christoph Schürz provided me with several valuable advices during my work and I am very thankful that they were always reachable during my work. The pleasant working atmosphere at the institute was helpful for realizing my Master thesis.

I want to sincerely thank my parents Elisabeth and Johannes who provided me with the opportunity to pursue my studies and gave me the freedom I needed throughout this process. I also want to thank my sister Theresa and my friends for their continuous support and encouragement. Special thanks go to my grandmother who supported me with special tissues. Without my BOKU colleagues, the study time would not have been that rich in experiences and that easy-going during stressful times. Finally I want to thank my girlfriend Steffi for believing in what I was doing, her patience and her constant emotional support from the very beginning although it was not always easy for her to stand my rapidly changing moods.

Statutory Declaration

I declare that I have developed and written the enclosed Master thesis completely by myself, and have not used sources or means without declaration in the text. Any thoughts from others or literal quotations are clearly marked. The Master thesis was not used in the same or in a similar version to achieve an academic grading or is being published elsewhere.

Benedikt Grath Vienna, 20. June 2016

Abstract

Austria is a water-rich country and the overall water quality is considered as good, however the nitrate pollution especially in the Raab catchment is still a main issue. The Raab catchment (988km²), located in south-east Austria, is strongly affected by agriculture and industry. This catchment is also well-known for its industry induced foam formation on the river Raab. The implementation of prediction models for water flow and nitrate-nitrogen (NO_3-N) loads (such as SWAT) support the development of adaptation strategies. Five discharge gauges for calibration and validation of flow are available in the Raab watershed. Two water quality monitoring stations (for the parameter NO_3-N) at Takern II (online monitoring data, 5 minute interval) and at Neumarkt/Raab (GZÜV, monthly grab samples) are existent in the study area. The objective of this Master thesis is the establishment of a calibrated SWAT model in order to be used for further research of the simulation NO_3-N loads. The SWAT model is subdivided into 30 subbasins and into 665 HRUs. The average annual discharge at outlet Neumarkt/Raab is 6.91 m³/s while the Raab catchment is characterized by moderate precipitation with an annual average precipitation of 756 mm/yr at Neumarkt/Raab. The land use in the Raab catchment is characterized by forest (44%), agriculture (25%), grassland zones (20%) and urban areas (11%). The main cultivated crops in Raab catchment are corn, oil pumpkin, vegetables, apples, wheat and soybean. Management application data such as tillage operations and fertilizer applications are applied in the SWAT model of the Raab catchment. The sequential calibration of the SWAT model is carried out with the SUFI-2 algorithm. The calibration period for discharge is set from 2003 to 2008; the validation period is performed from 2009-2012. The calibration and validation of streamflow is performed on daily and monthly basis and show a *satisfying* respectively a *very good* model fit. The calibration of NO_3-N load estimations shows an inappropriate model performance at both outlets (Takern II and Neumarkt/Raab), the model is not able to capture the peaks on monthly basis (simulated mean NO_3-N loads 45.20 t/month, observed mean NO_3-N loads 64.15 t/month). The Nash-Sutcliffe efficiency values (NSE, -0.24 and -0.14) and coefficient of determination (R^2) (0.01 and 0.00) indicate a very poor model accuracy. A consideration of point sources (treatment plants) may increase the accuracy of the NO_3-N simulation, however it is unclear to which extent diffuse sources (fertilizer application) and point sources (treatment plants) will affect the simulation of NO_3-N loads in the Raab catchment.

Zusammenfassung

Österreich weist generell eine hohe Wasserqualität und –quantität auf, jedoch ist die Nitratbelastung speziell im Einzugsgebiet der Raab nach wie vor ein Problem. Das Einzugsgebiet der Raab (988 km²), im Südosten von Österreich gelegen, wird stark durch Industrie und Landwirtschaft beeinflusst. Die Raab ist bekannt für die hohe Schaumbildung in Ungarn, welche durch die Industrie verursacht wird. Das Ziel dieser Diplomarbeit ist das Aufsetzen eines kalibrierten SWAT-Modells, um daraus weitere Forschungsmöglichkeiten für die Simulation von NO_3-N Frachten ableiten zu können. Fünf Abflusspegel werden für die Kalibrierung und Validierung auf den Durchfluss im Einzugsgebiet der Raab herangezogen. Zwei Wasserqualitätsmessstellen (für NO_3-N) in Takern II (Online Messdaten in einer 5-minütlichen Auflösung) und Neumarkt/Raab (monatliche GZÜV Daten) sind im Untersuchungsgebiet verfügbar. Das SWAT-Modell ist unterteilt in 30 Teileinzugsgebiete und in 665 HRUs (hydrologic response units). Der mittlere Jahresabfluss *MQ* am Pegel Neumarkt/Raab beträgt 6.91 m³/s. Der mittlere Jahresniederschlag in Neumarkt an der Raab beträgt 756 mm/a. Die Landnutzung im Einzugsgebiet ist durch Waldflächen (44%), landwirtschaftliche Flächen (25%), Wiesen bzw. Weiden (20%) und urbane Flächen (11%) geprägt. Die vorrangig kultivierten Pflanzenarten sind Getreide (Mais), Ölkürbis, Gemüse, Äpfel, Weizen und Sojabohnen. Landwirtschaftliche Managementoptionen wie z.B. die Bestellung von Äckern oder die Aufbringung von Düngemitteln sind im SWAT-Modell berücksichtigt. Die Kalibrierung des SWAT-Modells wird mit der SUFI-2 Methode durchgeführt. Der Abfluss wurde für die Jahre 2003-2008 kalibriert und für die Jahre 2009-2012 validiert. Die Kalibrierung und Validierung des Durchflusses auf täglicher und monatlicher Basis ergibt eine *zufriedenstellende* bzw. eine *sehr gute* Anpassungsgüte. Die Kalibrierung der berechneten NO_3-N Stofffrachten zeigt eine nicht zufriedenstellende Anpassungsgüte in Takern II und Neumarkt/Raab. Sowohl die Nash-Sutcliffe Effizienz (NSE) von -0.24 und -0.14 für die Gebietsauslässe Takern II und Neumarkt/Raab als auch das Bestimmtheitsmaß (R^2) mit 0.01 und 0.00 zeigen eine sehr schwache Modellanpassungsgüte. Das SWAT Modell kann die gemessenen NO_3-N Frachtspitzen auf monatlicher Basis nicht erfassen (berechnete bzw. gemessene NO_3-N Monatsfrachten liegen bei 45.2t bzw. 64.2t). Der Einsatz von Punktquellen (Kläranlagen) kann die Modellgenauigkeit verbessern, es ist jedoch unklar inwiefern sich diffuse Stickstoffquellen (Eintrag durch Düngung) und Stickstoff-Punktquellen (Kläranlagen) auf berechnete NO_3-N Frachten genau auswirken.

Table of Content

1 Introduction and Objective

The water quality and quantity of Austrian water bodies are considered to be good in almost all areas (Umweltbundesamt 2014). Austria is a country rich in water resources since only 3% of the available Austrian water resources are used in Austria (Umweltbundesamt 2014). All surface water quality measuring points in Austria show average nitrate (NO_3) concentrations below the threshold level of 50 mg/l (BMLFUW 2012a) which indicate a good water quality in Austrian surface water bodies. However it is unsure, how the water quantity and quality will develop under climate change conditions. The global warming trend due to climate change inclines to an increase of extreme weather events such as more extreme draught periods or more intensive rainfall events, even in Austria (BMLFUW 2010). Another substantial water related issue is to prevent Austrian water bodies from deterioration of the ecological status in future which is also the main approach of the European Water Framework Directive (WFD), established by the European Union in the year 2000 (EC 2000). The good level of the Austrian water quality is partly deteriorated due to high NO_3 pollution, especially in the north-east or south-east part of Austria (BMLFUW 2012a, see chapter 1.2).

To provide reliable adaptation strategies and to cope with all these water related issues in future, prediction models of water flow and nutrient flow are strongly needed to be applied, so they can support policy makers as well as water resources manager in their decision-making process for water management adaptation strategies (BMLFUW 2010). Consequently, this Master thesis is conducted within the research project named *UnLoadC³*. The UnLoadC³ project aims at developing and applying an extended uncertainty estimation framework for water quantity and quality (N,P) modelling under climate change conditions (Schulz 2014).

Since protection of the European's water bodies has a very high priority within the European Union (EU), the European Water Framework Directive (2000/60/EG) (EC 2000) was established to fulfil the high standards for environmental protection. The Water Framework Directive (WFD) aims to protect European water resources, ensuring fresh water supply and to obtain a *good status* of all European water bodies by the year 2015. Furthermore, the water status of European surface water and groundwater bodies shall not deteriorate (EC 2000). The WFD guidelines (EC 2000) provides five categories for classifying the overall ecological status of a surface water body: high, good, moderate, poor and bad. A *good status* of a water body is given by a *good ecological* respectively by a *good chemical status* in surface water bodies or by a *good quantitative and chemical status* in groundwater bodies (EC 2000). As a substantial progress of the WFD, the implementation of river basin districts (RBDs) and river basin management plans (RBMPs) facilitate the management and maintenance of European watersheds (Andersson et al. 2012).

The map in Figure 1.1 illustrates the ecological classification of river Raab according to the WFD guidelines, therefore just over 50% of the river Raab is classified as *natural surface water bodies* (yellow and orange solid line) and the remaining 50% of river Raab (yellow-grey dashed line) is determined as *artificial and heavily modified surface water bodies*. As a result, the main tributaries in the Raab watershed are allocated to a *moderate to poor* ecological status according to the WFD guidelines which indicates a poor condition of the Raab.

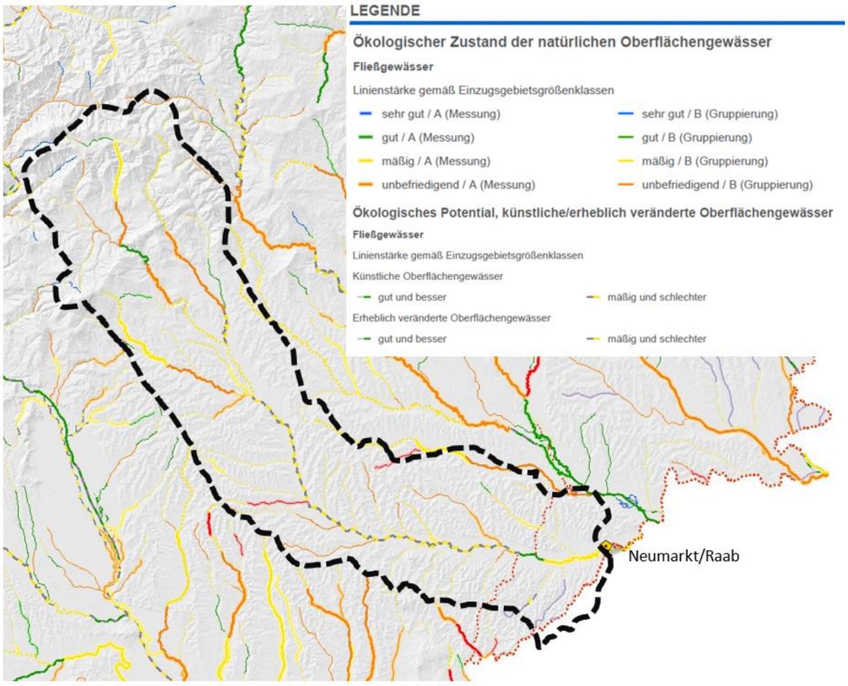

Figure 1.1: Classification of the ecological status of river Raab according to the WFD guidelines, modified after WISA (BMLFUW 2015)

The selected study area is the Austrian part of the Raab watershed with an area of 988.16 km² located in the Federal States Styria and Burgenland. The study area was designated for the Master thesis due to the present high NO_3 pollution by diffuse sources such as agriculture as well as by point sources such as waste water treatment plants or industry. According to BMLFUW (2011), more than 500 tons/year of nitrate-nitrogen (NO_3-N) loads were observed at the gauge Neumarkt/Raab in the Raab catchment (see chapter 1.2). Consequently, this catchment is well-known for its industry induced foam formation on the river Raab (Ruzicka et al. 2009; BMLFUW 2014a) which is discussed in chapter 1.1 in detail.

For the present and for similar scientific purposes worldwide, the physically based Soil and Water Assessment Tool (SWAT) model developed by Arnold et al. (1998) is a commonly used hydrological water quality model.

In this Master thesis, the SWAT model is considered for the hydrological simulation of water flow and nutrient (NO_3-N) flow of river Raab. The objectives of this Master thesis are in detail:

(i) The simulation of streamflow (on a daily & monthly basis) and of NO_3-N loads (monthly time step).

(ii) Implementation of calibration and validation steps for streamflow (daily basis) and NO_3-N loads (monthly basis).

(iii) Determine the uncertainty ranges of the streamflow and nutrient loads prediction model on the basis of 95% prediction uncertainty bands and of additional statistical parameters.

1.1 Raab foam formation issue

In 2007, increased foam formations on the river Raab were observed on the Hungarian side. Several reclamations and complaints by the Hungarian population followed and public interest on this issue became huge (BMLFUW 2014a). As a consequence, Austrian authorities established a comprehensive monitoring program in Raab catchment and launched an action program to minimize foam formations. The monitoring program (task force) identified three leather manufacturer along the river Raab (Wollsdorf, Feldbach, Jennersdorf) and the inlet of uncleaned wastewater from the geothermal facility in Fürstenfeld as the four main indicators of foam formations (BMLFUW 2014a). The monitoring program consisted also the implementation of two long-term online monitoring stations for water quality parameters. The online monitoring stations are located at Neumarkt/Raab and at Takern II (see Figure 2.2) and provide continuous data series of several water quality parameters (such as NO_3-N) in a 5-minute time interval. The consequences of the Raab task force were manifold, e.g. the waste water treatment plants along the river Raab were modernized to state-of-the-art standards, and further improvements such as ecological rehabilitation are planned (BMLFUW 2014a). In year 2012, reduced time periods of high foam formations were observed although the foam formation is still present on low level (BMLFUW 2012b).

1.2 Nitrate (NO_3) situation in Raab catchment and in Austria

The NO_3 levels in the lower Raab river basin at the gauge Neumarkt/Raab (see Figure 2.2) can be considered as high since there are measured nitrogen loads with more than 500 tons per year (comparable catchments show nitrogen loads of around 300-350 tons/year) (BMLFUW 2011). The main sources for nitrogen pollution in Raab catchment are the agricultural sector (fertilizer application) and waste waters from point sources like municipalities (waste water treatment plants) and industry (BMLFUW 2011). Study results by BMLFUW (2012a) show that the average NO_3 content in the river Raab ranges from 10 mg/l to 50 mg/l (mean respectively maximum value) at the gauge Neumarkt/Raab (Figure 1.2). Only few monitoring stations (7 of 81 examined stations) in the north-east and in the south-east of Austria show higher NO_3 contents with maximum concentrations beyond 40 mg/l which is the second worst quality class in the classification of NO_3 pollution in surface water bodies (BMLFUW 2012a). The areas in the north-east and south-east parts of Austria are affected by small precipitation rates (500-800 mm/yr, (BMLFUW 2014b)) and have high agricultural usage which increase the NO_3 pollution (BMLFUW 2012a).

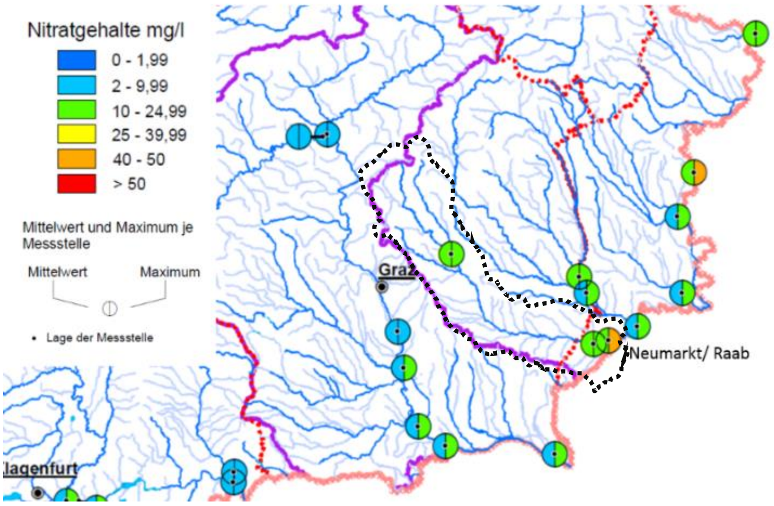

Figure 1.2: NO_3 concentrations (mg/l) in surface waters, average value and maximum for time period 2007-2011, modified after BMLFUW (2012a)

In general, the NO_3 levels throughout Austria can be considered as low since the measured average NO_3 concentrations in 97.5% of all monitoring stations are below the threshold level of 25 mg/l which is the third best water quality class (green classification in Figure 1.2, as per BMLFUW (2012a)). According to BMLFUW (2012a) the Austrian-wide main pathways of nitrogen sources can be determined as follows:

- Agriculture (especially fertilizer application in agriculture, ammonia (NH_3)-deposition and drainages) (49.7%)
- Municipality and industry (point sources, waterborne inputs (urban areas) and airborne inputs (Nitrogen oxide (NO_x)-deposition) (36.9 %)
- Further background emissions from natural sources such as precipitation (rain and snow) (13.4%)

On average in Austria, four fifths (80%) of the nitrogen emissions input stems from diffuse sources (such as agriculture and its fertilizer application) and the remaining one fifth (20%) originates from point sources (such as industry and waste water treatment plants) (BMLFUW 2012a).

2 Material and Methods

2.1 Study Area

The total length of the river Raab is approximately 250 km whereas one third is located in Austria and two thirds of the river flows through Hungary. The Raab river has its source in a crystalline low mountain range in Austria and flows into the Danube in the city Györ, central Hungary (Ruzicka et al. 2009). The designated study area is located in the Austrian part of the Raab watershed and covers an area of 988.16 km² as shown in Figure 2.1. The partial length of the river Raab in the study area can be specified as having a length of 80.6 km. The study area is found in the south-eastern part of Austria and covers two federal provinces, mostly Styria and to a small extent Burgenland. The second largest Austrian city Graz is located about 30 km west of the study area (see Figure 2.1).

The upper watershed is dominated by a pre-alpine topography and continues into a lower watershed with more fertile shallow areas characterized by high agriculture usage and industrial settlement. The altitudes in Raab watershed range from 1540 m a.s.l (at the origin) to 208 m a.s.l at the outlet Neumarkt/Raab, directly located at the Austrian-Hungarian border. The climate is characterized by moderate precipitation with an annual average precipitation of 756 mm/year (BMLFUW 2014c). The precipitation distribution shows higher average precipitation sums, up to 250 mm/month, during the summer period (May-September). According to the *Hydrografisches Jahrbuch* (BMLFUW 2014c), the average annual flow of Raab river at the discharge gauge Neumarkt/Raab is 6.91 m³/s (MQ, reporting period 1991-2012).

The moderate precipitation in the study area results in seasonal low discharge conditions with investigated flow around 1.85 m³/s ($MJNQ_T$, gauge 210468 Neumarkt/Raab, reporting period 1991-2012, (BMLFUW 2014c)).

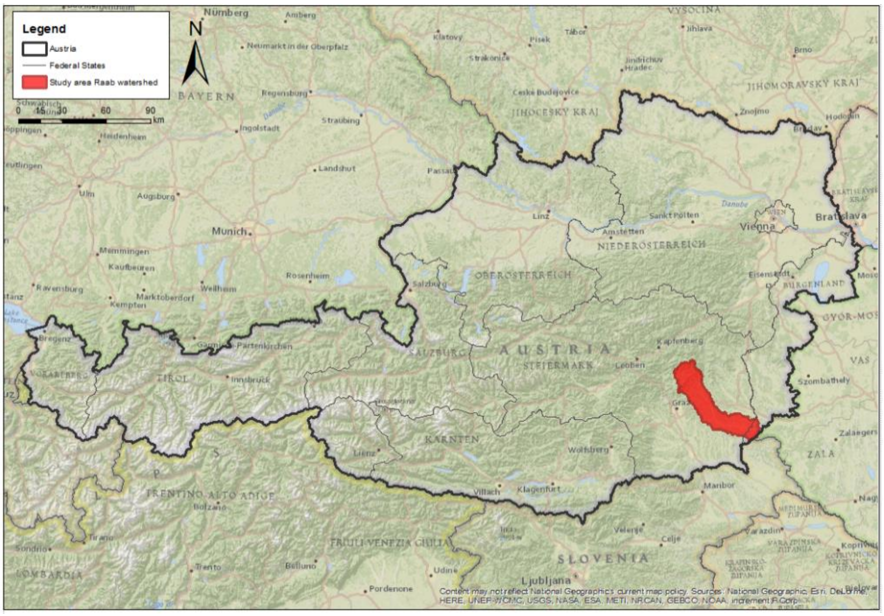

Figure 2.1: Austrian map locating the project area Raab watershed

As shown in Figure 2.2, the land use within the catchment is clearly dominated by forest areas with a fraction of nearly 44 percent (EEA 2015). The northern catchment with its hilly pre-alpine topography is mostly covered with forest (deciduous, evergreen and mixed forest) and is barely affected by human impact (Ruzicka et al. 2009). In the lower altitudes of Raab river basin more agricultural areas due to better climatic conditions and more fertile soil are present. In total, about 25 percent of the watershed area is cultivated by agriculture. Almost 20 percent of the watershed area are classified as grassland, the remaining part of 11 percent are primarily settlements as well as urban areas (see Figure 2.2) (EEA 2015).

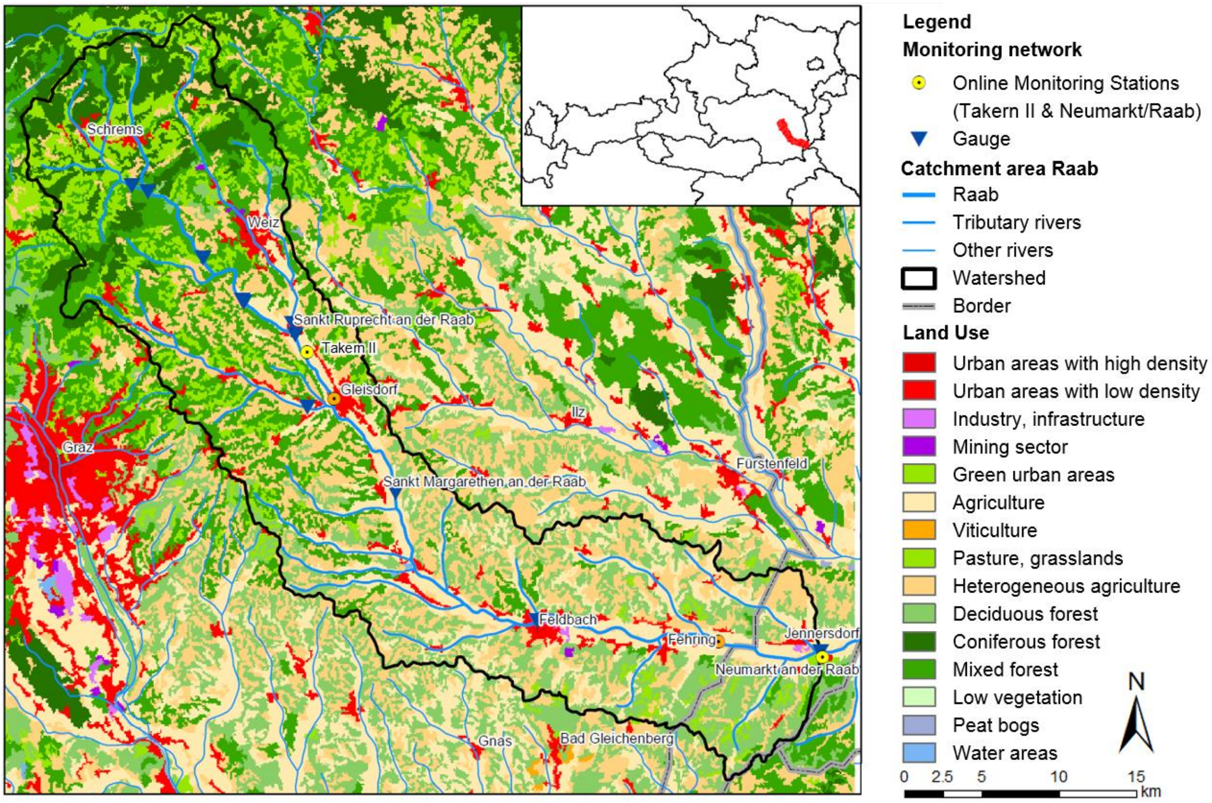

Figure 2.2: Overview map of land use classification in Raab watershed, its monitoring network (Online monitoring stations OM Takern II and OM Neumarkt/Raab, gauges), and the Raab rivers with its tributary rivers.

Although the Raab catchment comprises a high level of settlement areas, in total there are only eight settlements with more than 2000 inhabitants, as listed in Table 2.1.The rural districts in the watershed are Weiz, Graz-Umgebung, Südoststeiermark (all Styria) and Jennersdorf (Burgenland).

Table 2.1: List of settlements > 2000 inhabitants in Raab catchment

Settlement > 2000 inhabitants	Number of inhabitants
Feldbach	13 110
Weiz	11 316
Gleisdorf	10 278
Fehring	7 329
Schrems	5 540
St. Ruprecht/Raab	4 969
Jennersdorf	4 078
St. Margarethen/Raab	3 989

Data source: Statistik Austria (2015a)

The river Raab is a strongly impacted river due to the high level of industrialization and agricultural usage in this river basin area (diffuse sources). Additionally amplifying negative impact are the frequent small hydropower plants (around 15) along the stream which affect the aquatic ecosystem in a harmful way. The poor water quality is also triggered by contaminated waste waters from the regional leather industry (point sources). Due to the lack of shore vegetation respectively alluvial forests and due to excessive nutrient deposition in the river, eutrophication is a very likely threat for the river Raab (BMLFUW 2014a). The nutrient deposition in Raab catchment is characterized by high NO_3 load input observed in the lower river basin (BMLFUW 2011), as already discussed in chapter 1.2. In general, in the lower watershed the aquatic ecosystem and the ecological status can be considered as being very poor and weak, respectively (BMLFUW 2014a).

2.2 SWAT – Soil Water Assessment Tool

2.2.1 Introduction

The Soil and Water Assessment Tool (SWAT) is a river basin scale model developed by Arnold et al. (1998) for the USDA Agricultural Research Service (ARS). It was developed to predict the impact of land management practices on water, sediment, agricultural chemical yields in large complex watersheds with varying soils, land use and management conditions over long periods of time (Neitsch et al. 2011). Numerous features are implemented in the model to fulfil these objectives.

The SWAT model is a physically-based, distributed river basin model operating on a daily time step (Neitsch et al. 2011). SWAT requires specific information about weather, soil properties, topography, vegetation, and land management practices in the watershed to directly model the physical processes. These physically based processes comprise in general water movement, sediment transport, crop growth or nutrient cycling. The benefits of this approach are: watersheds with no monitoring data (such as discharge gauges) can be modeled and the relative impact of alternative input data (e.g. changes in climate) on e.g. water quality (NO_3) can be examined. The minimum required data to perform a model run is generally accessible from national authorities. SWAT allows the user to investigate long-term impacts with model runs covering several decades. The SWAT model is not designed to simulate detailed, single-event flood routings since the model is determined as a continuous time model (Neitsch et al. 2011).

2.2.2 Examples of SWAT application

The SWAT model was successfully applied in various watershed projects in the world and in several water quality modeling studies. Examples of such studies include the following publications and their titles:

- Evaluating the impacts of climate change and crop land use change on streamflow, nitrates and phosphorus - A modeling study in Bavaria (Germany) (Mehdi et al. 2015b)
- Influence of different nitrate–N monitoring strategies on load estimation as a base for model calibration and evaluation (Saxony, Germany) (Ullrich, Volk 2010)
- Modelling point and diffuse source pollution of nitrate in a rural lowland catchment using the SWAT model (Schleswig-Holstein, North Germany) (Lam et al. 2010)
- Modelling hydrology and water quality in the pre-alpine/alpine Thur watershed (Switzerland) using SWAT (Abbaspour et al. 2007)
- A continental-scale hydrology and water quality model for Europe (Abbaspour et al. 2015)
- Water resources of the Black Sea Basin at high spatial and temporal resolution (Rouholahnejad et al. 2014)
- Simulated impacts of climate change and agricultural land use change on surface water quality in Quebec, Canada, with and without adaptation management strategies (Mehdi et al. 2015a)

2.2.3 Development of SWAT

The USDA Agricultural Research Service (ARS) primarily deals with agricultural application as well as with agricultural management related scientific issues. Behind this approach, a previous model of SWAT with main focus on impacts of agricultural applications was developed: CREAMS, which stands for Chemicals, Runoff and Erosion from Agricultural Management Systems (Knisel 1980). A further key area of the ARS research was the development of a water quality assessment tool respectively sediment yield model system (GLEAMS, Groundwater Loading Effects on Agricultural Management Systems (Leonard et al. 1987)). The present SWAT growth model is based on the EPIC method (Erosion-Productivity Impact Calculator (Williams et al. 1984)), which was built as a comprehensive agricultural management and nonpoint source loading model. Based on these predecessor models the SWAT model evolved to its present structure (Neitsch et al. 2011).

Since SWAT was developed in early 1990s, it has undergone continued review and its functions were expanded continually. Worth noting are the implementations of the Green & Ampt infiltration method and an improved weather generator which allow the generation of data for daily solar radiation, relative humidity, and wind speed in SWAT2000 (Neitsch et al. 2011). The model interface itself was developed in Windows (Visual Basic), GRASS and ArcView.

The latest version SWAT2012 (Neitsch et al. 2011) was applied in this Master thesis and the ArcSWAT 2012 ArcGIS extension is used as a graphical user interface for the SWAT model. The SWAT model requires several input data such as DEM, land use, soil, weather, agricultural management data, in order to ensure a successful simulation for a specific period of time (Winchell et al. 2013).

2.2.4 Model components

The watershed delineation process divides the watershed into several sub-watersheds (subbasins) and further into Hydrologic Response Units (HRUs) (Figure 2.3). HRUs are based on similar soil texture, land uses and soil types and form the smallest units of a SWAT model (Arnold et al. 2012) as shown in Figure 2.3. All SWAT model computations are performed at the HRU level (Arnold et al. 2012). Streamflow, sediment and nutrient loadings from each HRU are aggregated for each subbasin and then routed through the hydrological network (Neitsch et al. 2011). The benefits of HRUs are the increased accuracy in the loading predictions from the subbasin as well as the diversity of plant cover remains in the model at a higher level (Arnold et al. 2012).

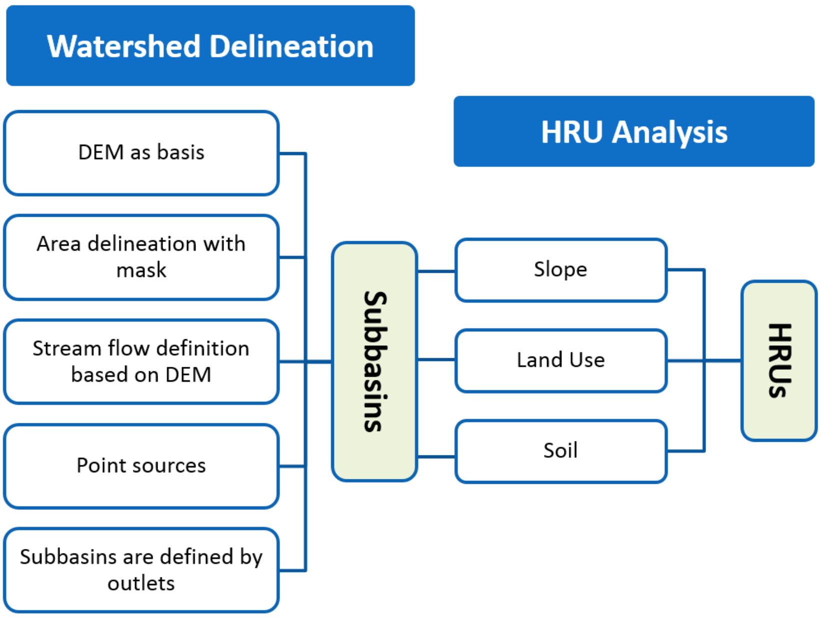

Figure 2.3: Schematic concepts of the watershed delineation in the SWAT model (subbasins) respectively of the HRU concept

The hydrology in the SWAT model can be divided into two major parts, namely into the land phase (upland processes) and the routing phase (channel processes) (Figure 2.4) (Neitsch et al. 2011). The upland processes control the amount of water, sediment and nutrients loadings to the main channel in each subbasin. The channel processes describe the movement of water, sediments etc. through the channel network of the watershed to the outlet (Neitsch et al. 2011).

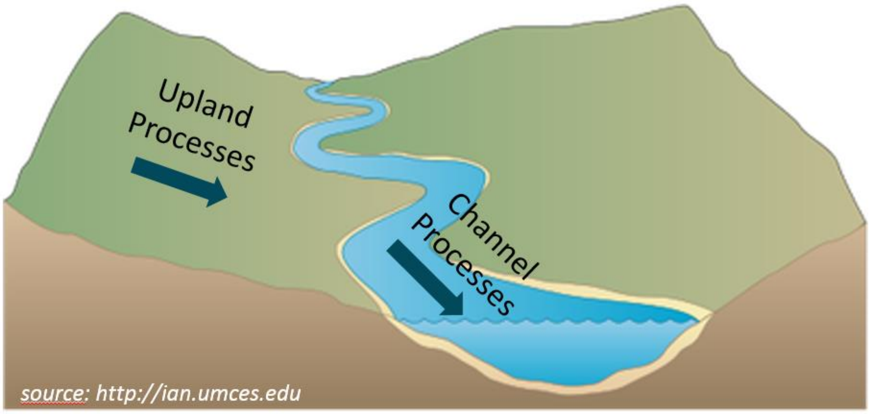

Figure 2.4: Conceptual model of the hydrology simulation in the SWAT model (upland processes and channel processes), modified after Schürz (2015, pers. comm., 2. July)

2.2.4.1 Land phase of the hydrologic cycle

In the land phase, SWAT calculates the hydrologic cycle based on the water balance equation (Neitsch et al. 2011):

$$SW_t = SW_0 + \sum_{i=1}^{t} \left(R_{day} - Q_{surf} - E_a - w_{seep} - Q_{gw} \right) \qquad (2.1)$$

where SW_t is the final soil water content (mm H_2O), SW_0 is the initial soil water content on day i (mm H_2O), t is the time (days), R_{day} is the amount of precipitation on day i (mm H_2O), Q_{surf} is the amount of surface runoff on day i (mm H_2O), E_a is the amount of evapotranspiration on day i (mm H_2O), w_{seep} is the amount of water entering the vadose zone from the soil profile on day i (mm H_2O) and Q_{gw} is the amount of return flow on day i (mm H_2O) (Neitsch et al. 2011).

A schematic representation of the hydrologic cycle is shown in Figure 2.5.

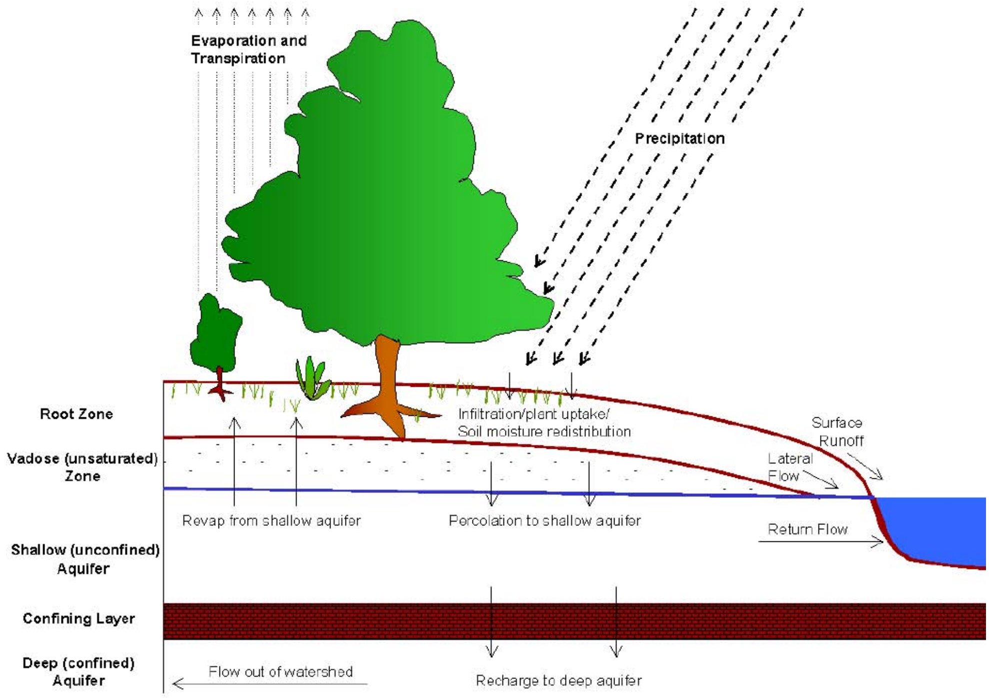

Figure 2.5: Schematic representation of the hydrologic cycle in SWAT (Neitsch et al. 2011)

To calculate the water movement in a HRU, SWAT includes several hydrological processes in the land component such as infiltration, surface runoff, base flow, lateral flow, evapotranspiration and canopy storage (Figure 2.5):

- Infiltration: defines the process by which water from the soil surface enters the soil profile. The rate of infiltration decreases with time until the soil becomes saturated. The “Green-Ampt Mein-Larson” infiltration method (Green, Ampt 1911; Mein, Larson 1973) calculates the infiltration based on sub-daily precipitation data.
- Surface runoff: is an overland flow which occurs along a sloping surface. SWAT models surface runoff volumes and peak runoff rates for each HRU. The surface runoff volume is calculated by using a modification of the SCS curve number method (USDA Soil Conservation Service, 1972) or the “Green-Ampt Mein-Larson” infiltration method (Green, Ampt 1911; Mein, Larson 1973).
- Return flow: also base flow, describes the volume of streamflow contributing from groundwater. The baseflow describes the percolation between shallow and deep aquifers in the SWAT model.
- Lateral flow: describes the lateral movement of water in the unsaturated zone of the soil profile (0-2m).

- Evapotranspiration: includes all processes at or near the earth's surface which turn water in the liquid or solid phase into atmospheric water vapor. The evapotranspiration processes comprises evaporation, transpiration (differentiation between potential and actual evapotranspiration) and the sublimation from ice and snow surfaces. SWAT provides three options for calculating potential evapotranspiration: Hargreaves, Priestley-Taylor and Penman-Monteith.
- Canopy storage: Canopy storage is the water intercepted by vegetative surfaces where it is available for evapotranspiration (Neitsch et al. 2011).

2.2.4.2 Climate

Climatic conditions control the water balance and ensure moisture and energy input in the SWAT model. The required variables for calculating the climate in SWAT are daily precipitation, maximum/minimum air temperature, solar radiation, wind speed and relative humidity. These data can be gathered from records of observed data or by using the built-in weather generator in case of incomplete data records. The weather generator calculates the total amount of the precipitation for the day; then the distribution of rainfall within the day is computed. The weather data set is individually generated for each subbasin as there is no spatial correlation between the subbasins (Neitsch et al. 2011).

2.2.4.3 Plant Growth

The plant growth model of SWAT is based on a simplified version of the EPIC (Williams et al. 1984) model. The phenological plant development is based on daily accumulated heat units which are a function of minimum and maximum air temperatures (PHU concept, for detailed information see below). Factors such as temperature, water or nitrogen stress affect plant growth. The growth cycle of a plant is controlled by plant attributes such as the base temperature (T_{base}) or optimum temperature (T_{opt}) which are specified in the SWAT plant growth database as well as by the timing of field operations listed in the SWAT management file. Plant growth also indicate the removal of water and nutrients from the root zone in the SWAT model (Neitsch et al. 2011).

2.2.4.4 PHU Concept

In SWAT, the cycle of plant growth is modeled by the plant heat unit (PHU) concept. Each plant has its own temperature range, such as the minimum, optimum and maximum temperature for growth. A minimum or T_{base} must be reached before any growth will take place. Each degree of the daily mean temperature above T_{base} is equal to one heat unit. Crop growth will only occur on those days where the mean daily temperature exceeds T_{base}. The heat unit accumulation for a given day is calculated with the equation (Neitsch et al. 2011):

$$HU = \bar{T}_{av} - T_{base} \ when \ \bar{T}_{av} > T_{base} \tag{2.2}$$

where HU is the number of heat unit accumulated on a given day, $\bar{T}_{av}$ is the mean daily temperature (°C), and T_{base} is the plant's base or minimum temperature for growth (°C) (Neitsch et al. 2011). The total number of heat units required for a plant to reach maturity is calculated as follows:

$$PHU = \sum_{d=1}^{m} HU \tag{2.3}$$

where PHU is the total heat units required for plant maturity, HU is the number of heat units accumulated on day d where $d = 1$ on the day of planting and m is the number of days required for a plant to reach maturity (Neitsch et al. 2011).

The crop maturity is reached when the total number of HU (PHU) is exceeded. An example for the PHU concept is given in Figure 2.6, where the mean daily temperature during 1992 for Greenfield, Indiana, is plotted. In this example, the blue line represents the plant base temperature (T_{base}) which has to be exceed by the mean daily temperature (red graph) to initiate plant growth (Neitsch et al. 2011).

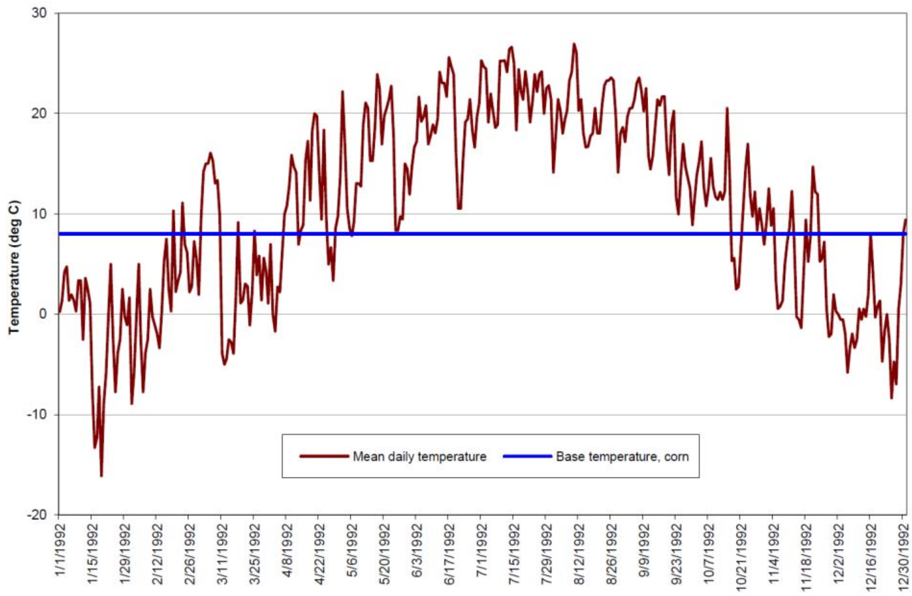

Figure 2.6: Plant Heat Unit (PHU) Concept - Mean daily temperature recorded for Greenfield in Indiana. When the mean daily temperature (red graph) exceeds the T_{base} threshold (blue line), the plant will start to grow (Neitsch et al. 2011).

2.2.4.5 Nutrients (Nitrogen)

In SWAT, several forms of nutrients such as nitrogen, NO_3 and phosphorus can be modeled in the watershed. Nutrients are transported into the main channel of the watershed through surface runoff and lateral subsurface flow. Nitrogen is an essential parameter for plant growth among other important elements including carbon, oxygen and hydrogen. In SWAT, the nitrogen cycle is modeled in the soil profile and in shallow aquifer. Since nitrogen may exist in several valance states (such as NO_3, ammonium (NH_4^+) or elemental nitrogen (N_2) etc.), SWAT operates with five different pools of nitrogen in the soil to reflect the complexity of the nitrogen cycle (Figure 2.7) (Neitsch et al. 2011). Two pools represent inorganic forms of nitrogen (the mineral nitrogen NH_4^+ and NO_3^-) whereas the other three pools constitute of organic forms of nitrogen. The active and stable organic nitrogen pools are linked to the soil humus while the fresh organic nitrogen is associated with crop residue (Figure 2.7).

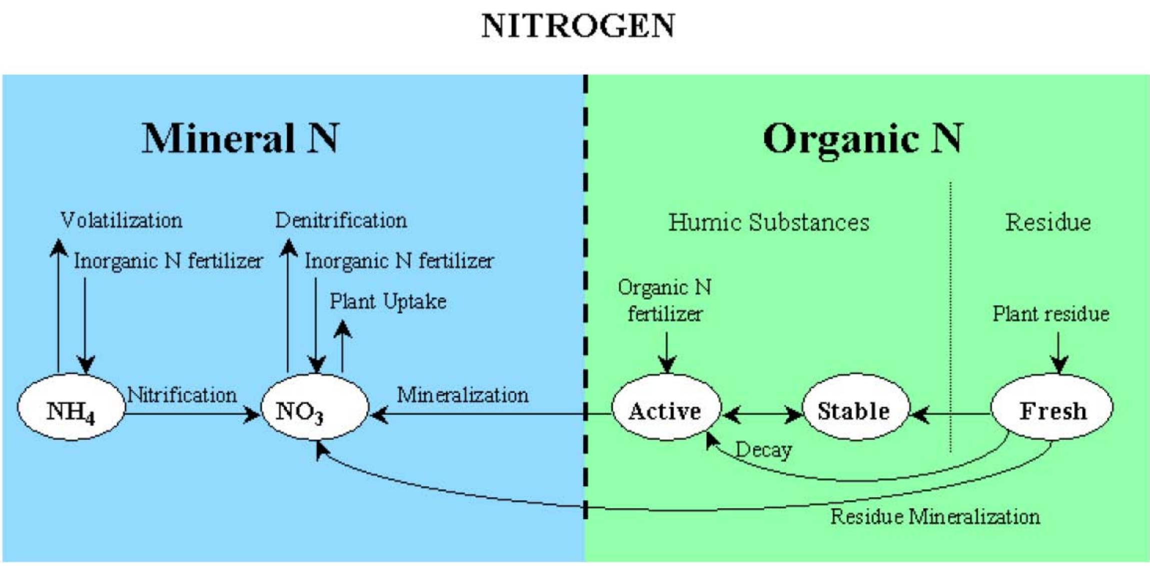

Figure 2.7: SWAT soil nitrogen pools and processes that move nitrogen in and out of pools (Neitsch et al. 2011)

As depicted in Figure 2.8, the SWAT algorithm contains several driving forces in the nitrogen cycle, namely mineralization, nitrification, denitrification, atmospheric deposition, water transport and leaching. Nitrogen may be added to the soil in form of fertilizer, manure or residue application, bacteriological application and rain (see Figure 2.8). It can be removed from the soil through plant uptake, soil erosion, leaching, volatilization and denitrification (Neitsch et al. 2011). NO_3 may be transported with surface runoff, lateral flow or percolation. The amount of NO_3 loads transported with the water is calculated by multiplying the NO_3 concentration in the streamflow by the volume of streamflow (Neitsch et al. 2011).

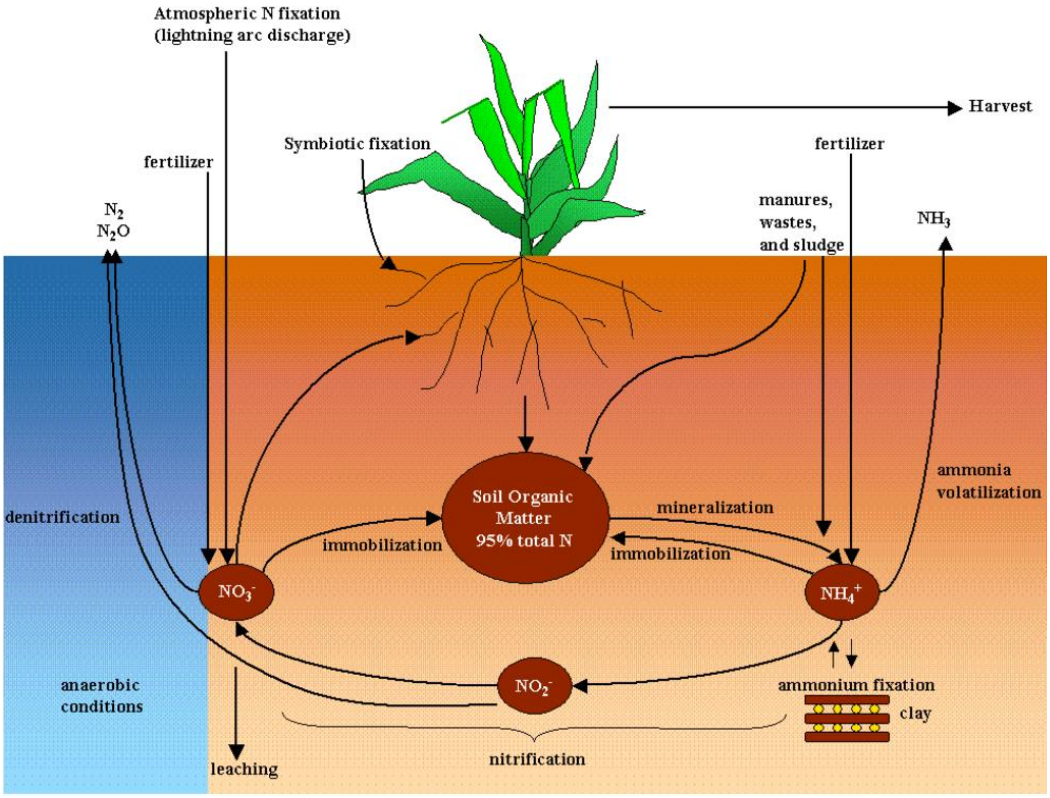

Figure 2.8: The major components in the nitrogen cycle in the SWAT model (Neitsch et al. 2011)

The SWAT in-stream water quality algorithms are partially based on the QUAL2E model (Brown, Barnwell 1987) which contains major interactive factors such as the nitrogen cycles, algae production and biological oxygen demand (Neitsch et al. 2011).

2.2.4.6 Agricultural Management Practices

A strength of the SWAT model is the quantification of the impact of land management and of the respective land use on the water supply and quality. For this reason, SWAT enables the user to define numerous land management practices taking place in every HRU. The management practices may be specified by basic management operations such as beginning or ending of growing season, timing and amounts of fertilizer application, timing and type of tillage operations or timing of harvest respectively seeding. Additional management options are the definition of the schedule of biomass removal as well as the determination of crop rotations in the watershed (Neitsch et al. 2011).

2.2.4.7 Point Source Loadings

To simulate the loadings of water and pollutants from sources not associated with a land area (point sources such as waste water treatment plants), SWAT is able to consider point source information along the channel network. In general, one point source in each subbasin can be implemented in SWAT. The point source loadings can be provided on a daily, monthly, yearly or mean annual basis and may contain loads of such as water, sediments, ammonium, nitrate, nitrite and metals (Neitsch et al. 2011).

2.2.4.8 Erosion

SWAT estimates the erosion and sediment yield for each HRU with the Modified Universal Soil Loss Equation (MUSLE) (Williams 1975). MUSLE uses the amount of runoff to model erosion and sediment yield. The main strengths of MUSLE are the prediction accuracy and the possibility of estimating the sediment yields of single storm events. (Neitsch et al. 2011)

2.2.4.9 Routing Phase of the Hydrologic Cycle

After determining the loadings of water, sediment, nutrients and pesticides to the main channel, the loadings are routed through the stream network. SWAT next transforms the chemicals in the stream and streambed in order to model the mass flow. In SWAT, the routing process in the main channel is described by four components: water, sediment, nutrients and organic chemicals (Neitsch et al. 2011).

- Flood routing: Several processes may influence the mass balance of water flowing downstream. Losses may appear due to evaporation and transmission as well as due to removal of water for agricultural or anthropogenic activities. Flow may be added by rain fall directly or by point source discharges. SWAT provides two methods for flood routing: the variable storage coefficient method or the Muskingum routing method.
- Sediment routing: Sediment transport is controlled by two simultaneously occurring processes, deposition and degradation.
- Nutrient routing: Nutrient transformations are controlled by the in-stream water quality component of the SWAT model that was adapted from the QUAL2E model.
- Channel pesticide routing: The major in-stream processes simulated by the model are settling, burial, resuspension, volatilization, diffusion and transformation (Neitsch et al. 2011).

2.3 Additional Software

The ArcSWAT2012 extension was used on the basic software ArcGIS 10.1. Additional to the ArcSWAT2012 software, the auto-calibration tool SWAT-CUP was used.

2.3.1 SWAT-CUP (SWAT Calibration & Uncertainty Program)

SWAT-CUP stands for Calibration and Uncertainty Programs and is an automated model calibration tool for the SWAT model. This tool was developed by the aquatic research institute Eawag located in Switzerland (Abbaspour 2015). SWAT-CUP is a public domain program and uses a generic interface. Different sensitivity analysis, calibration, validation and uncertainty analysis are possible within SWAT-CUP. Five different uncertainty algorithms (SUFI-2, PSO, MCMC, ParaSol and GLUE) are implemented in SWAT-CUP (Abbaspour 2015). In SWAT-CUP the uncertain model parameters are systematically changed; the model is run. Then the required outputs are extracted from the model output files and compared with the measured data.

2.3.2 ArcGIS

ArcSWAT was run on an ArcGIS 10.1 platform developed by ERSI (2012), which is an interface for geographic information systems. ArcGIS enables to view and edit spatial data, create layered maps and to perform spatial analysis.

2.4 Model Input

In the following sections (chapters 2.4.1 - 2.4.6), the several required SWAT input data sets are described, such as where the data was collected from or how the data was prepared and edited to the required SWAT input file format.

Unless otherwise written, the data collection and preparation was carried out by me personally. In particular, I collected the required SWAT input data for describing the land use classes, tillage operations, fertilizer applications, crop yield and biomass values, conventional tillage method and determining the PHU values.

The data aggregating and processing of DEM, land use, soil and field management practices data was done with the contribution of PhD student Christoph Schürz, who was carrying out his PhD within the UnLoadC³ project.

The Raab watershed delineation was carried out by myself with holding several reviews by my co-supervisors Dr. Bano Mehdi and PhD student Christoph Schürz. All collected data sets and data sources are summarized in the appendix, Table 8.1.

2.4.1 Watershed Delineation

The delineation of subwatersheds (subbasins) is based on a procedure using the DEM data but the user may predefine the limits of the size and number of subbasins (Winchell et al. 2013). When delineating the watershed in SWAT, a uniform distribution of the subbasins in size within the model area should be obtained to avoid potential problems in the routing process at subbasins inlets/outlets (Winchell et al. 2013). Thus, the Raab SWAT model was divided into 30 subbasins, with an average subbasin area of around 33km² (Figure 2.9). The delineated subbasin segments show an average size between 2% to 5% of the entire watershed which also complies with the recommendations of delineating subbasins (Jha et al. 2004).

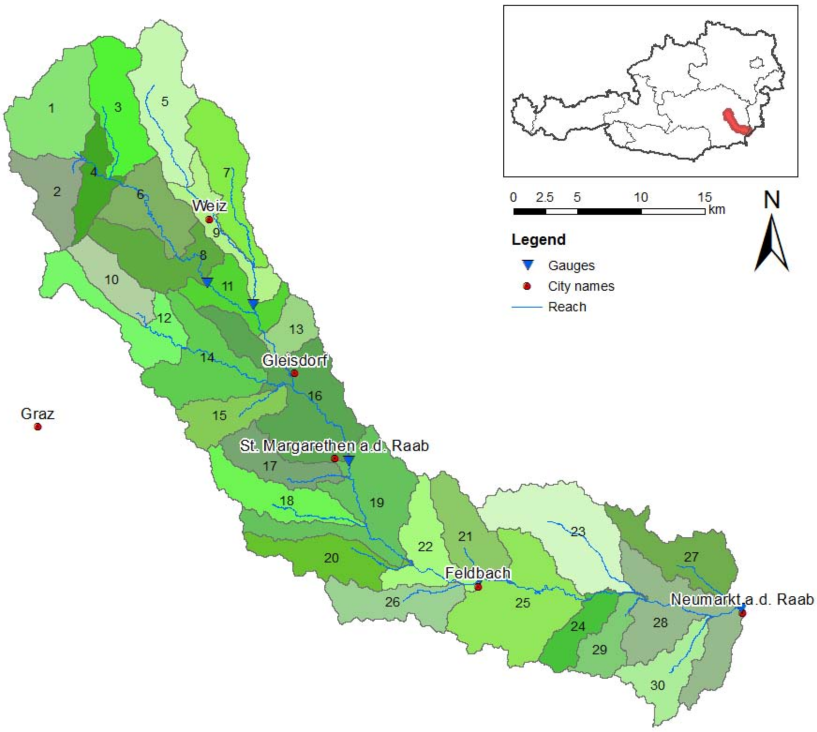

Figure 2.9: Delineation of Raab watershed into 30 subbasins based on the DEM

As shown in Table 2.2, five further subdivisions to the Raab watershed were made. The subdivisions were based on the available discharge and water quality monitoring stations for the calibration and validation process.

Table 2.2: Watershed Delineation - number of subbasins and HRUs; applied discharge gauges for calibration and validation; specific land use distribution in 5 subdivided watershed areas.

Watershed Outlet	Subbasins	No. of Subbasins	No. of HRUs	Watershed Area (km²)	Land Use Type (%)			
					Forest	Agriculture	Pasture	Urban
Mitterdorf/ Raab	*1 - 4, 6, 8*	6	84	184.15	58.8	6.0	32.7	2.5
St.Ruprecht/Raab	*5, 7, 9*	3	67	99.69	57.4	5.4	23.3	13.9
Takern II	*10 - 16*	7	134	215.09	49.7	22.5	5.5	22.2
Feldbach	*17-20, 22, 26*	6	151	191.10	37.4	35.8	14.8	12.0
Neumarkt/ Raab	*21,23-25,27-29,30*	8	229	298.13	40.2	37.2	15.2	7.4
Total	-	30	665	988.16	-	-	-	-

2.4.2 Meteorological Data

The INCA climate dataset for Austria (Haiden et al. 2010) was applied as input for the required temperature and precipitation data in the SWAT model weather data set. This weather data set provides a 15 minutes temporal resolution for the model time period 2003 – 2012 in a 1km x 1km grid. To take greater account of the different climatic conditions in the Raab catchment, a virtual weather station for each subbasin was compiled by Schürz (2015, pers. comm., 23. Oct.) which results in total 30 virtual weather stations for the entire Raab watershed, see Figure 2.10. The area precipitation as well as the temperature data based on the INCA dataset was aggregated in a 15 minutes interval for each virtual weather station. Additionally, the minimum and maximum daily temperature for the same spots and timeframes were computed (Schürz 2015, pers. comm., 23. Oct.).

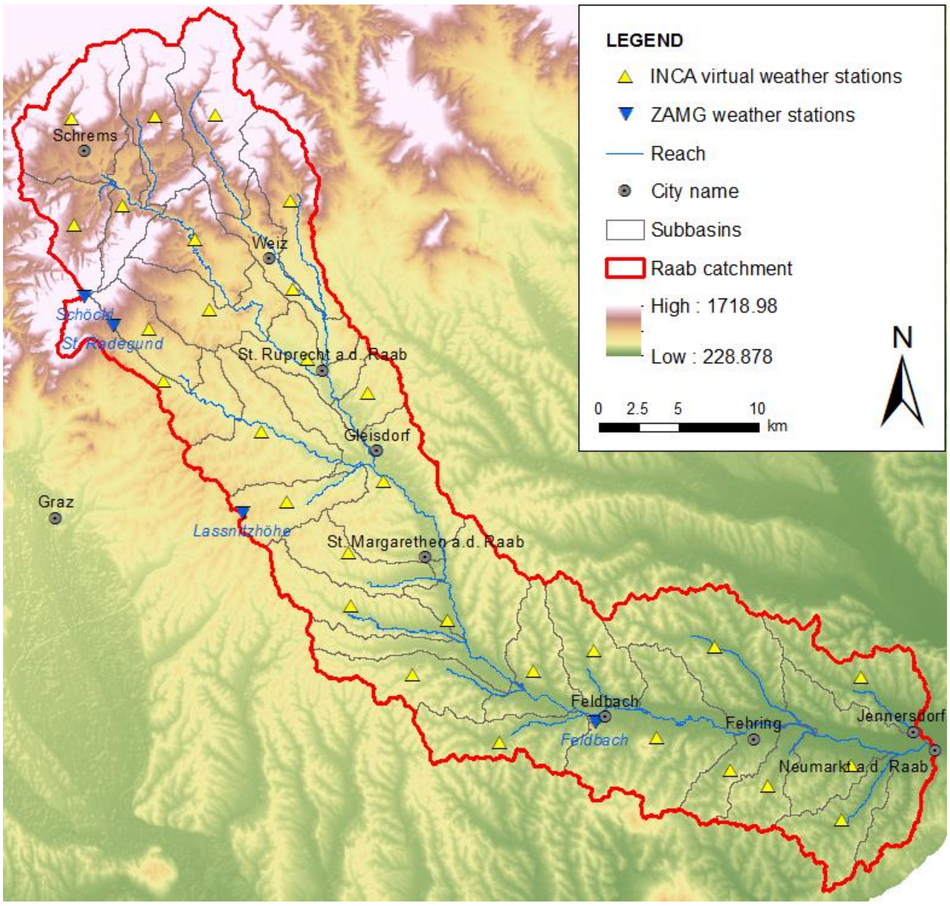

Figure 2.10: Overview map of Raab catchment representing the virtual INCA weather stations (yellow icons, in total 30); the ZAMG weather stations (blue triangles) and the subbasins.

Weather data by the Zentralanstalt für Meteorologie und Geodynamik (ZAMG 2015) such as the daily accumulated global radiation, mean relative humidity and mean daily wind speed were necessary for the model (Schürz 2015, pers. comm., 23. Oct.). In Raab catchment, only four ZAMG monitoring stations for all abovementioned monitoring parameters were available and are depicted in Figure 2.10 (Feldbach, St. Radegund, Schöckl and Lassnitzhöhe, labeled as blue triangles).

Remaining missing weather data is generated by the built-in SWAT weather generator on basis of long-time weather records.

2.4.3 DEM (Digital Elevation Model)

The digital elevation model (DEM) of the Raab watershed was generated by using the Laserscan dataset (Geoland.at 2015) which is available in a 10 m spatial resolution for entire Austria (Figure 2.10). This Laserscan dataset was created by means of elevation data based on Airborne Laserscan flights (Geoland.at 2015).

2.4.4 Soil Data

Obtaining data on the physical soil parameters for Raab catchment turned out to be a great challenge. The model structure of SWAT requires continuous data for the whole catchment as well as information about depth-related soil properties. Due to the lack of adequate, affordable national soil data in Austria, the global soil data set SoilGrids1km by ISRIC (ISRIC 2013) was applied. The SoilGrids1km worldwide dataset provides interpolated soil parameters in six different soil layers and in a 1km by 1km spatial resolution. To fulfil the requirements for an appropriate SWAT soil dataset, Schürz (2015, pers. comm., 12. Aug.) aggregated the soil information into a top- and a subsoil layer (conceptual model see Figure 2.11). As some required soil parameters were still not covered by the SoilGrids1km dataset, Schürz (2015, pers. comm., 12. Aug.) used a pedotransfer-function to calculate the required soil properties. The final SWAT soil dataset contains more than 150 soil classes in Raab catchment which are related to the pixels in the SWAT model as depicted in Figure 2.12. The Raab catchment is characterized by soil types such as brown soil, gley and pseudogley.

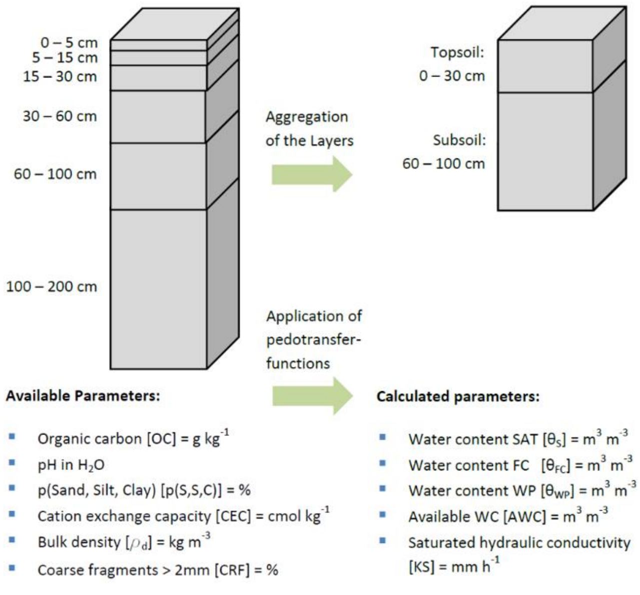

Figure 2.11: Conceptual model of the aggregation and calculation of soil data as input for SWAT, modified after (Schürz 2015, pers. comm., 4. Dec.)

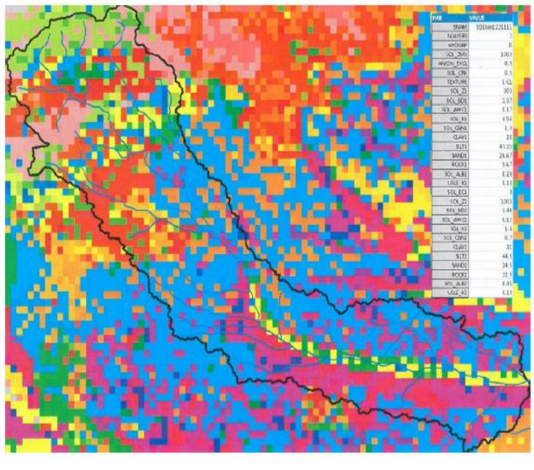

Figure 2.12: Final distribution of soil classes in Raab watershed based on SoilGrids1km (ISRIC 2013), modified after (Schürz 2015, pers. comm., 4. Dec.)

2.4.5 Land Use Data

As a basis for the SWAT land use map the CORINE Land Cover dataset (EEA 2015) was used. The CORINE Land Cover dataset covers all areas throughout Europe in a maximum spatial resolution of 1 ha (100m x 100m). However, the dataset provides only very coarse data about agricultural land use areas and no detailed information about the cultivated crops was available in Raab catchment. For the Raab catchment 22 land use classes, thereof only 6 agricultural classes, were available in the CORINE land cover dataset. Since the CORINE data set did not provide the required accuracy for the Raab catchment (detailed information about cultivated crops was not available), additional agricultural information was collected from the "Agrarstrukturerhebung 2010" (Statistik Austria 2015c). The data sets contain additional information about numerous cultivated field crops at a municipal level resolution given in hectares for the Raab catchment (in total 97 crop classes for the Raab catchment). Subsequently, Schürz (2015, pers. comm., 22. June) merged the grid data of the CORINE land use data set with the additional tabular crop data to achieve a more detailed land use dataset. This newly generated data set contained in total 72 land use classes, thereof 62 crop classes, for the Raab catchment.

Obtaining all necessary information for the specification of the land use was a very time-consuming task since the access to the data of the Agrarstrukturerhebung 2010 on municipality level was only possible via a library account of the WU Vienna (Vienna University of Economics and Business). Compiling the land use data, including data acquisition as well as the reallocation procedure, took about six months until it was completed.

2.4.6 Agricultural Management Practices

SWAT requires management operations for agricultural land uses to model the agricultural impacts on soil, hydrology and nutrients impacts (Neitsch et al. 2011). Including management data results in much better nutrient and crop yield outcomes in the SWAT model. SWAT allows management operations to be scheduled by day (fixed dates) or by fraction of potential heat units (Neitsch et al. 2011). For the Raab catchment, the scheduling of management operations (cultivation operation) was specified by predefined days. The predefined days were determined with the help of the *simple rule based model* (RBM) developed by Schürz et al. (2016). The RBM follows three simple rules (Schürz et al. 2016) to set a specific date for a management operation: (i) cultivation operation schedules are temperature dependent (e.g. warmer temperature results in earlier operation dates in spring), (ii) operations are randomized in a time span of 5 days around the calculated dates, (iii) and are only set during dry periods with no rainfall and low soil moisture (Schürz et al. 2016).

The management input data for the definition of the specific operation days in the RBM required information from the results of the field experiments carried out by the

Landwirtschaftliche Schulen NÖ (LAKO 2015), Landwirtschaftskammer NÖ (LK NÖ 2009), "Versuchsreferat Steiermark" (2013) and by the AGES (2015a). The obtained management input data is summarized in the appendix, Table 8.2.

2.4.7 Slope Classes & Thresholds for HRU Definition

In the HRU definition step, three slope classes were specified as shown in Table 2.3, where the last slope class (8 - ∞ %) represents non-arable lands with no cultivation patterns (Mehdi 2015, pers. comm. 2. Nov.).

Threshold levels of soil, land use and slope types were determined below which unique soil, land use and slope areas are not considered in subbasins (Winchell et al. 2013). The use of threshold levels reduces the number of HRUs in the SWAT model and optimizes the SWAT model as well as the computing demand (Winchell et al. 2013). Since it was important to keep the land use variety, only a low threshold value of 10% was applied to the land use classes (Table 2.3). Considering the high number of different soil classes in the SWAT model (more than 150 soil classes), a higher threshold of 20% was applied to the soil type. The threshold value for slope classes was specified with 15%.

Table 2.3: HRU definition - used slope classes in the slope discretization step and applied threshold levels in SWAT

Slope discretization	
Slope classes	0 – 3 %
	3 – 8 %
	8 – ∞ % [a)]
Threshold levels	
Land Use	10 %
Soil	20 %
Slope	15 %
Total HRUs	665

[a)] *non-arable lands, no cultivation patterns*

2.4.8 SWAT Set-Up

SWAT offers various methods to model the potential evapotranspiration, the rainfall-runoff balance and the infiltration processes. To simulate the potential evapotranspiration (PET) processes in the SWAT model, the Hargreaves equation was selected as the PET calculation method. The Hargreaves method requires only air temperature (maximum and minimum daily temperature) as input data (Neitsch et al. 2011). Another very essential component for the calculation of the hydrological model is built on the rainfall-runoff method. In this model, the "Green-Ampt Mein-Larson" infiltration method was used for estimation of the surface runoff. The channel routing in SWAT is modeled by using the variable storage routing method, which is a variation of the kinematic wave model (Neitsch et al. 2011). The simulation period was set from the years 2003 until 2012 (10 years); the warmup period consists of five years (1998 – 2002). The entire SWAT model set up for Raab catchment is summarized in Table 2.4.

Table 2.4: Model parameter settings in SWAT, Raab watershed

Parameter setting	
Simulation period	2003 – 2012 (10 years)
Warmup period	1998 – 2002 (5 years)
PET-method	Hargreaves method
Rainfall-Runoff method	Green & Ampt infiltration method Sub daily Rainfall- Hourly Route
Channel Routing	Variable Storage Routing method

2.5 Calibration and Validation Observed Data

2.5.1 Discharge Data

In general, the discharge and water levels are observed in an Austrian wide monitoring network which is operated by the hydrographic services of the federal states. Long-term time series of several decades are provided and freely available via the website eHYD respectively via annual published reports (BMLFUW 2014b). In the Raab catchment, eleven gauges were available covering several decades with discharge measurements in a daily resolution. One gauge was discontinued due to a replacement with a newly higher equipped monitoring station (Mitterdorf an der Raab), another gauge (Raabklamm) was discontinued five decades ago. The gauge Arzberg was excluded since it is located along a small tributary river (Moderbach), therefore the gauge is not directly positioned on the main river Raab. Three remaining gauges were not considered due to spatial distribution issues (stations were too close together). In conclusion, five discharge gauges with daily monitoring data were applied for the calibration and validation of the hydrological model:

- 211599 Mitterdorf an der Raab
- 210963 St. Ruprecht an der Raab (Weizbach)
- 210971 Takern II
- 210989 Feldbach
- 210468 Neumarkt an der Raab (watershed outlet)

Two of the gauge stations, Takern II and Neumarkt/Raab, are discussed in detail since water quality parameters such as nitrate-nitrogen (NO_3-N) are observed by the both stations. The gauge station Neumarkt/Raab represents as well the outlet of the entire SWAT watershed model. The monthly mean discharges of station 210468 Neumarkt/Raab are summarized in

Table 2.5 (model period 2003-2012); the mean discharge (MQ) in period 1991 – 2012 amounts to 6.91m³/s (BMLFUW 2014c). In August 2005 and in August 2009, two flood events with an annuality of 10 years (HQ10) were observed and documented in Raab watershed (Land Steiermark) and are evident by the peaks in Figure 2.13. The discharges in Neumarkt/Raab may be influenced by hydropower plant operations.

Table 2.5: Monthly mean discharges of 210468 Neumarkt/Raab (2003-2012)

m³/s	I	II	III	IV	V	VI	VII	VIII	IX	X	XI	XII
2003	4.66	3.48	4.33	2.69	1.90	2.07	1.96	1.20	2.59	3.78	3.50	3.70
2004	3.82	2.65	11.77	7.05	6.01	21.77	10.15	4.69	3.70	4.64	4.71	4.02
2005	3.49	3.02	8.21	7.00	4.83	3.14	6.77	25.96	11.06	8.30	5.08	6.75
2006	5.58	7.66	10.43	8.86	12.00	8.78	4.94	4.44	4.42	4.14	3.90	3.05
2007	3.97	3.76	7.95	4.10	3.62	3.68	2.37	3.27	8.52	5.06	3.84	5.97
2008	3.40	2.70	2.75	2.76	2.81	7.78	8.54	7.45	3.97	3.86	4.23	10.06
2009	7.86	12.63	8.43	5.53	6.14	22.26	21.70	22.12	15.58	7.73	8.75	10.37
2010	7.11	9.45	8.63	5.64	4.64	10.37	3.99	6.80	12.10	8.39	9.49	12.94
2011	8.39	5.48	7.71	5.60	4.33	11.49	5.75	5.87	5.14	5.54	3.42	2.98
2012	2.30	2.33	2.60	2.85	4.56	5.95	12.53	4.38	5.91	10.12	16.29	6.34

The discharges may be influenced by hydropower plant operations.

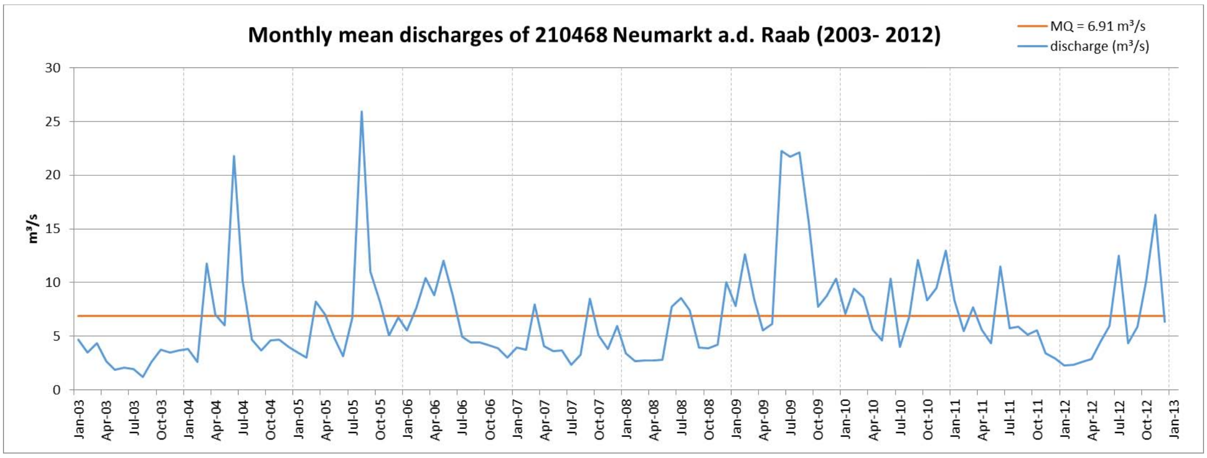

Figure 2.13: Monthly mean discharges of 210468 Neumarkt/Raab (2003-2012)

The monthly mean discharges of station Takern II (station number 210971) are summarized in Table 2.6 (model period 2003-2012); the mean discharge of Takern II (MQ) in period 1991 – 2012 amounts to 4.03m³/s (BMLFUW 2014c). In August 2005 and in August 2009, two flood events with an annuality of 10 years (HQ10) were observed in Raab watershed (Land Steiermark) and are evident by the peaks in Figure 2.14.

Table 2.6: Monthly mean discharges of 210971 Takern II (2003-2012)

m³/s	I	II	III	IV	V	VI	VII	VIII	IX	X	XI	XII
2003	2.75	2.12	2.21	1.72	1.31	1.53	1.29	1.09	1.42	2.10	2.53	2.32
2004	2.49	2.21	5.42	4.60	4.45	10.91	7.39	3.54	2.96	3.31	3.42	3.39
2005	2.47	2.00	4.75	4.51	3.10	2.11	4.77	17.20	7.41	5.32	2.85	2.54
2006	2.41	3.12	4.91	5.07	6.07	4.34	3.81	3.17	3.16	2.57	2.25	1.97
2007	2.45	2.14	3.64	2.52	2.16	3.01	1.82	2.38	4.91	3.09	2.55	3.23
2008	2.31	1.85	1.87	2.11	2.28	6.42	6.99	4.76	2.10	1.96	2.39	6.53
2009	4.00	5.83	6.20	4.84	4.58	8.38	11.74	14.22	14.19	6.39	6.44	6.72
2010	3.75	4.65	4.86	2.93	3.17	6.88	3.52	5.53	5.86	4.04	4.64	5.88
2011	4.13	2.92	4.80	3.17	2.85	7.26	3.55	3.71	3.71	3.15	2.24	2.00
2012	1.65	1.90	1.95	2.21	2.61	5.12	11.89	4.04	4.48	6.31	10.31	3.75

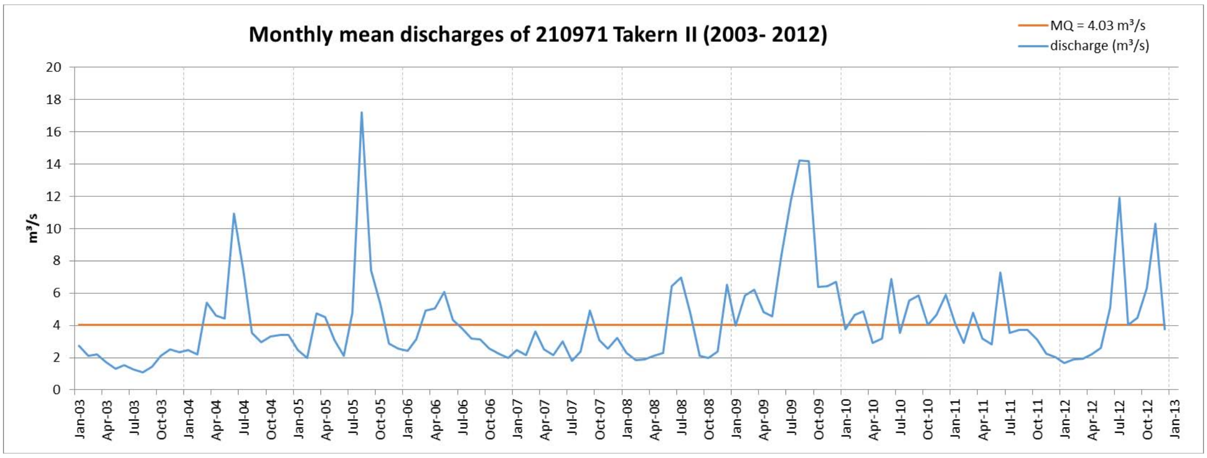

Figure 2.14: Monthly mean discharges of 210971 Takern II (2003-2012)

The observed discharge data for the remaining three gauges in Raab watershed (Mitterdorf/Raab, St. Ruprecht/Raab and Feldbach) are depicted in the appendix, tables 8.3 - 8.5.

2.5.2 Nitrate-Nitrogen (NO_3-N) Data

The water quality parameters such as NO_3-N in the Raab watershed are observed in Takern II and in Neumarkt/Raab. Due to the foam issue in river Raab (as described in chapter 1.1), the Raab watershed has a very comprehensive monitoring network with two online monitoring stations, referred as OM Takern II and OM Neumarkt/Raab, and one GZÜV water quality station, referred as GZÜV Neumarkt/Raab. The locations of the two online monitoring stations (OM Takern II and OM Neumarkt/Raab) as well as the GZÜV water quality sample point (GZÜV Neumarkt/Raab) are depicted in Figure 2.2.

In Austria, the standard monitoring network (GZÜV) carried out by the Austrian authorities has only monthly standardized samplings which are examined by authorized laboratories resulting in around 12 data recordings per year (BGBl. II Nr. 465/2010). In the Raab catchment, the GZÜV network provides one water quality monitoring station at the gauge Neumarkt/Raab (GZÜV Neumarkt/Raab).

The average monthly NO_3-N concentrations (mg/l) observed within the GZÜV framework for the SWAT model period 2003-2012 are listed in Table 2.7 respectively shown in Figure 2.15, with minimum and maximum NO_3-N concentrations of 1.51 mg/l and 12.47 mg/l. The average NO_3-N concentration in the period 2003-2012 is 3.22 mg/l.

Table 2.7: Monthly average NO_3-N concentrations in mg/l, GZÜV Neumarkt/Raab data series for the years 2003-2012

mg/l	I	II	III	IV	V	VI	VII	VIII	IX	X	XI	XII
2003	-	4.03	4.67	3.70	3.19	2.65	2.97	4.98	3.57	5.74	3.88	3.30
2004	3.34	3.84	12.47	3.97	5.50	6.85	3.32	3.36	4.01	3.29	3.22	3.02
2005	-	4.08	5.08	3.85	3.02	3.22	2.54	3.90	3.10	2.44	3.17	-
2006	4.63	6.44	7.60	3.60	7.00	3.65	3.59	2.96	3.38	2.92	2.70	3.36
2007	3.66	-	3.50	2.94	2.86	3.27	3.48	1.94	5.30	3.86	2.99	3.40
2008	3.12	3.05	2.38	2.36	2.25	4.28	3.30	2.87	2.63	2.02	2.08	3.26
2009	2.99	5.03	4.12	2.23	3.09	3.41	2.81	2.97	2.54	6.08	2.45	2.46
2010	3.03	3.46	3.26	2.58	2.22	2.65	2.42	2.02	2.80	2.34	2.17	2.91
2011	2.98	2.89	2.89	2.33	2.20	3.20	2.38	2.21	1.87	2.56	2.61	2.78
2012	3.46	2.95	2.48	2.37	6.32	2.32	2.40	2.13	2.35	2.45	3.20	2.92

Years 2003-2007: 1 sampling per month was taken, in total 12 samplings per year
Years 2008-2012: 2 samplings per month were taken, in total 24 samplings per year (given as the average value per month), unit (mg/l)

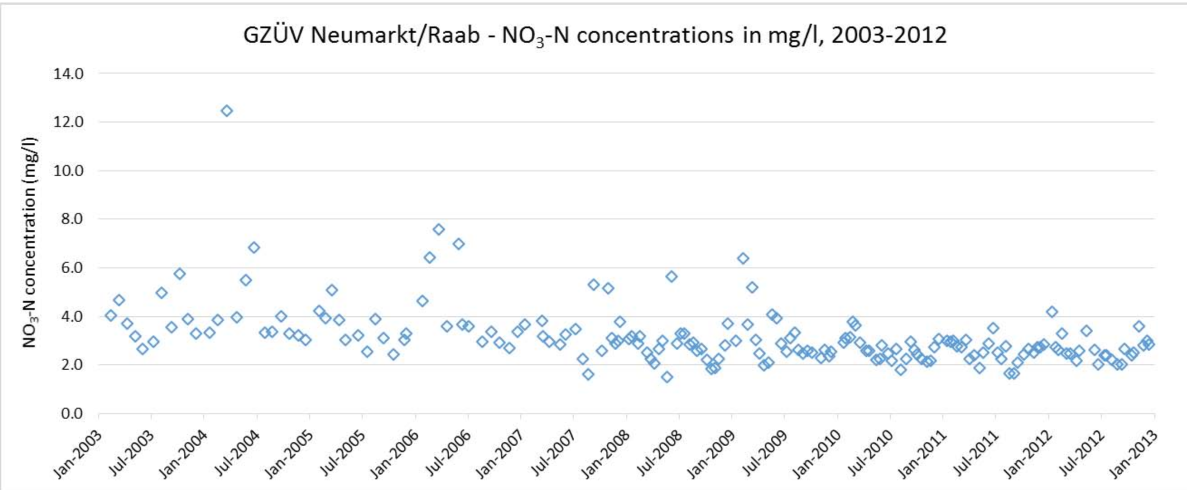

Figure 2.15: Monthly NO_3-N concentrations in mg/l, GZÜV Neumarkt/Raab time series for the years 2003-2012 at gauge Neumarkt/Raab; (years 2003-2007: 1 sampling per month, years 2008-2012: 2 samplings per month)

The online monitoring station OM Neumarkt/Raab is maintained by the TU Vienna and is located in Neumarkt/Raab. The online monitoring station OM Takern II is located in Takern II and is maintained by TBS Water Consult. These online monitored data are available in a 5 minute time interval. The OM Neumarkt/Raab and the OM Takern II data were only provided as raw and unverified data series.

Each online monitoring station requires regular review and if necessary a calibration of the online measuring probe has to be carried out. Thus, there are numerous reference measurement data available for the data series OM Neumarkt/Raab, carried out as samples examined by an external laboratory. The reference measurement data (referred as RM Neumarkt/Raab) are provided for a time period from April 2006 to Dec 2012, as shown in Figure 2.16 respectively in Table 2.8; in total 611 data points (around 7 samplings per month) were collected. The minimum and maximum NO_3-N concentrations in the RM Neumarkt/Raab data set are 1.25 mg/l and 6.20 mg/l. The average NO_3-N concentration in the period 2006-2012 is 2.85 mg/l which is lower than the average GZÜV concentration. For the OM Takern II data series, no reference measurement datasets were provided.

Table 2.8: Monthly average NO_3-N concentrations in mg/l, reference samplings (RM Neumarkt/Raab) for the years 2006-2012 carried out by TU Vienna, in total 611 samplings (around 7 samplings per month)

mg/l	I	II	III	IV	V	VI	VII	VIII	IX	X	XI	XII	n
2006	-	-	-	3.47	3.12	3.02	2.56	1.80	2.89	3.29	2.31	3.15	*90*
2007	3.20	3.64	5.96	2.83	3.02	2.97	3.03	2.59	2.94	2.82	3.17	3.47	*124*
2008	3.34	3.20	-	2.29	2.27	2.51	3.15	2.77	2.71	2.48	2.13	4.15	*75*
2009	-	3.78	3.68	2.41	1.76	2.54	2.88	2.90	2.52	2.86	2.41	3.11	*62*
2010	2.97	2.97	2.60	3.77	2.47	3.81	1.89	1.88	2.90	2.41	-	3.34	*85*
2011	3.15	2.94	3.11	2.39	4.44	3.13	2.34	1.58	1.78	1.65	2.04	2.46	*105*
2012	3.41	2.72	2.70	2.30	2.65	2.57	1.67	1.81	2.43	2.21	3.01	2.79	*70*

n… number of reference samplings, in total 611 samplings
values are given as the average value per month, unit in mg/l

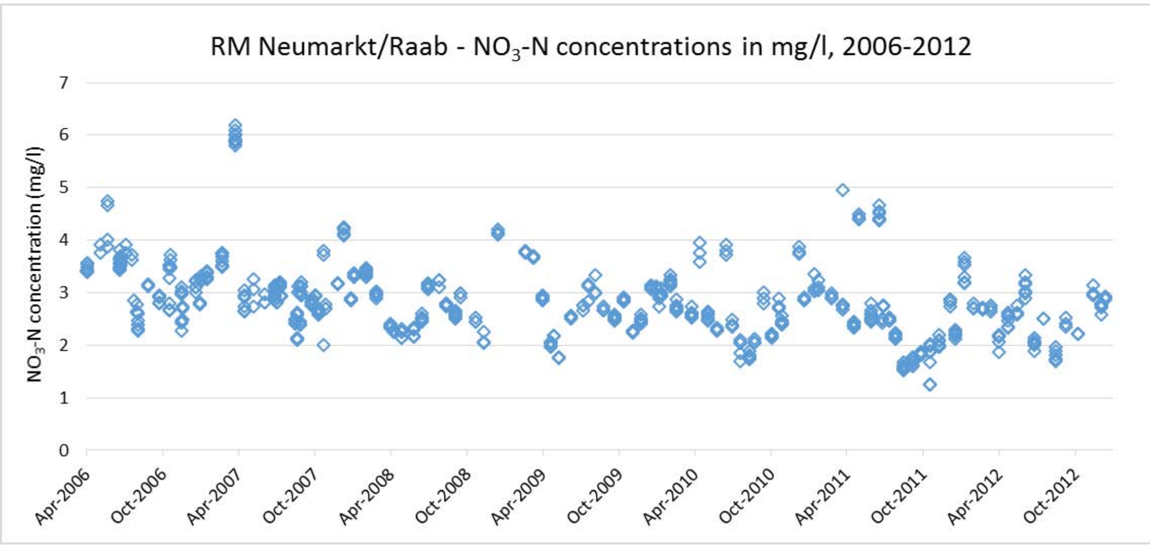

Figure 2.16: Monthly NO_3-N concentrations in mg/l, RM Neumarkt/Raab time series for the years 2006-2012 carried out by TU Vienna, in total 611 samples (around 7 samplings per month)

The OM Neumarkt/Raab time series of NO_3-N concentrations (raw data) is available for the years 2006-2012 and is shown in the appendix, Figure 8.9. The online monitored NO_3-N concentrations at Takern II are available for the years 2009 (Aug-Dec), 2010-2012 and are found in the appendix, Figure 8.8.

2.6 Calibration and Validation – Uncertainty Analysis

According to Moriasi et al. (2007) model calibration is the process of estimating model parameters by comparing model predictions (output) for a given set of assumed conditions with observed data for the same conditions and periods. Model validation involves running a model in a different time period, using input parameters measured or determined during the calibration process. The validation step is also performed to prove the strength of a model.

Manual calibration as well as the auto-calibration was used during the calibration and validation processes. The manual calibration contained the calibration of crop yield. The SUFI-2 algorithm (see chapter 2.6.3), available in the SWAT-CUP software package, was used for auto-calibration where 26 parameters were adjusted during the discharge calibration task and 7 parameters (see chapter 3.5 and 3.6.3) were adjusted during the NO_3-N calibration task.

The calibration process was carried out sequentially, since the model strongly depends on the hydrological processes in the subbasins above the outlets. Additional, the sequential calibration process enables a regional parameterization to consider the diversity of land use classes and agricultural crops in the Raab river basin (such as the forest-dominated areas in the pre-alpine regions and the agricultural areas in the lower Raab watershed region). During the calibration, only one outlet was specified as the main objective function, therefore no weighting of objective functions was needed. Since the NO_3-N loads strongly depends on the stream flow, the hydrological model was calibrated first and after achieving satisfactorily discharge results, the NO_3-N loads could be calibrated.

The sequential calibration process is carried out as recommended in the calibration protocol elaborated by Abbaspour et al. (2015):

(1) Set up the model with ArcSWAT by using the best parameter estimates based on the available data, literature and analyst's expertise (pre-calibrated SWAT model).

(2) Determination of most sensitive parameters by using the sensitivity analysis tool (*t-stat* and *p-value*)

(3) Based on the parameters identified before, initial calibration ranges are assigned to parameters. Additional, user-defined parameter ranges may be specified.

(4) Model is run 500 times (great time savings can be made by using the parallel processing option in SWAT-CUP).

(5) After an iteration is finished, post processing options are computed, where the objective function and the 95% prediction uncertainty for all observed variables are calculated as well as new parameter range sets are provided.

(6) Based on new suggested parameter range sets another iteration is performed with modified parameter ranges. The procedure is continued until satisfactory model results are reached in terms of NSE and R^2 (usually minimum 3 iterations needed).

2.6.1 Nash-Sutcliffe Efficiency

The SWAT model was optimized by using the Nash-Sutcliffe Efficiency (NSE) (Nash, Sutcliffe 1970) since its common application provides extensive information on reported values (see Table 2.10, (Moriasi et al. 2007)) as well as it was applied in several hydrological studies using SWAT such as in Mehdi et al. (2015b). The statistical criterion NSE was chosen as the primary objective function because the discharge peaks were well simulated. The NSE determines the relative magnitude of the variance of the residuals compared to the variance of the observed data and is calculated as follows (Nash, Sutcliffe 1970):

$$NSE = 1 - \frac{\sum_{t=1}^{n}\left(Q_{s,t} - Q_{o,t}\right)^2}{\sum_{t=1}^{n}\left(Q_{o,t} - Q_{o,mean}\right)^2} \qquad (2.4)$$

where n is the number of time steps, $Q_{s,t}$ is the simulated value at time step t , $Q_{o,t}$ is the observed value at time step t , and $Q_{o,mean}$ is the mean of the observed values.

According to Moriasi et al. (2007) the NSE ranges between infinite (- ∞) and 1.0 where an NSE of 1.0 represents the optimal value. Values between 0.0 and 1.0 are generally viewed as acceptable levels of performance, whereas values lower than 0.0 indicates unacceptable performance (which indicates that the mean observed value is a better predictor than the simulated value). As per Moriasi et al. (2007), a model performance considering for monthly time steps can be evaluated as *very good* if a NSE > 0.75 is reached, on the other hand, the model performance is evaluated as *unsatisfactory* when no better NSE than 0.50 is achieved (Table 2.9).

Table 2.9: General performance ratings for selected statistics for a monthly time step, modified after Moriasi et al. (2007)

Performance Rating	NSE	PBIAS (%)	
		Streamflow	N, P
Very good	0.75 < NSE ≤ 1.00	PBIAS < ±10	PBIAS < ±25
Good	0.65 < NSE ≤ 0.75	±10 ≤ PBIAS < ±15	±25 ≤ PBIAS < ±40
Satisfactory	0.50 < NSE ≤ 0.65	±15 ≤ PBIAS < ±25	±40 ≤ PBIAS < ±70
Unsatisfactory	NSE ≤ 0.50	PBIAS > ±25	PBIAS > ±70

Moriasi et al. (2007) performed a literature study on the performance of SWAT models in different studies and found in several studies that calibration and validations results manifested in a very wide range of possibly NSE values (for the constituents streamflow and NO_3-N) as shown in Table 2.10. Median values instead of means are included in the table because medians are less sensitive to extreme values. Although, the NSE for daily calibrated streamflow models ranges widely from -0.23 to 0.95, the median value of 0.89 indicate a very good model accuracy for most of the simulations. The daily validation yields in greater ranges, beginning from -1.81 to 0.89 with a median value of 0.67. In general, validation efficiencies have lower NSE than calibration efficiencies. For NO_3-N, only two studies respectively NSE values were reported by Moriasi et al. (2007) (Table 2.10). The monthly calibration and validation process show lower median NS efficiencies (0.26 and 0.70). No values were reported for daily calibration and validation time steps.

Table 2.10: Summary statistics of reported NSE values, based on the literature review by Moriasi et al. (2007)

Nash-Sutcliffe Efficiency (NSE)		Calibration		Validation	
Constituent	Statistic	Daily	Monthly	Daily	Monthly
Streamflow (Q)	*n*	*92*	*33*	*128*	*70*
	Minimum	-0.23	0.14	-1.81	-3.35
	Maximum	0.95	0.91	0.89	0.93
	Median	0.89	0.79	0.67	0.63
NO_3-N	*n*	*0*	*2*	*0*	*2*
	Minimum	na	-0.08	na	0.64
	Maximum	na	0.59	na	0.75
	Median	na	0.26	na	0.70

n = number of reported values (sample size); na = not available (used when *n*=0)

2.6.2 Sensitivity Analysis

The selection of calibration parameters was based on their significance on the simulated output. The parameter significance was determined by trial & error, by literature research and by using the built-in sensitivity analysis tool of SWAT-CUP.

The sensitivity analysis of calibration parameters was carried out with the sensitivity analysis tool in SWAT-CUP which uses the statistical parameters *t-stat* and *p-value* for determining the parameter sensitivity. The *t-stat* is the coefficient of a parameter divided by its standard error and a low *p-value* (< 0.05) indicates that the null hypothesis can be rejected. Summed up, the larger the absolute value of *t-stat* and the smaller the *p-value* is, the more sensitive the parameter (Abbaspour 2015).

2.6.3 SUFI-2 algorithm

The Sequential Uncertainty Fitting algorithm (SUFI-2) (Abbaspour et al. 2004) in SWAT-CUP was used for calibrating and validating the SWAT model. According to Abbaspour et al. (2004) SUFI-2 is a semi-automated inverse modeling tool that is used for calibrating the SWAT model outputs to the available time series data of streamflow and NO_3-N.

In SUFI-2, the model and parameter uncertainties are mapped onto a set of parameter ranges. Initially, a set of meaningful parameter ranges are assigned to calibrating parameters based on literature, knowledge on site processes, and sensitivity analyses. The ranges of parameters are divided by the Latin hypercube samples algorithm. Then a set of Latin hypercube samples are drawn from the parameter ranges, and the objective function is calculated for each parameter set.

In the SUFI-2 algorithm there are two indicators to quantify the strength of the calibration and uncertainty of the model, namely the *P-factor* and *R-factor*. The *P-factor* is the percentage of observed data bracketed by the 95% prediction uncertainty (95PPU) (Abbaspour 2015). The 95PPU is the quantification at the 2.5% and 97.5% levels of the cumulative frequency distribution of all simulated output values, disallowing 5% of the very bad simulations. The *P-factor* varies from 0 to 1 where 1 means that 100% of the observed data lies within the model prediction uncertainty and indicate a good model accuracy (Abbaspour 2015). The *R-factor* is the ratio of the average thickness of the 95PPU band and the standard deviation of the observed variables (Abbaspour et al. 2015). It ranges from 0 to infinite where 0 reflects a perfect match with the observed values. According to Abbaspour (2015), a *P-factor* of > 0.7 (>70%) while having an *R-factor* of around 1 for discharge indicate a satisfying model accuracy. A simulation that exactly corresponds to observed data would be described by a *P-factor* of 1 and an *R-factor* of 0 (Abbaspour 2015).

In SUFI-2, an initial parameter can be modified through different methods to define new parameter ranges which are specified by the operators *v, a* and *r*. The operator *v* replaces the existing parameter by a given value (most common operator), the operator *a* adds a given value to the existing parameter value and the operator *r* multiplies an existing value by (1+ a given value) (Abbaspour 2015).

2.6.4 Statistical Parameters for Evaluation of Model Prediction

To evaluate the model prediction, besides the NS efficiency following model evaluation statistics were used: coefficient of determination (R^2), percent bias (PBIAS), standard deviation (SD) and ratio of mean root square error (RSR). These statistical parameters are described in the present section.

The coefficient of determination (R^2) indicates the quality of relationship between observed and simulated results and is calculated as follow:

$$R^2 = \frac{\left[\sum_i (Q_{m,i} - \bar{Q}_m)(Q_{s,i} - \bar{Q}_s)\right]^2}{\sum_i (Q_{m,i} - \bar{Q}_m)^2 \sum_i (Q_{s,i} - \bar{Q}_s)^2} \tag{2.5}$$

where Q is a variable (e.g. discharge), m and s stand for measured and simulated, i is the i^{th} measured or simulated data. The higher the R^2 value, the better the model accuracy and the lower the error variance (Moriasi et al. 2007). A value of R^2=1.0 indicate the ideal situation, while a R^2 of 0.0 ratifies a very poor prediction accuracy.

The percent bias (PBIAS) measures the average tendency of the simulated data to be larger or smaller than the observations (Gupta et al. 1999) and is calculated as follow:

$$PBIAS = 100 * \frac{\sum_{i=1}^{n} (Q_m - \bar{Q}_s)_i}{\sum_{i=1}^{n} Q_{m,i}} \tag{2.6}$$

where Q is a variable (e.g. discharge), m and s stand for measured and simulated, respectively. The optimal value of PBIAS is 0.0, which indicate an accurate model simulation. The PBIAS is commonly used to quantify water balance errors and its use can be easily extended to load errors (Moriasi et al. 2007).

To evaluate the quality of model simulations, the standard deviation (SD) as well as the ratio of the root mean square error to the standard deviation of measured data (RSR) were used. The standard deviation (SD) is calculated based on equation (2.7).

$$SD = \sqrt{\frac{\sum_{i=1}^{n}(Q_{m,i} - \bar{Q}_m)^2}{n}} \tag{2.7}$$

where Q is a variable (e.g. discharge), m stands for e.g. measured data (simulated data is as well considered in the SD), n is the number of observations (or of simulated data).

The ratio of root mean square error to the standard deviation of measured data (RSR) is calculated as follow:

$$RSR = \sqrt{\frac{\sum_{i=1}^{n}(Q_m - \bar{Q}_s)_i^2}{\sum_{i=1}^{n}(Q_{m,i} - \bar{Q}_m)^2}} \tag{2.8}$$

where Q is a variable (e.g. discharge), m and s stand for measured and simulated, respectively. According to Moriasi et al. (2007), a model simulation is considered as satisfactory, if RSR < 0.70.

2.7 Calibration and Validation - Set up

The SWAT simulation carried out covers a period of 15 years, starting in 1998 with a five years warm up period and ending in 2012, that means a model period of 10 years from 2003 – 2012. Precipitation data and discharge data, both available in a daily resolution, are continuous available for the entire model period (2003 -2012). The calibration period was determined as a six years period (2003 – 2008) with the objective of holding all possible hydrological events (floods, dry periods, snow melting, etc.). The validation period consists of the remaining four years (2009 – 2012) which holds as well several significant hydrological events to prove the strength of the SWAT model. The sequential calibration process was started with the calibration of streamflow on a monthly basis, subsequently the calibration on daily streamflow was carried out.

Having the hydrological model satisfactorily calibrated (by achieving a NSE > 0.75, see chapter 2.6.1), the validation process for both daily and monthly discharges was performed. After accomplishing the calibration/validation steps for discharge with satisfying results, the same sequential calibration process was applied on the water quality parameter NO_3-N. During the calibration processes, extensive input data like crop data, discharge data and monitoring records of NO_3-N are needed respectively were discussed in detail in the previous sections.

3 Results and Discussion

3.1 Land Use Class Definition

During the definition step of the land use classes in the SWAT model of the Raab catchment, the land use input data set was summarized from 72 classes into 15 different SWAT land use classes which were based on the built-in SWAT land use and crop database files. The 15 summarized land use classes are described in Table 3.1. The SWAT model of the Raab catchment was subdivided into seven different agricultural land use classes (crop classes), three forest classes (FRST, FRSD, FRSE), three different grassland zones, one urban area class and one class for wetlands and peat bogs.

The seven agricultural classes are characterized by the crop types CORN, OELK, SGBT, SOYB, SUNF, SWHT and WWHT (Table 3.1). The crop classes OELK, SOYB and FESI were newly created in the SWAT crop database since none of the pre-defined SWAT crop classes were compatible to the three crop types and specific plant growth parameter values such as T_{base} or T_{opt} were required for the SWAT crop database. The information of the required parameters was collected by carrying out a literature study, for example the values for the parameters T_{base} and T_{opt} for the crop OELK were collected from Bavec et al. (2002). The other required crop parameters such as maximum root depth or leaf area index were taken from the SWAT crop data set for watermelon. The parameter values for the crop class SOYB were modified with data from a report about soybeans by LK NÖ (2009). The crop class FESI is a modified FESC data set where minor alterations in cultivation usage and fertilizer application were made with crop information provided by Mehdi (2015, pers. comm., 7. Oct.).

Table 3.1: Classification of land use classes in Raab watershed and in the SWAT model, percentage distribution of land use

SWAT crop class	Area (km²)	Fraction of Area (%)	SWAT full crop name	Typical crop class/ land use in Raab watershed
FRST	184.93	18.72	Forest-Mixed	Forest Mixed
FRSD	153.57	15.54	Forest-Deciduous	Forest Deciduous
CORN	119.77	12.12	Corn	Corn and Corn-Cob-Mix (CCM)
URML	118.90	12.03	Urban Residential Med/ Low Density	Settlements, industry and barren land
FESC	116.47	11.79	Tall Fescue	Grassland, meadow and pasture
FESI	84.64	8.57	Tall Fescue Intensive	Grassland, meadow and pasture (intensive use)
FRSE	78.21	7.92	Forest-Evergreen	Forest Evergreen
OELK	31.59	3.20	Oelkuerbis	Oil pumpkin ("Styrian gold")
SGBT	30.43	3.08	Sugarbeet	Several vegetables
ORCD	30.24	3.06	Orchard	primarily Styrian apples
WWHT	18.53	1.88	Winter Wheat	Winter wheat, winter barley
SWHT	9.78	0.99	Spring Wheat	Spring wheat, spring barley
ALFA	5.98	0.61	Alfalfa	Clover grass
SOYB	4.44	0.45	Soybean	Soybean
WETL	0.55	0.06	Wetlands-Mixed	Wetland, peat bog
total	988.18	100.00		

Figure 3.1 gives an overview about the spatial distribution of the 15 SWAT land use classes in the Raab watershed. In the north-west part of the catchment, the land use characteristic is clearly dominated by forest (almost 44% of the area, green labels (FRST, FRSE, FRSD)). The proportion of agricultural land use increases eastbound (in total around 25%) and is indicated by orange-beige labels (e.g. SGBT, ORCD or WWHT) or orange surfaces (CORN). Grassland zones (light green surfaces, land use classes ALFA, FESC and FESI) represent around 20% percent of the Raab catchment. The remaining areas are settlements and urban areas (indicated by red labels) and result in approximately 11 % of the entire watershed area. Most of the bigger settlements are primarily located along the river Raab as well as along the tributary stream, Weizbach.

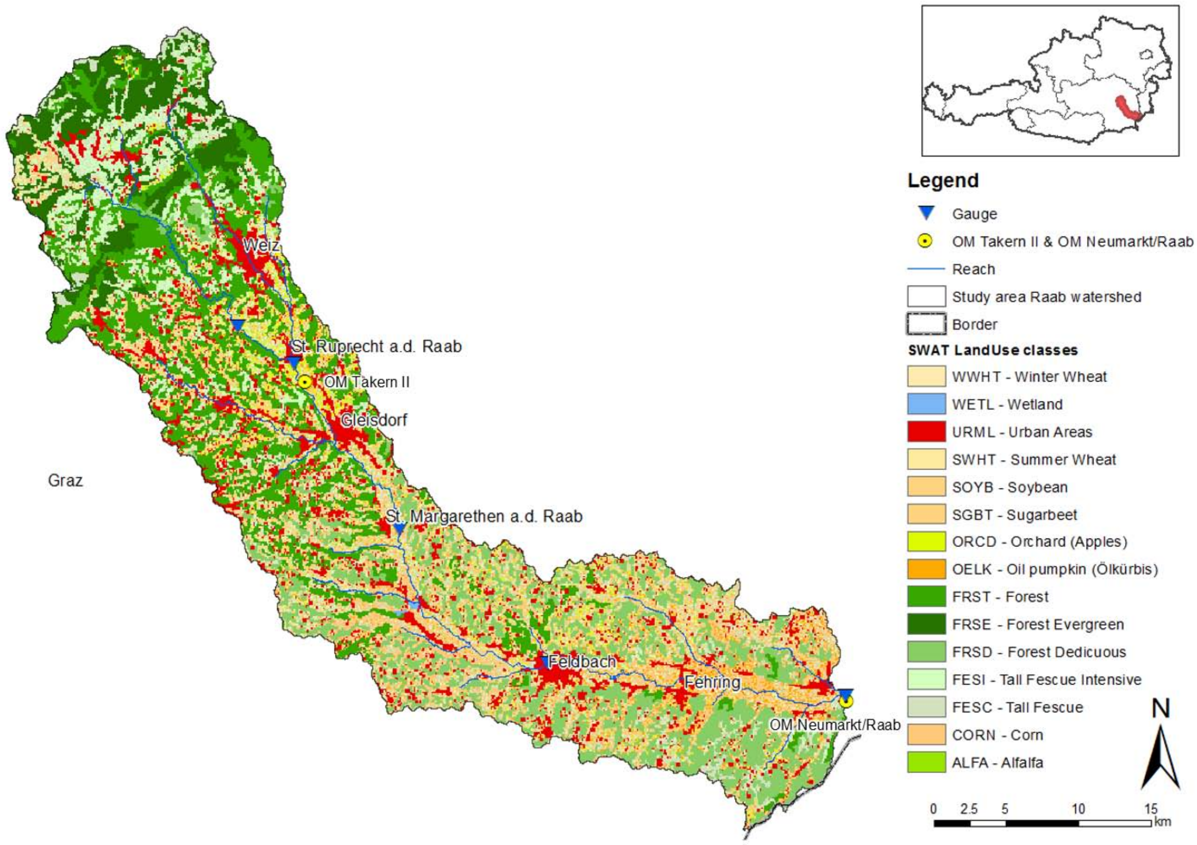

Figure 3.1: Land Use distribution with the 15 SWAT Land Use classes in Raab watershed

3.2 Agricultural Management Practices

The compilation of management practices data was another time-consuming task due to the fact that the first approaches by using management data collected from KTBL and by using the built-in scheduling method in SWAT for applying management operations based on the fractions of potential heat units (PHUs) were proved as inappropriate.

First, because the KTBL data stems from Germany as it was assumed that the agricultural conditions in Germany behave similarly as in Austrian Raab catchment but they did not. Second, the applied dates of tillage operations and fertilizer amounts turned out to be completely different compared to Austrian cultivation operation schedules. Third, the scheduling method based on the fractions of PHUs showed some weaknesses, such as the planting or harvesting dates were set too early or too late since the fractions of PHUs are sensitive to seasonal variability of temperature. The timing of fertilizer application was applied during wet periods which can lead to peaks in simulated NO_3-N loads, especially during heavy rainfall events (Mehdi et al. 2015b). Normally, no fertilizer is applied by farmers during a wet period since the applied fertilizer will be eroded immediately by surface runoff triggered by rainfall. Due to the weakness of the scheduling method based on the fractions of PHUs, it was decided to use the RBM (see chapter 2.4.6) for calculating the fixed dates for the application of agricultural management operations in the Raab catchment.

The workflow for the definition step of agricultural management practices (including the collection of the required input data) as well as the determination step of PHU values (chapter 3.3) is illustrated in Figure 3.2.

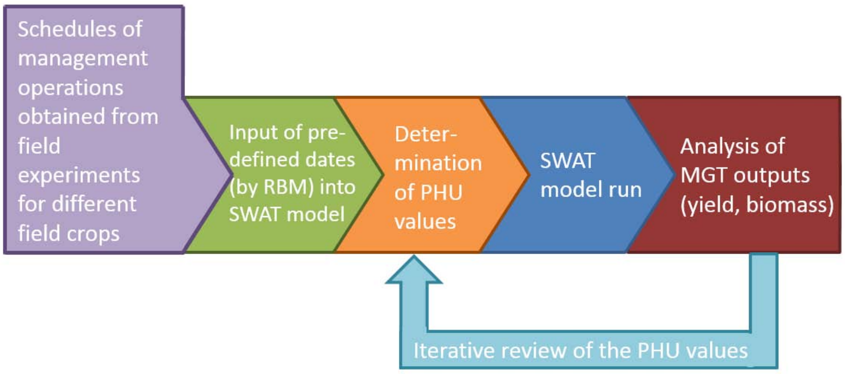

Figure 3.2: Schematic workflow of the PHU value determination step and of preparation the SWAT management input files

After the KTBL data was not useful, the management data was collected from the results of the field experiments carried out by the Landwirtschaftliche Schulen NÖ (LAKO 2015), Landwirtschaftskammer NÖ (LK NÖ 2009), Versuchsreferat Steiermark (2013) and by the AGES (2015a).

The obtained parameters from the field experiments consist of annual figures for the cultivation operations in the Raab catchment such as seeding date, harvest date, tillage operation, crop yield in tons per hectare, and amount or date of fertilizer application as shown in Table 8.2 in the appendix. According to the Agrarstrukturerhebung 2010 (Statistik Austria 2015c), *conventional tillage* is the primarily used management operation type in Raab watershed which was applied to the SWAT model. A typical characteristic of conventional tillage in the SWAT model is the application of *generic plowing* or of the *generic field cultivator* operations.

After computing the management input files with RBM, the final SWAT input data sets based on fixed dates for all agricultural operations were implemented to the SWAT model. An example for the computation of management input files based on the RBM is provided in Table 3.2.

Table 3.2: Example of a schedule of management operations for the crops SWHT (spring wheat) and WWHT (winter wheat), considering the beginning and ending date of seed, harvest and fertilizer applications. Further information contains the type of fertilizer and tillage operation application, the amount of fertilizer and the PHU number of the crop (e.g. 1536).

CROP	MON_1	DAY_1	MON_2	DAY_2	OPERATION	OP_TYPE	OP_VAL_1	OP_VAL_2	OP_VAL_3	OP_VAL_4
					Fraction	100				
SWHT	3	3	3	14	Fertilizer	Elem-N			50	0
SWHT	3	3	3	14	Fertilizer	Elem-P			22	0
SWHT	3	3	3	15	Tillage	Fldcge15				
SWHT	3	4	3	18	Plant	SWHT			1536	0
SWHT	5	14	6	7	Fertilizer	Elem-N			50	0
SWHT	7	15	8	3	Harvest & Kill					
SWHT	11	6	12	4	Tillage	Fallplow				
SWHT					End of year					
WWHT					Initial crop	WWHT	1	200	1892	
WWHT	3	5	3	20	Fertilizer	Elem-N			50	0
WWHT	3	5	3	20	Fertilizer	Elem-P			22	0
WWHT	4	14	5	6	Fertilizer	Elem-N			40	0
WWHT	5	20	5	31	Fertilizer	Elem-N			30	0
WWHT	7	9	7	24	Harvest & Kill					
WWHT	9	22	10	18	Tillage	Fallplow				
WWHT	10	1	10	25	Plant	WWHT			1892	0
WWHT					End of year					

According to the example schedule file in Table 3.2, the *PHU* (plant heat units) value for the crop SWHT is set to 1536 units which means a crop maturity is reached after 1536 plant heat units. The parameters *MON_1, DAY_1, MON_2* and *DAY_2* are predefined time slots based on the field experiments in which an operation shall occur. The actual operation date is dependent on weather conditions, e.g. a seeding operation is not realized in a cold period or a fertilizer operation is not applied during a wet period and is calculated by the RBM. In this example, the fertilizer application on SWHT crops consist of 50 kg/ha elemental nitrogen and of 22 kg/ha elemental phosphorus. The applied fertilizer amounts of the other crops is described in chapter 3.3. An entire overview with all management operations for all applied crop types in the Raab catchment is given in Table 8.2 in the appendix.

3.2.1 Fertilizer Application

Table 3.3 shows the applied annual fertilizer amounts of each crop class. The data was collected during several literature researches including following data sources: the outcomes of the field experiments carried out by the Landwirtschaftliche Schulen NÖ (LAKO 2015), Landwirtschaftskammer NÖ (LK NÖ 2009), Versuchsreferat Steiermark (2013) and by the AGES (2015a). The crop class SGBT (sugar beet) requires the highest annual nitrogen fertilizer amounts (250 N kg/ha) respectively needs an annual phosphorus fertilizer amount of 50 kg/ha. The lowest nitrogen demand show the crop classes ALFA (alfalfa) and SOYB (soybean) since legumes such as alfalfa and soybeans fixate the nitrogen (Mehdi 2015, pers. comm., 15. July) and therefore show a lower nitrogen demand as well as their demand on phosphorus is increased (50 P kg/ha) as shown in Table 3.3.

Table 3.3: Applied annual fertilizer amount (elemental nitrogen and elemental phosphorus) per crop; used T_{base}, T_{opt} values and plant classifications in SWAT of each crop

Crop-class	Elemental-N (kg/ha)	Elemental-P (kg/ha)	T_{base} (°C)	T_{opt} (°C)	Plant classification in SWAT
ALFA	-	80	4	20	perennial legume
CORN	135	35	8	25	warm season annual
FESC	90	20.1	0 [3)]	15 [3)]	perennial
FESI	140	35	0 [3)]	15 [3)]	perennial
OELK	60	26.4	10 [1)]	20 [1)]	warm season annual
ORCD	70	15.4	7	20	trees
SGBT	250	50	4	18	warm season annual
SOYB	20	28.6	10 [2)]	25 [2)]	warm season annual
SWHT	100	22	0	18	cold season annual
WWHT	120	22	0	18	cold season annual
FRST	-	-	10 [3)]	30 [3)]	trees
FRSD	-	-	10 [3)]	30 [3)]	trees
FRSE	-	-	0 [3)]	30 [3)]	trees

Data sources:
[1)] Bavec et al. (2002)
[2)] LK NÖ (2009)
[3)] predefined values in the SWAT2012 crop database
All other T_{base} and T_{opt} values were obtained from Mehdi (2015, pers. comm., 7. Oct.)

3.2.2 Discussion Agricultural Management Practices

Although numerous collected management practices input data were used in the SWAT model, the data cannot be validated for the Raab catchment due to lack of regionally available field management data. Therefore, it is uncertain if the used management parameters such as fertilizer application, tillage operation dates etc. actually reflects the agricultural reality in the Raab region.

The fertilizer application information was obtained from literature which are best practice guidelines and may not reflect the reality. Due to this reason, the amounts of applied fertilizers may be underestimated in the SWAT model for the Raab catchment. A further weak point is the non-consideration of manure by cattle in the SWAT model (as natural fertilization) due to lack of corresponding data. Merely fertilizer application of elemental nitrogen and elemental phosphorus were considered in the SWAT model.

3.3 Crop Yield

In this calibration task, the plant heat units (PHUs) were revised in an iterative way until the results of the simulated crop yield were satisfying (Figure 3.2). The reference values of the average yield for each crop, which were collected from the literature study as described in chapter 2.4.6, were used for the manual calibration of crop yield (see Table 3.4).

The most sensitive parameters which influenced the crop yield and the biomass output in the SWAT model were the plant growth parameters such as T_{base}, T_{opt} and harvest parameters such as the harvest efficiency. In general, the crop yield and biomass in the SWAT model are influenced by the harvest index (HVSTI, defines the fraction of the biomass which is removed in a harvest operation), the harvest index override (HI_OVR, this parameter forces the ratio of yield to total biomass to the specified value) and the efficiency of the harvest operation (HARVEFF, for grain harvest: the harvest efficiency defines the fraction of yield biomass removed by the harvesting equipment with the remaining yield lost) (Arnold et al. 2012). The specified T_{base} and the T_{opt} parameters significantly affect the plant growth (Arnold et al. 2012) and were revised in the crop database as shown in Table 3.3.

Another essential part of the crop description in the SWAT model is an accurate plant classification of each crop class (last column in Table 3.3) which affects the simulation of nitrogen fixation, the root depth of each crop class and the behavior of the dormancy status of a crop (when a plant goes dormant) (Arnold et al. 2012).

The most crop yields could be calibrated in a satisfying way (Table 3.4); only the yields of the crop classes ORCD, SWHT and WWHT remained underestimated. The yield of the crop classes SWHT (3.9 t/ha, reference value 6-8 t/ha) and WWHT (4.4 t/ha, ref. value 6.3-9.1 t/ha) were underestimated most likely due to inappropriately adjusted harvest parameters and due to unsuitable initial plant growth variables such as T_{base} and T_{opt}. Although these parameters were modified with values provided by Austrian relevant literature such as from AGES (2015a), the edited T_{base} and T_{opt} parameters (0°C and 18°C, see Table 3.3) for the crops SWHT and WWHT remained unsuitable for the Raab catchment.

The SWAT model underestimated the yield of the crop class ORCD (Table 3.4) significantly (11.8 t/ha compared to 24-35 t/ha), a reason may be that the used SWAT crop class ORCD is not suitable for modeling of apple yields due to inappropriate T_{base} and T_{opt} values (7°C respectively 20°C, see Table 3.3) or due to insufficient assumptions on the harvest efficiency.

Although, the temperature values and harvest efficiency variables were modified for ORCD several times, no significant improvement of the yield outcome was achieved.

Table 3.4: Reference values for the annual average crop yield in the study area and specified PHUs for each crop

CROP		LITERATURE		SWAT model Raab	
Crop class	Crop class- full name	Yield (t/ha) BSL15[a)]	Yield (t/ha) LKO [a)]	Simulated Yield (t/ha)	Plant Heat Units (PHU)
ALFA	Alfalfa	12.6 TM	-	13.6	1258
CORN	Corn	-	7.5 - 14.0	8.1	1205
FESC	Tall Fescue	-	5 - 6 TM	7.9	1585
FESI	Fescue Intensive	-	7 - 12 TM	7.4	1585
OELK	Oil pumpkin	1.2	-	2.8	700
ORCD	Orchard (apples)	-	24 - 35[b)]	11.8	1730
SGBT	Sugar beet	11 - 170	-	16.8	2050
SOYB	Soybean	(3.5 - 4.0)	1.8 - 3.0	2.1	935
SWHT	Spring Wheat	6.5 - 7.3	6 - 8	3.9	1536
WWHT	Winter Wheat	6.3 - 9.1	-	4.4	1892
FRSD	Forest Deciduous	-	-	-	2440
FRSE	Forest Evergreen	-	-	-	2840
FRST	Forest Mixed	-	-	-	2640

[a)]*Data sources:*
BSL15: Österreichische Beschreibende Sortenliste 2015 (AGES 2015a)
LKO: Landwirtschaftskammer Österreich (LK Österreich)
CORN & SWHT: Landwirtschaftliche Schulen NÖ (LAKO 2015)
[b)] *ORCD: Statistik Austria (Statistik Austria 2015b)*

3.4 Water Balance

According to the water supply plan of the Federal State Styria (Wasserversorgungsplan 2015, (Land Steiermark 2015)), the average annual precipitation is 800-900 mm/yr for the Raab catchment based on a time series from 1987-2012. The SWAT model simulated an average precipitation of 881.1 mm per year (Table 3.5) which fits in very well compared to the literature value. Further reference precipitation values can be collected from eHYD (BMLFUW 2014b), where the average annual precipitation in the upper watershed region of Weiz is 990 mm and in the lower watershed region of Neumarkt is 760 mm. Therefore the simulated annual precipitation of 881.1 mm/yr lies completely within the range 760-990 mm of the collected values from eHYD.

According to Herrnegger (2013), the mean annual potential evapotranspiration of the Raab river basin is classified as 800.1 - 900 mm/yr which was calculated based on the PET methods Penman-Monteith and Hargreaves for the years 2007-2009. To a small extent (approximately 20%) of the Raab catchment, the annual potential evapotranspiration is to be 750.1 – 800 mm/yr as per Herrnegger (2013). The simulated average annual potential evapotranspiration amount of 801 mm/yr (Table 3.5) corresponds very well with the given literature values.

The average flow in the Raab river basin is given with 221 mm/yr (*Hydrografisches Jahrbuch* 2012, (BMLFUW 2014c)), which shows a good correlation with the simulated flow of 213.1 mm/yr (Table 3.5).

The ratio of the actual baseflow and total flow (baseflow factor) in the Raab catchment was calculated with the baseflow program (Arnold et al. 1995) based on the daily discharge time series from 1991 to 2012 at the gauge Neumarkt/Raab. The actual baseflow factor is 0.74 at the outlet Neumarkt/Raab which correlates well with the simulated baseflow of 0.79 in the SWAT model (Table 3.5). The reference ratio of streamflow and precipitation is 0.26 (based on literature values) which shows a very good accordance with the simulated ratio of 0.24 at the outlet Neumarkt/Raab.

Table 3.5: Simulated hydrological water balance in the SWAT model, with values of evapotranspiration, surface runoff and several ratios

Constituent	Unit	Simulated SWAT model ratios for Raab catchment	Literature review-ratios for Raab catchment
Precipitation	mm/yr	881.1	800 - 900[a)], 760 - 990[b)]
Potential Evapotranspiration	mm/yr	801	750.1 – 800[c)], 800.1 – 900[c)]
Streamflow	mm/yr	213.1	221[d)]
Water Balance Ratios			
Baseflow/Total Flow	[-]	0.79	0.74
Surface Runoff/Total Flow	[-]	0.21	0.26
Streamflow/Precipitation	[-]	0.24	0.26

Data sources:
[a)] *Wasserversorgungsplan 2015, (Land Steiermark 2015)*
[b)] *eHYD (BMLFUW 2014b)*
[c)] *Herrnegger (2013)*
[d)] *Hydrografisches Jahrbuch 2012 (BMLFUW 2014c)*

3.5 Streamflow Calibration

The auto-calibration using SUFI-2 was performed for each outlet separately. For the sequential calibration, 500 simulations per iteration were run after which the parameter ranges were adjusted. A total of 3 iterations per outlet were performed. Based on the sensitivity analysis, in total 26 parameters were chosen for the hydrological calibration in SUFI-2 (see Table 3.6); thereof 21 parameters were used for monthly hydrological calibration and additional 5 parameters were added for the daily hydrological calibration. Table 3.6 shows a list of the calibration parameters with the corresponding final calibration ranges determined after the 3rd iteration.

The hydrological calibration in the Raab watershed was based on four primary parameter groups which influenced the following hydrological processes as surface runoff, baseflow, snow and soil parameters.

The surface runoff processes control the formation of overland flow along sloping surfaces and the rate of infiltration into soil (Neitsch et al. 2011). The base flow parameters affect the volume of water that enters the reach from shallow aquifer, the groundwater flow and the hydraulic conductivity in soil (Neitsch et al. 2011). In the Raab SWAT model, the surface runoff as well as baseflow related hydrological processes were modeled by parameters such as CN2, SOL_AWC, ESCO, EPCO, SURLAG and LAT_TTIME.

The snow parameters are principally related to snow melt processes, the corresponding melting temperatures and the amount of snow water content (Neitsch et al. 2011). The snow processes were characterized by parameters such as SNO50CV, SNOCOMX, SFTMP, SMTMP, SMFMX, SMFMN and TIMP.

The soil parameters influence the soil water movement in the soil profile and the hydraulic conductivity in the Raab catchment. The soil conditions in the Raab catchment were specified by parameters such as CANMX, SOL_K(), CH_N1, CH_N2, CH_K1 or CH_K2.

The results of the sensitivity analysis showed that the groundwater parameters are the most sensitive parameters for the Raab catchment since the groundwater parameters showed a strong influence to the simulated discharge volumes. The groundwater components influence the interaction between surface water and shallow groundwater (Neitsch et al. 2011). The groundwater processes in the Raab catchment are driven by parameters such as GW_DELAY, GWQMIN, GW_REVAP and REVAPMN.

Table 3.6: List of the parameters adjusted during the auto-calibration process with the corresponding final minimum and maximum values of the calibrated parameter ranges (incl. short description of parameters)

Parameter	Description	Min	Max	Units
r__CN2.mgt	Initial SCS runoff curve number for moisture condition II	-13.40%	+20.00%	-
v__ALPHA_BF.gw	Baseflow alpha factor	0.803	0.920	1/days
v__GW_DELAY.gw	Groundwater delay times	327.883	479.751	days
v__GWQMN.gw	Threshold depth of water in the shallow aquifer	135.857	4692.798	mm
v__ESCO.hru	Soil evaporation compensation factor	0.096	0.282	-
v__GW_REVAP.gw	Coefficient for groundwater transfer from the shallow aquifer to the root zone	0.024	0.199	-
v__SNO50COV.bsn	Fraction of snow volume represented by SNOCOVMX that corresponds to 50% snow cover	0.036	0.407	-
v__CANMX.hru	Maximum canopy storage	0.06	24.58	mm
r__SOL_AWC().sol	Available water capacity of the soil layer	-1.73%	+19.77%	mm/mm
r__CH_N2.rte	Manning's "n" value for the main channel	-9.98%	+6.47%	-
r__CH_K2.rte	Effective hydraulic conductivity in main channel alluvium	-18.26%	+14.79%	mm/hr
r__CH_K1.sub	Effective hydraulic conductivity in tributary channel alluvium	-19.95%	+8.14%	mm/hr
v__ALPHA_BNK.rte	Baseflow alpha factor for bank storage	0.037	0.652	days
v__SURLAG.bsn	Surface runoff lag coefficient	2.214	22.905	-
v__TIMP.bsn	Snow pack temperature lag factor	0.377	0.957	-
v__SFTMP.bsn	snowfall temperature	-0.072	2.428	°C
v__SMTMP.bsn	snow melt base temperature	-5.127	2.889	°C
v__SMFMX.bsn	Melt factor for snow on June 21	0.301	4.988	mm/°C
v__SMFMN.bsn	Melt factor for snow on December 21	0.876	4.328	mm/°C
v__SNOCOVMX.bsn	Minimum snow water content that corresponds to 100% snow cover	57.02	452.46	mm
v__REVAPMN.gw	Threshold depth of water in the shallow aquifer for "revap"	69.077	698.821	mm
v__EPCO.hru	Plant uptake compensation factor	0.578	0.819	-
v__LAT_TTIME.hru	Lateral flow travel time	2.224	102.426	days
a__OV_N.hru	Manning's "n" value for overland flow	-0.037	-0.014	-
r__SOL_K().sol	Saturated hydraulic conductivity	-14.43%	+95.00%	mm/hr
v__CH_N1.sub	Manning's "n" value for the tributary channels	0.700	17.554	-

Parameters in italics were additionally implemented for calibration of daily discharge

The outlets Takern II and Neumarkt/Raab were considered for detailed discussions since the two NO_3-N monitoring stations are assigned with the outlets Takern II and Neumarkt/Raab. The following diagrams (Figure 3.3 and Figure 3.4) show the results on a monthly time step of the hydrological calibration and validation at the outlets Takern II and Neumarkt/Raab. Additionally, the 95% probability uncertainty band (95PPU) with the upper and lower limits during the calibration period are depicted in Figure 3.3 and Figure 3.4.

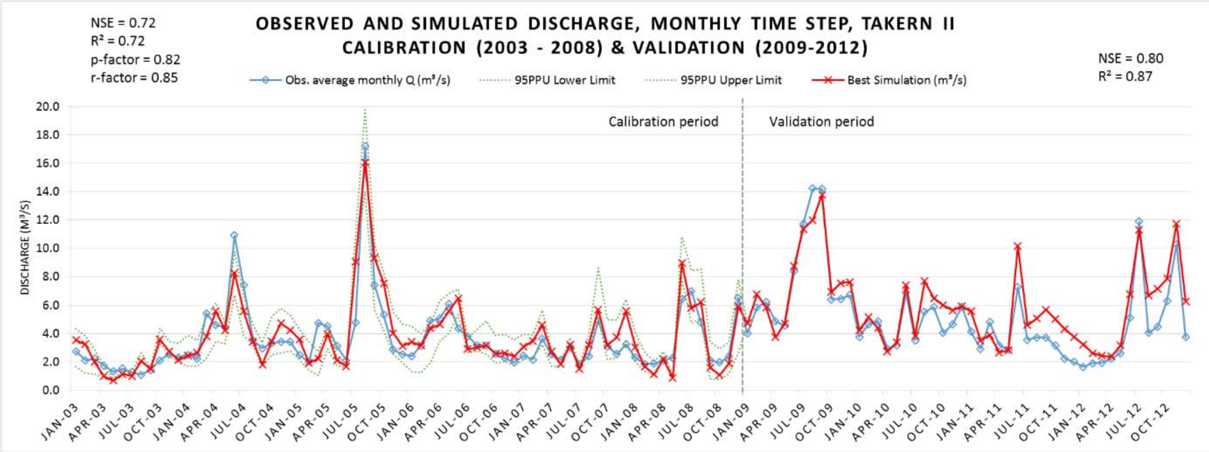

Figure 3.3: Discharge plot on a monthly time step of the observed values, the best simulation and the 95% probability uncertainty band according to auto-calibration with SUFI-2 for the outlet Takern II (calibration period 2003-2008 and validation period 2009-2012)

For both outlets Takern II and Neumarkt/Raab, the thickness of the 95PPU in the calibration period on monthly time step is much wider for low flows than for peak flow events (Figure 3.3 and Figure 3.4). Therefore, the lower flow events imply a higher model prediction uncertainty. The thickness of the 95PPU band at the outlet Takern II can be considered as relatively wide (r-factor 0.85) while the r-factor of 0.71 at the outlet Neumarkt/Raab indicate a smaller 95PPU band thickness. Further, it is notable that for both outlets almost all observed events are bracketed by the 95PPU band which is also indicated by the high p-factor of 0.83 at the outlet Neumarkt/Raab and by the p-factor of 0.82 at Takern II. Overall, the model is able to capture most peak flow events in both outlets, since all eight observed discharges events greater than 7.8 m³/s at Takern II (HJMQ, *Hydrografisches Jahrbuch* (BMLFUW 2014c)) were modeled. The eight observed discharge events greater than 12.4 m³/s at outlet Neumarkt/Raab (HJMQ, (BMLFUW 2014c)) were as well captured by the SWAT model (Figure 3.4).

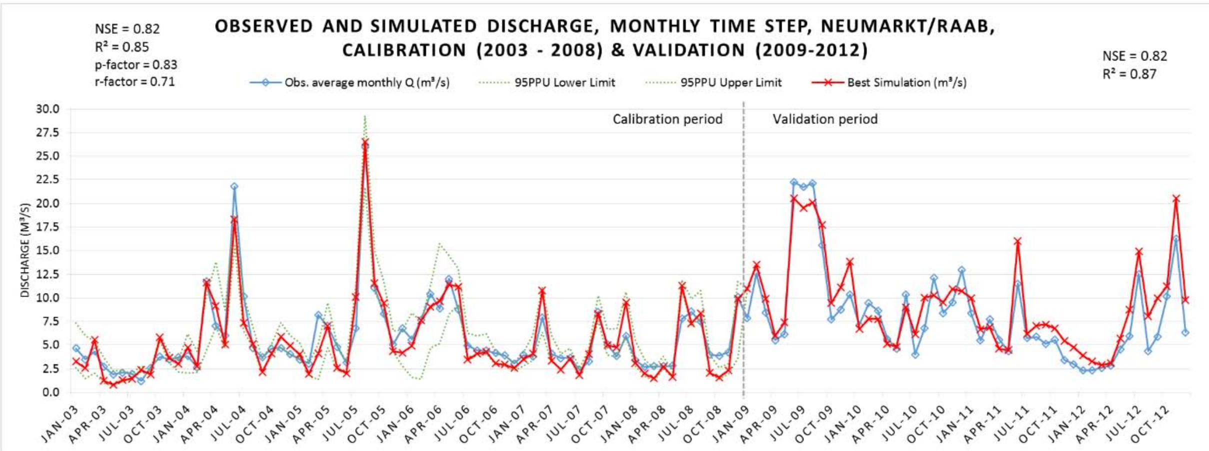

Figure 3.4: Discharge plot on a monthly time step of the observed values, the best simulation and the 95% probability uncertainty band according to auto-calibration with SUFI-2 for the outlet Neumarkt/Raab (calibration period 2003-2008 and validation period 2009-2012)

Figure 3.5 shows two correlation plots of the observed versus the simulated discharge data from 2003 to 2008 (calibration period) as well as from 2009 to 2012 (validation period) for the outlet Takern II. Both plots show a close fit of the regression line to the 1:1 line. The validation period however performs better since the majority of flow data points are closer to the 1:1 line compared to the calibration data. The same applies for the calculated NS efficiencies of both periods at Takern II (Figure 3.5); the validation period shows a better NSE (0.80) than the calibration period (NSE = 0.72).

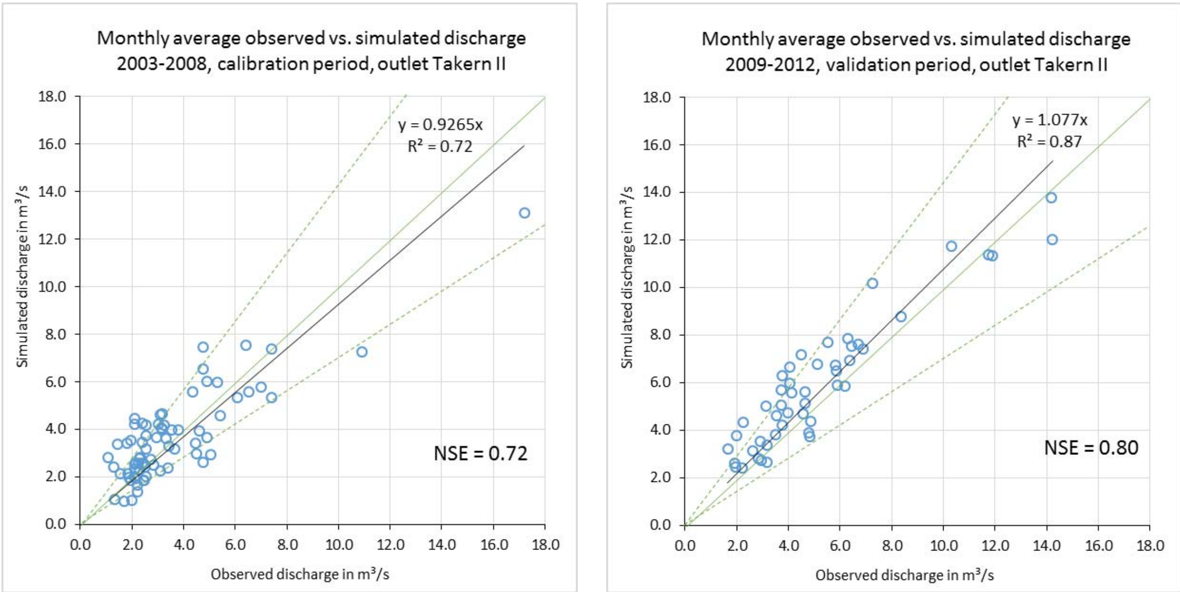

Figure 3.5: Evaluation of the observed vs. the simulated discharge data for outlet Takern II (left: calibration period 2003-2008, right: validation period 2009-2012), dashed green lines show a ±30% deviation.

Figure 3.6 shows the correlation plots of the calibrated and validated monthly values for the outlet Neumarkt/Raab. Both plots show a close fit of the regression line to the 1:1 line and present the same behavior for the calibration and validation period which is also proved by the similar NSE values (both periods have a NSE of 0.82). Notable is the good capability of the SWAT model to simulate the high peak flows (flows around 20m³/s) in the validation period.

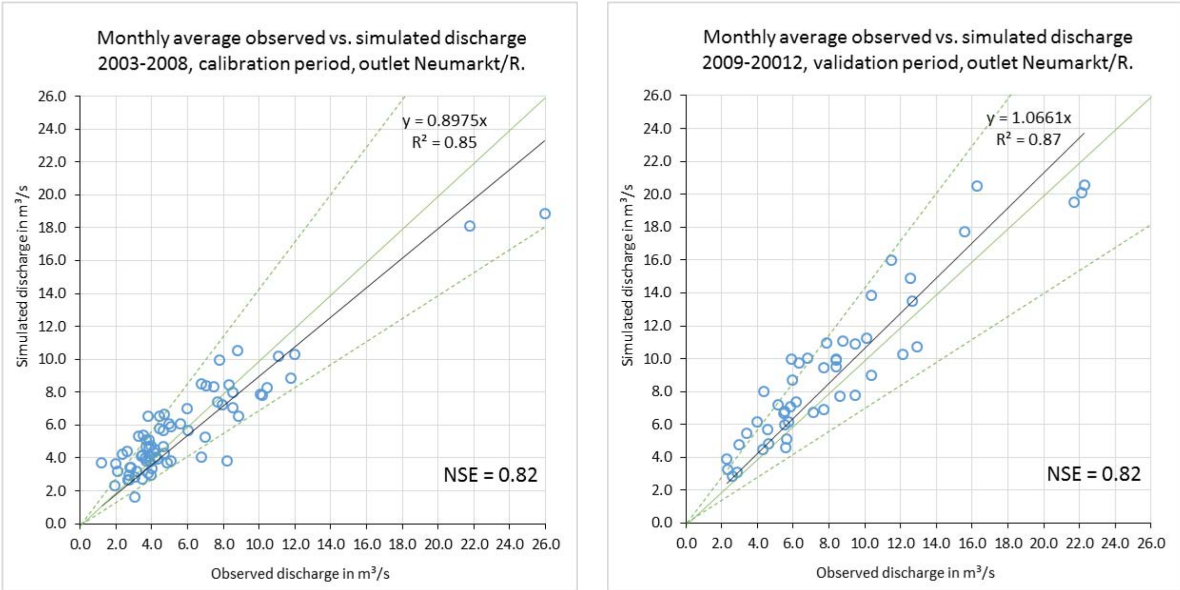

Figure 3.6: Evaluation of the observed vs. the simulated discharge data for outlet Neumarkt/Raab (left: calibration period 2003-2008, right: validation period 2009-2012), dashed green lines show a ±30% deviation.

The distribution of the observed and simulated discharge values at Takern II and Neumarkt/Raab for the calibration and validation periods are very accurate since the majority of the observed and simulated discharge values lie within the ±30% deviation range (displayed by green dashed lines in Figure 3.5 and Figure 3.6). The used ±30% deviation range is a widely accepted deviation range especially in Austrian scientific literature such as in the STOBIMO report (BMLFUW 2011).

As discussed in chapter 2.6, several statistical parameters were used to assess the goodness of model fit. Table 3.7 and Table 3.8 show an overview of the different statistical parameter with the according values for both outlets of daily and monthly calibration for the constituent discharge.

Table 3.7: Overview of NSE statistics of calibration and validation (daily and monthly time step) at outlets Takern II, Feldbach and Neumarkt/Raab for the constituent discharge

		Calibration (2003-2008)		Validation (2009-2012)	
Gauge Outlet		Daily	Monthly	Daily	Monthly
Takern II	NSE	0.64	0.72	0.56	0.80
Feldbach	NSE	0.67	0.78	0.53	0.68
Neumarkt/Raab	NSE	0.67	0.82	0.65	0.82
Total number of data points		2192 days	72 months	1461 days	48 months

Based on the model evaluation guidelines of Moriasi et al. (2007) the simulation results from the monthly calibration can be considered as *very good* at the outlets Feldbach and Neumarkt/Raab (NSE of 0.78 and 0.82); and *good* at outlet Takern II (NSE 0.72), see Table 3.7. The validation results of discharge on a monthly time step provide as well a *very good* model performance at the outlets Takern II and Neumarkt/Raab (0.80 and 0.82), while at the outlet Feldbach a *good* model performance is achieved (NSE 0.68). Due to the good model fit, the SWAT model is able to capture the most important hydrological events in Raab watershed and can be used with a reasonable confidence for further investigations. However, it is evident that the model performs significantly better for monthly calibrated discharge than for daily discharges.

Table 3.8: Overview of statistical parameters for evaluating the goodness of fit for the outlets Takern II and Neumarkt/Raab, calibration period 2003-2008, daily and monthly time step

Outlet	*NSE*	*p-factor*	*r-factor*	*R^2*	*PBIAS (%)*	*RSR*	*Mn Q_{sim}*	*Mn Q_{obs}*	*SD Q_{sim}*	*SD Q_{obs}*
					Daily time step					
Takern II	0.64	0.54	0.44	0.64	-3.5	0.60	3.66	3.53	3.47	4.10
Neumarkt/Raab	0.67	0.54	0.39	0.67	0.6	0.58	5.66	5.69	6.12	7.23
					Monthly time step					
Takern II	0.72	0.82	0.85	0.72	-3.7	0.53	3.65	3.52	1.93	2.39
Neumarkt/Raab	0.82	0.83	0.71	0.85	0.4	0.42	5.66	5.68	3.04	4.00

NSE	*Nash-Sutcliffe efficiency (Nash, Sutcliffe 1970)*
p-factor	*p-factor according to SUFI-2 algorithm (Abbaspour 2015)*
r-factor	*r-factor according to SUFI-2 algorithm (Abbaspour 2015)*
R^2	*Coefficient of determination*
PBIAS	*Percent bias*
RSR	*Ratio of root mean square error*
Mn Q_{sim}	*Mean simulated flow (m^3/s)*
Mn Q_{obs}	*Mean observed flow (m^3/s)*
SD Q_{sim}	*Standard deviation of simulated flow (m^3/s)*
SD Q_{obs}	*Standard deviation of observed flow (m^3/s)*

The R^2 values for the monthly calibration for outlets Takern II and Neumarkt/Raab are 0.72 and 0.85 which indicate a satisfying model fit. The daily calibration provides R^2 values of 0.64 and 0.67 which indicate a quite good model fit (see Table 3.8). According to Moriasi et al. (2007), the model accuracy can be considered as acceptable, since all R^2 parameters are greater than 0.5.

The PBIAS for daily calibration in the outlets Takern II and Neumarkt/Raab are -3.5% and 0.6% (Table 3.8) which indicate a *very good* model simulation (according to Moriasi et al. (2007)) with a minor overestimation model bias in Takern II and a minor model underestimation bias in Neumarkt/Raab. The PBIAS for monthly calibration range in a similar span (-3.7% and 0.4%) and in a similar tendency.

All RSR values for both outlets and for both time steps are below 0.70, consequently the model accuracy can be considered as reasonable according to Moriasi et al. (2007). The standard deviations for the simulated flow data range from 1.93 to 3.04 m³/s for the calibration period on monthly time step and for the outlets Takern II and Neumarkt/Raab.

3.6 Nitrate-Nitrogen (NO_3-N) Loads

3.6.1 NO_3-N Loads Calibration Data at outlet Neumarkt/Raab

The observed annual NO_3-N concentrations of all three data records at the gauge Neumarkt/Raab (OM Neumarkt/Raab, RM Neumarkt/Raab and GZÜV Neumarkt/Raab) show a wide variety of minimum, maximum, mean values as well as the range values and deviations as listed in Table 3.9 and Table 3.10.

The two discontinuous data records (RM Neumarkt/Raab and GZÜV Neumarkt/Raab) show smaller deviations to the mean value (deviations up to 200%, Table 3.9 and Table 3.10) as the OM Neumarkt/Raab data records (deviations up to 260%, Table 3.10). However, it must be taken into consideration that the OM Neumarkt/Raab data contain solely raw and unverified data. However, for the statistical review in Table 3.10, the observed NO_3-N concentrations with values < 0.06 mg/l or > 8.0 mg/l in the OM Neumarkt/Raab data were excluded.

Table 3.9: Observed annual NO_3-N concentrations in mg/l from GZÜV Neumarkt/Raab data series using different statistical parameters at gauge Neumarkt/Raab (2003-2012)

Year	Mean	Min	Max	Range (max-min)	Deviation to mean value (range/mean) in %
2003	3.88	2.65	5.74	3.09	79.7
2004	4.68	3.02	12.47	9.45	201.8
2005	3.47	2.44	5.08	2.64	76.1
2006	4.32	2.70	7.60	4.90	113.4
2007	3.30	1.63	5.30	3.67	111.1
2008	2.80	1.51	5.66	4.15	148.3
2009	3.36	1.97	5.19	3.22	95.8
2010	2.65	1.79	3.76	1.97	74.3
2011	2.57	1.64	3.52	1.88	73.1
2012	2.94	2.02	4.19	2.17	73.8

Table 3.10: Observed annual NO_3-N concentrations in mg/l from RM Neumarkt/Raab and (unverified and raw) OM Neumarkt/Raab data series using different statistical parameters at gauge Neumarkt/Raab (2003-2012)

Year	Mean		Min		Max		Range (max-min)		Deviation to mean value (range/mean) in %	
	a)	*b)*	*a)*	*b)*	*a)*	*b)*	*a)*	*b)*	*a)*	*b)*
2006	3.14	3.36	0.07	0.21	4.74	7.99	4.67	7.79	148.9	232.1
2007	3.26	3.54	2.01	2.09	6.20	6.30	4.20	4.22	128.7	119.1
2008	2.77	3.44	2.05	0.10	4.20	7.98	2.15	7.88	77.4	228.9
2009	2.70	3.35	1.75	0.52	3.79	5.97	2.04	5.45	75.4	162.7
2010	2.64	3.25	1.70	0.17	3.96	8.00	2.26	7.83	85.5	240.9
2011	2.47	3.02	1.25	0.07	4.96	7.99	3.71	7.92	150.2	262.7
2012	2.54	3.16	1.70	0.15	3.67	8.00	1.97	7.85	77.4	248.3

a) RM Neumarkt/Raab data;
b) OM Neumarkt/Raab – raw, unverified data (values <0.06 mg/l and >8.0 mg/l were excluded for the present statistical review)

The periodic grab samples (GZÜV and RM Neumarkt/Raab data) were taken at random times during the day; it is not clarified if the samples were adjusted to flow rates. The minimum and maximum observed NO_3-N concentrations in the RM Neumarkt/Raab data range from 1.25 to 6.20 mg/l (Table 3.10). The raw and unverified OM Neumarkt/Raab data records show significant outliers since there are measured NO_3-N concentrations > 8.0 mg/l, as depicted in Diagram 8.9 in the appendix. Due to lack of additional on-site information as well as sensor information on the precision values and effective measurement ranges of the measuring probe, a verification of the online measured data cannot be performed within the scope of this Master thesis.

The visual comparison of the observed OM, RM and GZÜV data at the outlet Neumarkt/Raab (Diagram 8.9 in the appendix) showed that the reliable and plausible NO_3-N concentrations lie in the range between 0.06 and 8 mg/l. The lower limit was set because observed concentrations <0.06 mg/l in the OM Neumarkt/Raab data show an inconsistent pattern, e.g. caused by monitoring device malfunctions. Further reason was that no observed NO_3-N concentration in the RM Neumarkt/Raab data was below 0.06 mg/l. The upper limit of 8.0 mg/l was set because the RM Neumarkt/Raab or the GZÜV Neumarkt/Raab data showed no values beyond 8.0 mg/l whereas the large outliers in the raw OM Neumarkt/Raab data (> 8.0 mg/l) occur unexpectedly, even in periods with low discharge and during dry days. These peaks have apparently no correlation with precipitation or flow volume (see Diagram 8.9, appendix). These sharp abrupt peaks are probably caused by device errors of the measuring sensor.

In general, as apparent in Diagram 8.9 (appendix), the OM Neumarkt/Raab data show in the years 2006 and 2011 after long rainfall periods (associated with an increase in the outflow) an increase and a slowly decrease of the NO_3-N concentration in the range of 0.06 to 8 mg/l, which is a good indicator for the presence of diffuse sources (nitrogen input due to agriculture).

Another possible reason for the high deviations in the online monitored data at the gauge Neumarkt/Raab may be caused by the point source pollution induced by industry along the river Raab. According to WISA (BMLFUW 2015), there are 6 registered point sources such as industry in the lower watershed area below the gauge Takern II. In the catchment above the gauge Takern II there are apart from municipal waste water treatment plants no industrial point sources such as PRTR plants, which may explain the more consistent data in online monitoring records at Takern II (Figure 3.7).

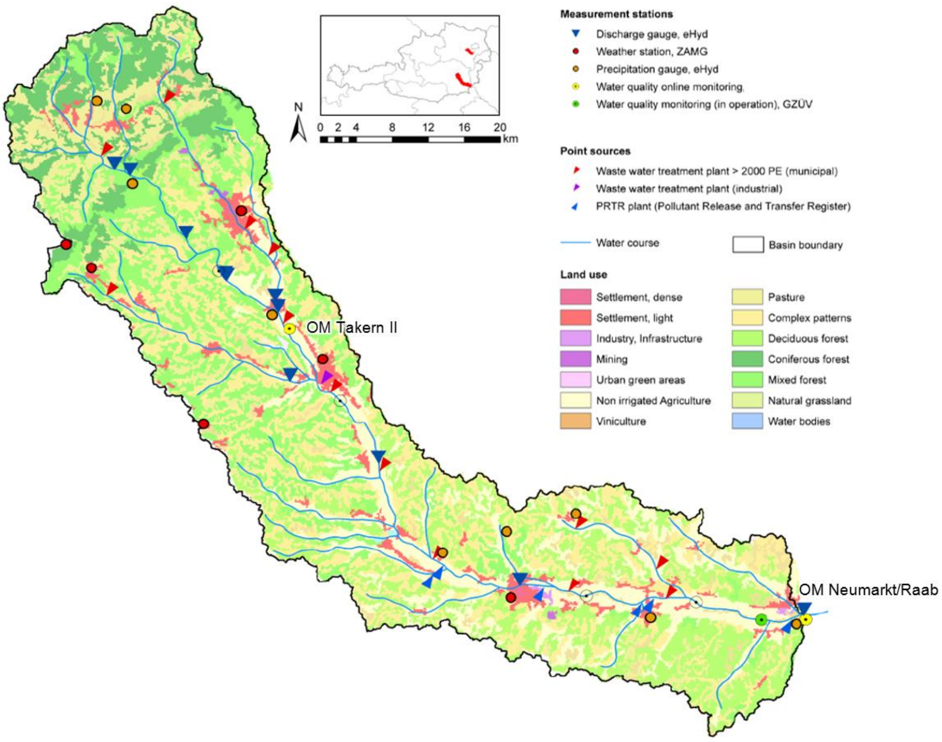

Figure 3.7: Overview of Raab watershed including locations of PRTR plants, waste water treatment plants (WWTP), the locations of the online monitoring (OM) stations Neumarkt/Raab and Takern II and the GZÜV water quality monitoring.

The raw OM Neumarkt/Raab data set was not suitable as a calibration input data set due to the unverified status, the sharp peaks in the observed data and due to the high deviations in the data records.

As an interim solution, the monthly GZÜV Neumarkt/Raab data set was used as input data for a first calibration approach, due to following reasons: (i) the GZÜV monitoring data follows standardized on-site sampling methods (as per BGBl. II (Nr. 465/2010)), (ii) the samples are evaluated in verified laboratories (BGBl. II Nr. 465/2010) and (iii) GZÜV data records are available for the entire simulation period (2003-2012) contrary to the RM Neumarkt/Raab or to the OM Neumarkt/Raab data sets (2006-2012).

3.6.2 NO_3-N Loads Calibration Data at the outlet Takern II

The water quality is monitored at the gauge Takern II with an online monitoring station in a 5 minutes time interval (referred as OM Takern II, time period 2009-2012). Due to lack of comparison data (there is no GZÜV observation station at the gauge Takern II and no reference measurement data available), the online monitoring data records neither can be verified. However, the deviation of the observed raw data in Takern II (deviation of 250%, Table 3.11) lies almost in the same deviation range as the GZÜV Neumarkt/Raab data (200%, Table 3.9). The data peaks were not excluded for the statistical review, since the visual examination of the OM Takern II data series (Diagram 8.8, appendix) show a normal and reliable pattern of observed NO_3-N concentrations. In general, the majority of observed NO_3-N concentrations in the OM Takern II data set lie in the range between 1.5 and 4.0 mg/l (sharp peaks below 1.5 mg/l were not considered).

Table 3.11: Observed annual NO_3-N concentrations in mg/l from OM Takern II data series, using different statistical parameters at gauge Takern II (2009-2012), raw and unverified data

Year	Mean	Min	Max	Range (max-min)	Deviation to mean value (range/mean) in %
2009	2.54	0.00	3.47	3.47	136.8
2010	2.76	0.00	3.99	3.99	144.5
2011	2.58	0.13	3.67	3.54	137.1
2012	2.61	0.00	6.59	6.59	252.8

3.6.3 Calibration NO_3-N Loads

Since the SWAT model simulates loads of nutrients instead of concentrations, the observed NO_3-N concentrations (mg/l) have to be converted into NO_3-N loads, which is a product of flow discharge and the corresponding NO_3-N concentration (in mg/l). The result is the NO_3-N load in weight per time unit (e.g t/month). Due to this conversion procedure, NO_3-N loads are strongly dependent on the daily or monthly discharge volume (NO_3-N loads increases proportional with the flow volume).

The calibration of NO_3-N loads at the gauge Neumarkt/Raab was performed on a monthly time step for the time period 2003-2008, with a total of 68 observed NO_3-N load values. The calibration of NO_3-N loads at the gauge Takern II was performed on a monthly basis comprising the years 2009 (Sep-Dec), 2011 and 2012, with a total of 26 observed NO_3-N load values.

The sequential calibration process was performed separately as the both outlets are hydrologically connected and therefore influencing each other. 500 simulations per iteration were run in in SWAT-CUP; one iteration was performed. Based on the sensitivity analysis, in total 7 parameters were used for the NO_3-N load calibration in SUFI-2 (see Table 3.12).

The NO_3-N load in SWAT is modeled by nitrogen related processes in the soil, such as mineralization and denitrification processes in the soil (parameters CMN and CDN, Table 3.12) (Neitsch et al. 2011). Further processes are the transport of nitrogen in soil (NPERCO) and the nitrogen uptake by roots and plants which is controlled by the parameter N_UPDIS. The main input source of nitrogen is the fertilizer application which may be controlled by the factor FRT_KG and by the fertilizer applications specified in the SWAT management input files (see chapter 3.2.1).

Another nitrogen related calibration parameters such as the concentration in rainfall (RCN), the initial concentrations of nitrogen in shallow aquifer or in the soil layer (SHALLST_N, SOL_ORGN) were insensitive and did not influence the simulation of NO_3-N loads at all.

Table 3.12 shows a list of the NO_3-N calibration parameters with the corresponding final calibration ranges determined and includes a short description to each corresponding NO_3-N calibration parameter. The validation process was not performed due to the poor model outcomes and due to the weak model accuracy in both outlets.

Table 3.12: List of the parameters adjusted during the calibration process for NO3-N with the corresponding minimum and maximum values of the calibrated parameter ranges (incl. short description of parameters)

Parameter	Description	Min	Max	Units
r__SOL_BD().sol	Moist bulk density	-0.2	0.2	mg/m³
v__SOL_NO3().chm	Initial NO3 concentration in the soil layer	22.8728	80.00	N/kg
v__CMN.bsn	Rate factor for humus mineralization of active organic nutrients (N and P)	0.0014	0.0025	-
v__CDN.bsn	Denitrification exponential rate coefficient	0	1.7078	-
r__FRT_KG.mgt	Amount of fertilizer applied to HRU	0.5	1.5	kg/ha
v__NPERCO.bsn	Nitrate percolation coefficient	0	1	-
v__N_UPDIS.bsn	Nitrogen uptake distribution parameter	0	100	-

Parameters in italics were additionally implemented for calibration of daily discharge (due to sensitivity purposes) (Arnold et al. 2012)

Figure 3.8 and Figure 3.9 show the results of the calibration of the NO_3-N loads at Takern II and at Neumarkt/Raab on a monthly time step. Additionally, the 95% probability uncertainty band (95PPU) with the upper and lower limits during the calibration period are depicted in Figure 3.8 and Figure 3.9.

The model is able to simulate the substantial NO_3-N loads in the magnitude of the observed loads at the outlet Takern II (Figure 3.8). However, the model is not able to capture the peaks of the observed NO_3-N loads within the corresponding timings. The simulated peaks show significant time lags with regards to the time points of the observed peaks at the outlet Takern II. It is notable that in Takern II the majority of observed NO_3-N loads is not bracketed by the 95PPU band (indicated by the small p-factor of 0.27), although the thickness of the 95PPU band can be considered as wide (shown by the r-factor of 1.05). In Figure 3.8, the lower limit of the 95PPU is identical with the best simulation graph.

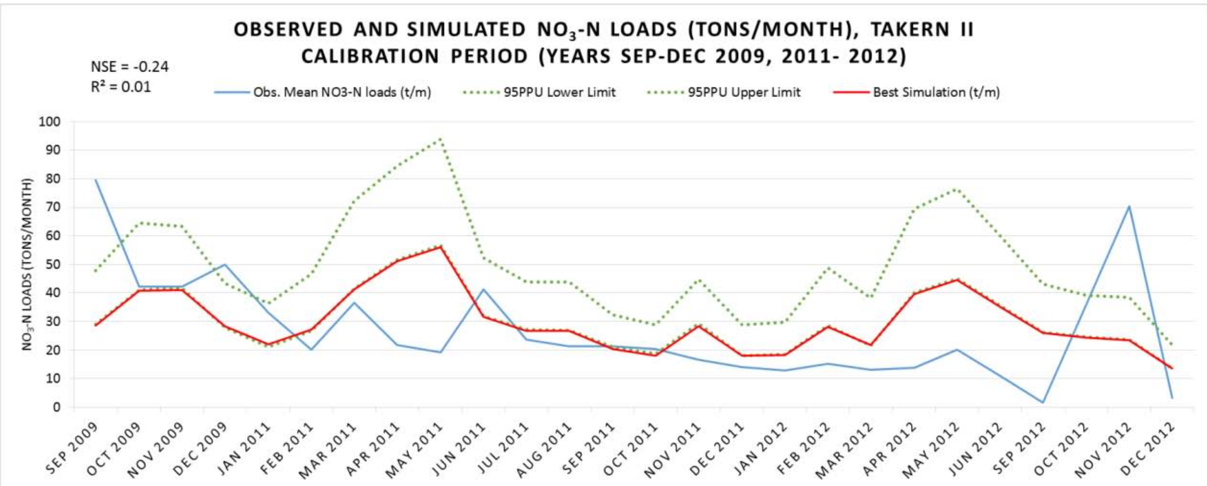

Figure 3.8: Online Monitoring- NO_3-N loads plot on a monthly time step of the observed values, the best simulation and the 95% probability uncertainty band according to auto-calibration with SUFI-2 for the outlet Takern II (calibration years Sep-Dec 2009, 2011 and 2012)

Figure 3.9 shows that the model significantly underestimated all peaks of the NO_3-N loads during the calibration period at the outlet Neumarkt/Raab. The simulated NO_3-N loads does not include any peaks (loads beyond 100 t/month) but the model is able to capture the NO_3-N loads in the range between 10 and 100 t/month (Figure 3.9). However, at the outlet Neumarkt/Raab, the thickness of the 95PPU band can be considered as slim (r-factor 0.10) for the entire calibration period. Only 36% of observed NO_3-N loads are bracketed by the 95PPU band (expressed by the low p-factor of 0.36).

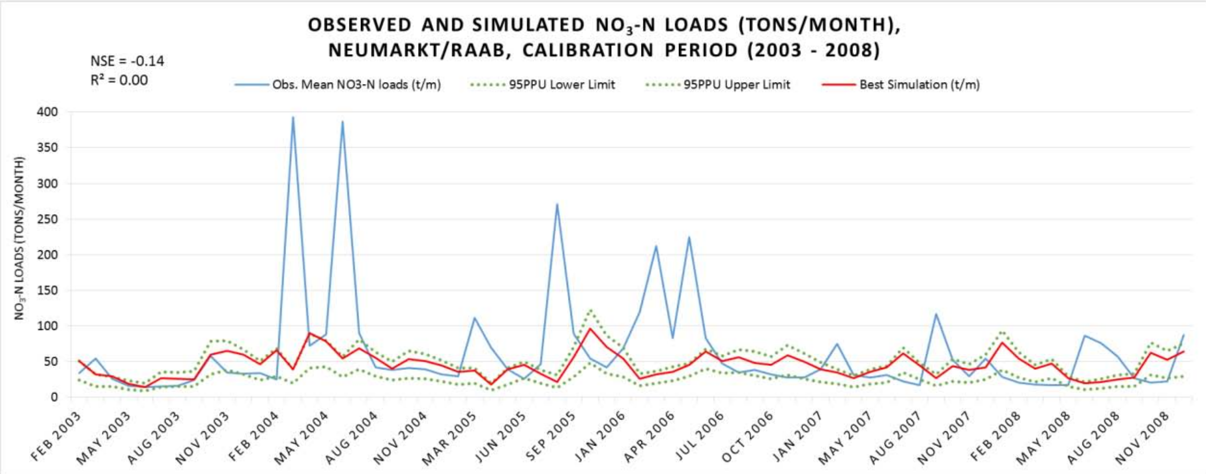

Figure 3.9: GZÜV- NO_3-N loads plot on a sub-monthly time step of the observed values, the best simulation and the 95% probability uncertainty band according to auto-calibration with SUFI-2 for the outlet Neumarkt/Raab (calibration period 2003-2008)

In general, the NO_3-N load simulation for Takern II performs better than Neumarkt/Raab since the model is able to simulate the observed loads much better at the gauge Takern II.

Figure 3.10 shows two correlation plots of the observed versus simulated NO_3-N load data for the calibration years 2009, 2011 and 2012 at the outlet Takern II and for the calibration period 2003-2008 at the outlet Neumarkt/Raab.

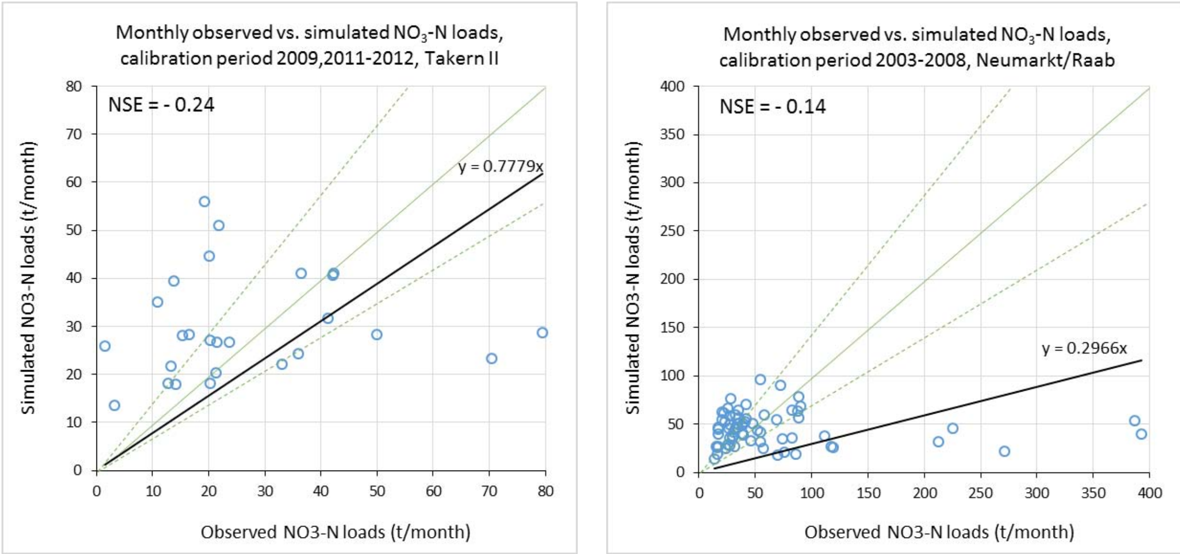

Figure 3.10: Evaluation of the observed vs. the simulated NO_3-N load data for outlets Takern II and Neumarkt/Raab (**left**: Takern II, calibration period Sep-Dec 2009, 2011-2012; **right**: Neumarkt/Raab, calibration period 2003-2008); dashed green lines show a ±30% deviation.

According to Figure 3.10, the simulation at the outlet Neumarkt/Raab shows a very poor fit of the regression line to the 1:1 line. The simulated NO_3-N loads are hardly captured by the ±30% deviation ranges, it seems that the majority of simulated NO_3-N loads lie beyond the ±30% deviation (Figure 3.10, dashed green line, diagram on right side). The distribution of Takern II data points seems to be more accurate since approximately the half of data points are within the ±30% deviation ranges (Figure 3.10, left side). Notable is the better NSE value of -0.14 in Neumarkt/Raab compared to Takern II, although it is obviously that the regression lines and the ±30% deviation ranges indicate better performance ratings for Takern II (NSE= -0.24). A possible reason is, that the NSE as an objective function applies a higher weight on peak events during the calibration period in order to make the model more reliable in estimating the peaks (Abbaspour 2015). Since the peaks in Takern II are simulated with a time lag (wrong peak prediction results in a lower NSE value) and the time series of Takern II contains fewer observed NO_3-N loads (the lower the data point number, the higher the weight on one inappropriate simulated peak), the NSE results in a lower value for Takern II (NSE= -0.24). The negative NSE values of -0.24 and -0.14 for both outlets indicate an unacceptable model performance for NO_3-N load estimation, as the NSE values are lower than 0.0.

Table 3.13 shows an overview of the different statistical parameters based on a monthly time step with the according values for both outlets.

Table 3.13: Overview of statistical parameters for evaluating the goodness of fit of the NO_3-N load simulation for the outlets Takern II and Neumarkt/Raab, calibration period, monthly time step

Outlet	*NSE*	*p-factor*	*r-factor*	*R^2*	*PBIAS (%)*	*RSR*	*Mn NO_3N_{sim}*	*Mn NO_3N_{obs}*	*SD NO_3N_{sim}*	*SD NO_3N_{obs}*
Takern II	-0.24	0.27	1.05	0.01	-11.5	1.11	30.01	26.92	10.52	18.40
Neumarkt/Raab	-0.14	0.56	0.38	0.00	29.5	1.07	45.20	64.15	17.27	73.76

NSE	*Nash-Sutcliffe efficiency (Nash, Sutcliffe 1970)*
p-factor	*p-factor according to SUFI-2 algorithm (Abbaspour 2015)*
r-factor	*r-factor according to SUFI-2 algorithm (Abbaspour 2015)*
R^2	*Coefficient of determination*
PBIAS	*Percent bias*
RSR	*Ratio of root mean square error*
Mn NO_3N_{sim}	*Mean simulated NO_3-N loads (t/month)*
Mn NO_3N_{obs}	*Mean observed NO_3-N loads (t/month)*
SD NO_3N_{sim}	*Standard deviation of simulated NO_3-N loads (t/month)*
SD NO_3N_{obs}	*Standard deviation of observed NO_3-N loads (t/month)*

The R^2 values for the calibration of NO_3-N loads on a monthly time step at outlets Takern II and Neumarkt/Raab are 0.01 and 0.00, respectively (Table 3.13) which indicate a very poor prediction accuracy, since the values are very close to 0.0. According to Moriasi et al. (2007), the model accuracy has to be considered as unacceptable, if all R^2 parameters are below 0.5.

The optimal value of PBIAS is 0.0 which indicate accurate model simulation (Moriasi et al. 2007). The PBIAS for the monthly calibration of NO_3-N loads in the outlets Takern II and Neumarkt/Raab are –11.5% and 29.5% (Table 3.13) which indicate a model simulation with a minor model overestimation bias in Takern II respectively a model underestimation bias in Neumarkt/Raab. According to Moriasi et al. (2007), the PBIAS performance rating for the outlet Neumarkt/Raab can be considered as *good* since the PBIAS lies in the range between 25-40 %.

The RSR values of both outlets (1.11 and 1.07, see Table 3.13) are beyond 0.70, consequently the model accuracy of the NO_3-N load simulation has to be considered as inappropriate. The standard deviations for the simulated NO_3-N loads range from 10.52 to 17.27 t/month for the outlets Takern II and Neumarkt/Raab (Table 3.13). Notable is the large standard deviation for the observed loads of 73.76 t/month at the outlet Neumarkt/Raab, which is very high compared to the standard deviation of Takern II (18.40 t/month).

3.6.4 Discussion Calibration NO_3-N Loads

Of particular importance in analyzing the NO_3-N simulation are the total applied nitrogen fertilizer and NO_3-N losses due to the plant uptake or denitrification in the SWAT model (Neitsch et al. 2011). When analyzing the SWAT output files, the initial annual organic nitrogen in the soil and the final annual soil organic nitrogen loads show similar values (21.3 kg/ha and 21.1 kg/ha) which indicates an appropriate fertilizer application of the crop needed organic nitrogen. However, the average simulated annual initial inorganic NO_3-N load in the soil is 49.0 kg/ha for the entire Raab watershed while the final annual simulated inorganic NO_3-N load in the soil amounts to 18.5 kg/ha which may indicate an under-fertilization during the simulation.

It is not clear if the total applied nitrogen fertilizer plus the NO_3-N losses due to plant uptake affect the total NO_3-N loads at the outlet Neumarkt/Raab of the Raab catchment, or if the lack of point sources is crucial for simulating the missing NO_3-N loads in the Raab watershed. A possible reason for the more accurate estimation of NO_3-N loads at the outlet Takern II may be the small fraction of agricultural areas in the Raab catchment, since in the upper basin area above the outlet Takern II only 13% of the land use area is cultivated by farmers. On the other hand, in the lower river basin area above the outlet Neumarkt/Raab, 37% of the land cover is cultivated by farmers: The simulated average NO_3-N load at the lower outlet Neumarkt/Raab (45.20 t/month) is only increased by 50% compared to the simulated average NO_3-N loads in the upper basin area at Takern II (30.01 t/month) while the average monthly observed NO_3-N load is increased by approximately 130% at the outlet Neumarkt/Raab (observed mean NO_3-N load of 64.15 t/month at Neumarkt/Raab; observed mean NO_3-N load of 26.92 t/month at Takern II, Table 3.13). An intensified fertilizer application due to the higher agricultural usage in the lower river basin area may explain the larger observed NO_3-N load values at the outlet Neumarkt/Raab.

For the years 2009-2012, the observed mean annual NO_3-N concentrations at Takern II (2.65 mg/l) are lower than the observed annual mean NO_3-N concentrations in Neumarkt/Raab (3.0 mg/l). Here the question still remains open, to which proportion the diffuse sources (agricultural usage) respectively the point sources (such as industry waste water inlet) amount to the nitrogen pollution in the SWAT model of the Raab catchment. However, the nitrate report (BMLFUW 2012a) states, that in Austria four fifths (80%) of the nitrogen emissions input stems from diffuse sources (such as agriculture and its fertilizer application) and the remaining one fifth (20%) originates from point sources (such as industry and waste water treatment plants). Considering the 20% fraction of point sources, the influence of implementing the point sources on the NO_3-N pollution in the Raab watershed may be minor, although the Raab catchment shows a very specific situation due to the strongly industrialized river basin (see chapter 1.2).

4 Summary and Conclusion

The objective of this Master thesis was the implementation of a calibrated SWAT model in the Raab watershed. The simulation comprises the hydrological model of flow and the calculation of NO_3-N loads. The calibration of the hydrological model and the simulation of NO_3-N loads was carried out in a sequential procedure. The model accuracy as well as the uncertainty ranges of flow and NO_3-N load simulation were determined by means of the 95% prediction uncertainty bands. The findings of this Master thesis should be used for further investigations of NO_3-N load modelling.

The study area covers an area of 988.16 km^2 which was subdivided into 30 subbasins with a total of 665 HRUs. Five discharge gauges for calibration and validation of flow were available in the Raab watershed. Two water quality monitoring stations (for parameters such as NO_3-N) at Takern II and Neumarkt/Raab were existent in the study area. The simulation period was set from the year 2003 to 2012, with a calibration period from 2003 to 2008 (6 years) and a validation period from 2009-2012 (4 years).

The calibration and validation of the hydrological model for the Raab catchment was performed in a sequential calibration procedure with the SUFI-2 algorithm. The calibrated NSE values for the outlets Takern II and Neumarkt/Raab on a monthly time step were 0.72 and 0.82 which is considered as a very good model performance. The validation period on a monthly time step provided as well a very good model performance since the validated NSE were 0.80 at the outlet Takern II and 0.82 at the outlet Neumarkt/Raab. Particular attention was paid to quantify the 95% prediction uncertainty during the calibration period on a monthly time step which turned out to be satisfactorily as the p-factor and the r-factor at the outlet Neumarkt/Raab were 0.82 and 0.71, respectively.

The simulation of NO_3-N loads showed a very poor and inappropriate model performance. A validation of the NO_3-N load simulation was not performed due to weak model performance. The calibration of NO_3-N loads on a monthly time step showed that the model has serious problems to model the NO_3-N loads at the outlets Takern II (NSE= -0.24) and Neumarkt/Raab (NSE= -0.14) in a satisfactory way. The 95% prediction uncertainty of the NO_3-N loads turned out to be large at the outlets Takern II and Neumarkt/Raab. In general, the simulation of NO_3-N load peaks in the Raab watershed was clearly underestimated, especially at the outlet Neumarkt/Raab.

A main problem was the unverified inappropriate online monitored input data (OM Neumarkt/Raab) at the outlet Neumarkt/Raab. The GZÜV Neumarkt/Raab data was more suitable as a reference data set for the calibration of NO_3-N loads but was only available on a monthly time step. For the outlet Takern II, the unverified but useful online monitoring data (OM Takern II) was used as a reference data set for calibration of the NO_3-N loads. Another problem was the lack of input data to simulate point source pollution in the SWAT model.

For further study research in the Raab watershed and for an appropriate simulation of the NO_3-N loads, an extensive verification of monitored data is recommended. A possible relationship between observed NO_3-N concentrations and discharge volumes must be examined. Additionally, the point sources as SWAT input data have to be prepared properly from all waste water treatment plants in the required format of loads since the SWAT model only accepts input data in terms of load volumes (and not in terms of concentrations). Point sources are e.g. industry related waste water or outflow by waste water treatment plants. The consideration of additional point source may improve the model prediction of NO_3-N loads. However, it is unclear, to which degree the applied nitrogen fertilizer, the nitrogen losses due to plant uptake and the applied crop types affect the simulation of NO_3-N loads especially in the Raab catchment.

The used fertilizer application (diffuse nitrogen sources) was based on best-practice literature data. Hence, the applied fertilizer amounts may be underestimated in the SWAT model. Expanded research of the actual fertilizer application in the Raab watershed is recommended. The model implementation of NO_3-N simulation cannot be considered as completed. Therefore, the findings of following research, especially nitrogen point sources and nitrogen diffuse sources, should be considered in the SWAT model in future. Hopefully the prospective calibration and validation of NO_3-N loads based on the improved input data sets will be more successful when the NO_3-N data has been verified.

5 References

Abbaspour, K. C. (2015): SWAT-CUP. SWAT Calibration and Uncertainty Programs. A User Manual. Swiss Federal Institute of Aquatic Science and Technology.

Abbaspour, K. C.; Johnson, C. A.; van Genuchten, M. Th. (2004): Estimating Uncertain Flow and Transport Parameters Using a Sequential Uncertainty Fitting Procedure. In *Vadose Zone Journal* 3 (4), pp. 1340–1352. DOI: 10.2113/3.4.1340.

Abbaspour, K. C.; Rouholahnejad, E.; Vaghefi, S.; Srinivasan, R.; Yang, H.; Kløve, B. (2015): A continental-scale hydrology and water quality model for Europe. Calibration and uncertainty of a high-resolution large-scale SWAT model. In *Journal of Hydrology* 524, pp. 733–752. DOI: 10.1016/j.jhydrol.2015.03.027.

Abbaspour, K. C.; Yang, J.; Maximov, I.; Siber, R.; Bogner, K.; Mieleitner, J. et al. (2007): Modelling hydrology and water quality in the pre-alpine/alpine Thur watershed using SWAT. In *Journal of Hydrology* 333 (2-4), pp. 413–430. DOI: 10.1016/j.jhydrol.2006.09.014.

AGES (2015a): Österreichische Beschreibende Sortenliste 2015 Landwirtschaftliche Pflanzenarten. ISSN 1560-635X (Schriftenreihe 21/2015).

AGES (2015b): Zuckerrüben ein- und mehrjährige Wertprüfung 2011-2014. ISSN 1560-635X. With assistance of Josef Rieppl. Institut für Nachhaltige Pflanzenproduktion. Wien (Schriftenreihe 4/2015).

Andersson, I.; Petersson, M.; Jarsjö, J. (2012): Impact of the European Water Framework Directive on local-level water management. Case study Oxunda Catchment, Sweden. In *Land Use Policy* 29 (1), pp. 73–82. DOI: 10.1016/j.landusepol.2011.05.006.

Arnold, J. G.; Allen, P. M.; Muttiah, R.; Bernhardt, G. (1995): Automated Base Flow Separation and Recession Analysis Techniques. In *Ground Water* 33 (6), pp. 1010–1018. DOI: 10.1111/j.1745-6584.1995.tb00046.x.

Arnold, J. G.; Kiniry, J. R.; Srinivasan, R.; Williams, J. R.; Haney, E. B.; Neitsch, S. L. (2012): Input/Output Documentation Version 2012. Texas Water Resources Institute. TR-439. Texas.

Arnold, J. G.; Srinivasan, R.; Muttiah, R. S.; Williams, J. R. (1998): Large area hydrologic modeling and assessment part I. model development. In *Journal of the American Water Resources Association* 34 (1), pp. 73–89. DOI: 10.1111/j.1752-1688.1998.tb05961.x.

Bavec, F.; Gril, L.; Grobelnik-Mlakar, S.; Bavec, M. (2002): Seedlings of oil pumpkins as an alternative to seed sowing: yield and production costs. Ölkürbis-Jungpflanzen als Alternative zur Aussaat: Ertrag und Produktionskosten (53 (1)), pp. 39–43.

BGBl. II Nr. 465/2010: Gewässerzustandsüberwachungsverordnung – GZÜV 14.12.2006. 479. Verordnung des Bundesministers für Land- und Forstwirtschaft, Umwelt und Wasserwirtschaft über die Überwachung des Zustandes von Gewässern (Gewässerzustandsüberwachungsverordnung – GZÜV), revised BGBl. II Nr. 465/2010 2006.

BMLFUW (2010): Anpassungsstrategien an den Klimawandel für Österreichs Wasserwirtschaft - Kurzfassung. Studie der ZAMG und der TU Wien im Auftrag von Bund

und Ländern. With assistance of W. Schöner, R. Böhm, K. Haslinger, G. Blöschl, R. Merz, A. P. Blaschke et al. Wien.

BMLFUW (2011): Stoffbilanzmodellierung für Nährstoffe auf Einzugsgebietsebene als Grundlage für Bewirtschaftungspläne und Maßnahmenprogramme (STOBIMO-Nährstoffe). Endbericht. Im Auftrag des BMLFUW - Sektion VII BMLFUW-UW.3.1.2/0029-VII/1/2008. With assistance of O. Gabriel, A. Kovacs, S. Thaler, M. Zessner, G. Hochedlinger, C. Schilling, G. Windhofer. Wien.

BMLFUW (2012a): EU Nitratrichtlinie 91/676/EWG Österreichischer Bericht 2012. Gemäß Artikel 10 der Richtlinie 91/676/EWG zum Schutz von Gewässern vor der Verunreinigung durch Nitrat aus landwirtschaftlichen Quellen über den Zeitraum 2007 - 2011. Wien.

BMLFUW (2012b): Schaum auf der Raab. Wien.

BMLFUW (2014a): Die Raab: Wasserinformationssystem Austria - WISA. Fachthema - Die Raab. Wien. Available online at http://wisa.bmlfuw.gv.at, checked on 4/8/2016.

BMLFUW (2014b): eHYD – der Zugang zu hydrographischen Daten Österreichs. Wien. Available online at http://ehyd.gv.at/, checked on 4/23/2016.

BMLFUW (2014c): Hydrografisches Jahrbuch von Österreich 2012. 120. Band Hydrografischer Dienst in Österreich. Wien.

BMLFUW (2015): Wasserinformationssystem Austria - WISA. Wien. Available online at http://wisa.bmlfuw.gv.at/wasserkarten/gewaesserbewirtschaftungsplan-2015/fluesse_und_seen/ngp_owk.html#, checked on 4/8/2016.

Brown, L.C.; Barnwell, T.O. Jr. (1987): The Enhanced Water Quality Models QUAL2E and QUAL2E-UNCAS: Documentation and User Manual. EPA (EPA/600/3-87/007).

EC (2000): Directive 2000/60/EC of the European Parliament and of the Council, Water Framework Directive. WFD, checked on 3/22/2016.

EEA (2015): Corine Land Cover 2006 raster data — European Environment Agency. Version 17 (12/2013). Available online at http://www.eea.europa.eu/data-and-maps/data/corine-land-cover-2006-raster-3, checked on 4/7/2016.

ESRI Inc. (2012): ArcGIS 10.1 SP1 for Desktop. Esri ArcMap 10.1. Version Build 3143.

Fuiko, R.; Kornfeind, L.; Schilling, K.; Winkelbauer, A. (2014): Nachhaltige Wassergütewirtschaft Raab, Online - Monitoring, Endbericht, Berichtsjahr 2013. Wien.

Geoland.at (2015): Digitales Geländemodell (DGM) Österreich - data.gv.at. OGD Austria Metadata 2.1. Land Kärnten; http://www.geoland.at, checked on 4/19/2016.

Green, W. H.; Ampt, G. A. (1911): Studies on Soil Phyics. The flow of air and water through soils. In *J. Agric. Sci.* 4 (1), pp. 11–24. DOI: 10.1017/S0021859600001441.

Gupta, H.; Sorooshian, S.; Yapo, P. (1999): Status of Automatic Calibration for Hydrologic Models: Comparison with Multilevel Expert Calibration. In *J. Hydrologic Eng.* (4(2)), pp. 135–143.

Haiden, T.; Kann, A.; Wittmann, C.; Pistotnik, G.; Bica, B.; Gruber, C. (2010): The Integrated Nowcasting through Comprehensive Analysis (INCA) System and Its Validation over the Eastern Alpine Region. In *Wea. Forecasting* 26 (2), pp. 166–183. DOI: 10.1175/2010WAF2222451.1.

Herrnegger, M. (2013): Zeitlich hochaufgelöste inverse Modellierung von Gebietsniederschlägen aus Abflussmessungen. Dissertation zur Erlangung des Doktorgrades an der Universität für Bodenkultur Wien. BOKU Wien, Wien. Institut für Wasserwirtschaft, Hydrologie und konstruktiven Wasserbau.

ISRIC (2013): ISRIC World Soil Information. SoilGrids: an automated system for global soil mapping. SoilGrids1km visualisation and distribution website. ISRIC. Available online at http://soilgrids.org/.

Jha, M.; Gassman, P. W.; Secchi, S.; Gu, R.; Arnold, J. (2004): Effect of watershed subdivision on SWAT flow, sediment, and nutrient predictions. In *J Am Water Resources Assoc* 40 (3), pp. 811–825. DOI: 10.1111/j.1752-1688.2004.tb04460.x.

Knisel, W. G. (1980): CREAMS: a field scale model for Chemicals, Runoff, and Erosion from Agricultural Management Systems. United States. Science and Education Administration.

LAKO (2015): Landwirtschaftliche Bildung in NÖ - Versuche. Versuchsberichte. Amt der NÖ Landesregierung Abteilung Landwirtschaftliche Bildung (LF2) - Landwirtschaftliche Koordinationsstelle für Bildung und Forschung.

Lam, Q. D.; Schmalz, B.; Fohrer, N. (2010): Modelling point and diffuse source pollution of nitrate in a rural lowland catchment using the SWAT model. In *Agricultural Water Management* 97 (2), pp. 317–325. DOI: 10.1016/j.agwat.2009.10.004.

Land Steiermark: Die Hochwasserereignisse im August 2005 (Teil 1). Graz.

Land Steiermark (2015): Wasserversorgungsplan Steiermark 2015. Ein Leitfaden für die öffentliche Wasserversorgung. Abteilung 14 - Wasserwirtschaft, Ressourcen und Nachhaltigkeit. Graz.

Leonard, R. A.; Knisel, W. G.; Still, D. A. (1987): GLEAMS. Groundwater Loading Effects of Agricultural Management Systems. In *Transactions of the ASAE* 30 (5), pp. 1403–1418. DOI: 10.13031/2013.30578.

LK NÖ (2009): Sojabohne (Glycine max.). With assistance of F. Lembacher, J. Schmiedl, J. Wasner. St. Pölten.

LK Österreich: Obsternte 2013 in Österreich. Wien.

Mehdi, B.; Lehner, B.; Gombault, C.; Michaud, A.; Beaudin, I.; Sottile, M.-F.; Blondlot, A. (2015a): Simulated impacts of climate change and agricultural land use change on surface water quality with and without adaptation management strategies. In *Agriculture, Ecosystems & Environment* 213, pp. 47–60. DOI: 10.1016/j.agee.2015.07.019.

Mehdi, B.; Ludwig, R.; Lehner, B. (2015b): Evaluating the impacts of climate change and crop land use change on streamflow, nitrates and phosphorus. A modeling study in Bavaria. In *Journal of Hydrology: Regional Studies* 4, pp. 60–90. DOI: 10.1016/j.ejrh.2015.04.009.

Mein, R. G.; Larson, C. L. (1973): Modeling infiltration during a steady rain. In *Water Resour. Res.* 9 (2), pp. 384–394. DOI: 10.1029/WR009i002p00384.

Moriasi, D. N.; Arnold, J. G.; Van Liew, M. W.; Bingner, R. L.; Harmel, R. D.; Veith, T. L. (2007): Model Evaluation Guidelines for Systematic Quantification of Accuracy in Watershed Simulations. In *Transactions of the ASABE* 50 (3), pp. 885–900. DOI: 10.13031/2013.23153.

Nash, J. E.; Sutcliffe, J. V. (1970): River flow forecasting through conceptual models part I — A discussion of principles. In *Journal of Hydrology* 10 (3), pp. 282–290. DOI: 10.1016/0022-1694(70)90255-6.

Neitsch, S. L.; Arnold, J. G.; Kiniry, J. R.; Williams, J. R. (2011): Soil and Water Assessment Tool Theoretical Documentation Version 2009. (No. Technical Report No. 406). Texas Water Resources Institute, Temple. Texas.

Rouholahnejad, Elham; Abbaspour, Karim C.; Srinivasan, Raghvan; Bacu, Victor; Lehmann, Anthony (2014): Water resources of the Black Sea Basin at high spatial and temporal resolution. In *Water Resour. Res.* 50 (7), pp. 5866–5885. DOI: 10.1002/2013WR014132.

Ruzicka, Katerina; Gabriel, Oliver; Bletterie, Ulrike; Winkler, Stefan; Zessner, Matthias (2009): Cause and effect relationship between foam formation and treated wastewater effluents in a transboundary river. In *Physics and Chemistry of the Earth, Parts A/B/C* 34 (8-9), pp. 565–573. DOI: 10.1016/j.pce.2009.01.002.

Schulz, K. (2014): UnLoadC³. Uncertainty assessment of water flow and nutrient loads under future climate change conditions. Publizierbarer Zwischenbericht. Wien.

Schürz, C.; Mehdi, B.; Schulz, K. (2016): A simple rule based model for scheduling farm management operaons in SWAT. Institute of Water Management, Hydrology and Hydraulic Engineering, BOKU Vienna. Vienna.

Statistik Austria (2015a): Einwohnerzahl 1.1.2015 nach Gemeinden, Gebietsstand 1.1.2015. Wien.

Statistik Austria (2015b): Obsternte Jahre 2012-2013. Wien. Available online at http://www.statistik-austria.at, checked on 11/19/2015.

Statistik Austria (2015c): STATCube - Statistische Datenbank von STATISTIK AUSTRIA: Agrarstrukturerhebung 2010 - Bodennutzung - data.statistik.gv.at, checked on 6/6/2015.

TBS Waterconsult (2015): Datensatz des Wasserqualitäts-Onlinemoning an der Raab, Messstelle Kraftwerk Takern II, betrieben von TBS WaterConsult, Dateneigentum: BMLFUW. Wien. Available online at http://www.onlinemonitoring.at/Projekte/Raab/Detail.htm, checked on 4/23/2016.

Ullrich, Antje; Volk, Martin (2010): Influence of different nitrate–N monitoring strategies on load estimation as a base for model calibration and evaluation. In *Environ Monit Assess* 171 (1-4), pp. 513–527. DOI: 10.1007/s10661-009-1296-8.

Umweltbundesamt (2014): Wasservorkommen in Österreich. Wien.

Versuchsreferat Steiermark (2013): Ölkürbis 2010 bis 2012: Sorten- und Reihenweitenversuch. Versuchsbericht 2012. Amt der Steiermärkischen Landesregierung – Abteilung 6. Hatzendorf.

Williams, J. R. (1975): Sediment routing for agricultural watersheds. In *Water Resources Bulletin* 11 (5), pp. 965–974. DOI: 10.1111/j.1752-1688.1975.tb01817.x.

Williams, J. R.; Jones, C. A.; Dyke, P. T. (1984): A Modeling Approach to Determining the Relationship Between Erosion and Soil Productivity. In *Transactions of the ASAE* 27 (1), pp. 129–144. DOI: 10.13031/2013.32748.

Winchell, M.; Srinivasan, R.; Di Luzio, M.; Arnold, J. (2013): ArcSWAT Interface for SWAT2012. User's Guide. Texas.

ZAMG (2015): Ausgewählte Stationsdaten der klimatischer Parameter; betrieben von der Zentralanstalt für Meteorologie und Geodynamik (ZAMG). Available online at http://www.zamg.ac.at, checked on 4/19/2016.

6 List of Figures

7 List of Tables

8 Appendix

8.1 Overview of the acquired data sets for Raab catchment

Overview of the catchment characteristics data sets acquired for building up the water quantity and water quality models.

Data content	Data source	Type
Digital elevation map (DEM) Extent covering whole Austria at a resolution of 1 are (10m x 10m).	Laserscan Geoland.at (2015)	GeoTIFF, raster format
Soil map 1. SoilGrids1km: Worldwide dataset holding soil properties such as soil fractions, bulk density, organic carbon, etc. at a 1 km x 1km resolution and in 6 layers.	ISRIC – World Soil Information (2013)	GeoTIFF, raster format
Land use CORINE Land use land cover map: European wide data set classifying the land surface into 44 land uses, such as continuous/discontinuous urban fabric, non-irrigated arable land, etc. The spatial resolution is 100m x 100m, whereas the lower threshold for assigning a class to an area is 25ha.	EEA (2015)	GeoTIFF, raster format
Tabular crop data on municipality level holding the cultivated area per crop for the year 2010.	Statistik Austria (2015c)	Tabular
Management practices Management practices obtained from the field experiments, carried out by the Landwirtschaftliche Schulen NÖ	LAKO (2015)	Tabular
Additional management information provided by the Landwirtschaftskammer NÖ and “Versuchsreferat Steiermark” (for crop OELK)	LK NÖ (2009) Versuchsreferat Steiermark (2013)	Tabular
Management information for the crop class SGBT was obtained from the AGES	(AGES 2015b)	Tabular

Overview of available input- and calibration/validation data sets.

Data content	Data source	Type
Meteorological data		
Sub daily time series (15 minute interval) of precipitation and min.& max. temperature.	INCA dataset (Haiden et al. 2010)	georeferenced location tables
Solar radiation, mean relative humidity and mean wind velocity for several station points over long time periods (+10 years)	ZAMG (2015)	georeferenced location tables
Discharge		
Time series of mean daily discharge for several station points (over long time periods (+10 years)	eHYD (BMLFUW 2014b)	georeferenced location tables
Water quality		
1. 5 minute interval time series for Nitrogen for the years 2006 to 2014 (Neumarkt a.d. Raab, TU Vienna) and 2009 to 2013 (KW Takern II, TBS Consult) in the Raab catchment.	iwr TU Vienna (Fuiko et al. 2014), TBS Waterconsult (2015)	georeferenced location tables
2. Sampling data on monthly basis according to the surveillance monitoring in Austria (GZÜV) holding several water quality parameters.	WISA database (BMLFUW 2014a)	georeferenced location tables

8.2 Results of management practices collected from literature research (field studies)

SWHT- Summerwheat

Durum, Sommerweizen

Anbau	Ernte	Pflug 1	Saatbettkomb	Ertrag tha	Düngung					
15.3.2010	28.7.2010		13.3.2010	6.04	10.3.2010	50 kg N/ha in	30.4.2010	50 kg N	29.5.2010	40 kg N
15.3.2011	16.7.2011	25.11.2010	11.3.2011	6.04	14.3.2011	50 kg N/ha in	2.5.2011	40kg N	25.52011	50 kg N
12.3.2012	18.7.2012	6.11.2011	9.3.2012	5.26	7.3.2012	50 kg N/ha in Form von NAC (27:0:0)				
11.3.2013	30.7.2013	12.11.2012	11.3.2013	6.12		50		40		50
18.3.2010	2.8.2010	Herbst	11.3	5.7	8.3.2010	170 kg/ha NA	9.3.2010	250 kg/ha DC	7.6.2010	185 kg/ha NAC
11.3.2011	3.8.2011	Herbst	7.3.2011	5.9	3.3.2011	330 kg 17:15:	20.4.2011	150 kg/ha NA	30.5.2011	100 kg NAC

Sommergerste

Anbau	Ernte	Pflug 1	Saatbettkomb	Ertrag tha	Düngung			
11.3.2011	19.7.2001	Herbst	7.3.2011	6.6	3.3.2011	330 kg (17:15:	20.4.2011	150 kg NAC
15.3.2011	9.7.2011	25.11.2010	11.3.2011	6.01	14.3.2011	50 kgN in Form von NAC (27:0:0)		
10.3.2015	16.7.2015	11.11.2014	10.3.2015	7	9.3.2015	50 kgN in Form von NAC (27:0:0)		
5.3.2014	15.7.2014	4.12.2013	3.3.2014	6.7	3.3.2014	50 kgN in Form von NAC (27:0:0)		
12.3.2012	7.7.2012	14.11.2011	12.3.2012	5.5	7.3.2012	50 kgN in Form von NAC (27:0:0)		

WWHT - Winter wheat

Winterweizen

Anbau	Ernte	bodenbearb.	bodenbearb.	Ertrag tha	Düngung					
9.10.2010	13.7.2011	30.9.2010		7.48	15.3.2011	45 kg N NAC	28.4.2011	42 kg N NAC	25.5..2011	30 kg NAC
19.10.2012	18.7.2013	18.10.2012	19.10.2012	6.67	----					
3.10.2014	15.7.2015	1.10.2014		5.12	-----					
21.10.2010	20.7.2011	23.9.2010	30.9.2010		3.3.2011	330kg (17:5:5)	20.4.2011	200 kg NAC (2	25.5.2011	100 kg NAC (27:0:0)

Wintergerste

Anbau	Ernte	Plug	Kreiselegge	Ertrag	Düngung					
4.10.2010	7.7.2011	29.9.2010	2.10.2010	9.3	28.9.2010	40 kgN	1.3.2011	60 kgN	11.4.2011	54 kgN
3.10.2012	10.7.2013	1.10.22012	3.10.2012	6.3	1.10.2012	45 kgN	18.3.2013	53 kgN	16.4.2013	50 kgN
30.9.2014	3.7.2015	18.9.2014	29.9.2014	7.2	10.3.2015	51 kgN	14.4.2015	27 kgN	18.5.2015	27 kgN
Anbau	Ernte	Grubber	Kreiselegge	Ertrag	Düngung					
1.10.2010	7.7.2011	23.9.2010	30.9.2010	7.2	3.3.2011	56 kgN	20.4.2011	200 kg NAC	25.5.2011	100 kg NAC
1.10.2012	15.7.2013	27.9.2012	-	7.3	13.3.2012	48 kgN	30.4.2012	76 kgN	8.5.2012	25 kgN
6.10.2014	6.7.2015	22.9.2014	kurz v. Anbau	8.3	9.3.2015	51 kgN	27.4.2015	81 kgN	-	-

CORN

Körnermais

Anbau	Ernte1	Ernte2	Begrünung	Pflug	Saatbettkomb	Ertrag tha	Düngung			
22.4.2009	8.10.2009		Herbst 2008	16.11.2008	1.4.2009	14.3	13.4.2009	30 m^3 Schwei	20.4.2009	80 kg N (Harnstoff)
14.4.2011	28.9.2011	17.10.2011	13.8.2010	16.11.2011	11.4.2011	14.6 (ernte2)	5.8.2010	32 m^3 Schwei	11.4.2011	130 kg Harnstoff/ha, 60 kg N
26.4.2013	27.9.2013	10.10.2013	24.10.2012	?	?	13.3 (ernte2)	16.4.2013	28 m^3 Schwei	27.4.2013	300 kg NAC/ha (81 kg N)
23.4.2013	1.10.2015	19.10.2015	18.8.2014	?	?	10.2 (ernte2)	10.4.2015	25 m^3 Schwei	22.4.2015	350 kg NAC/ha (94 kg N)

Quelle:
http://www.lako.at/de/versuche/?lang=de&a=179&a_urlname=versuche&versuche_a=1&versuche_b=5&versuche_c=6

SOYB - SOYBEAN

Sojabohne

Anbau	Ernte	Grubber	Saatbettkombi	Ertrag tha	Düngung	
21.4.2010	23.9.2010	9.4.2010	21.4.10	3.95	--	
28.4.12	18.9.12	Aug 11	27.4.12	3.91	--	
25.4.14	28.9.14	Aug 13	24.4.14	3.55	--	
28.4.2011	27.9.2011	17.11.2011	25.04.2011	4.31	--	
26.4.2012	11.9.2012	9.11.2012	18.4.2012	2.92	--	
30.4.2014	25.9.2014	8.11.2013	16.4.2014	2.66	1.4.2014	Mischdünger (30:100:100) 30 kg/ha N

OELK - OIL PUMPKIN

Ölkürbis

Anbau	Ernte	Hacken1	Hacken2	Ertrag tha	Düngung			
28.4.2010	15.9.2010	27.5.2010	8.6.2010	-	vor d. Anbau	400 kg/ha Volldünger (15:15:15) (60 kg N)		
27.4.2011	13.9.2011	-	-	-	vor d. Anbau	400 kg/ha Volldünger (15:15:15) (60 kg N)		
30.4.2012	7.9.2012	-	-	-	vor d. Anbau	400 kg/ha Volldünger (15:15:15) (60 kg N)		
1.5.2014	14.9.2014	25.5.2014	14.6.2014	1.93 (1.1TM)	26.4.2014	400 kg/ha +S11 (15:15:15)		
26.4.2014	27.9.2014	21.5.2014	12.6.2014	3.15 (1.1TM)	2.4.2014	Schweine- u. I	23.4.2014	185 kg NAC
2010				0.52 TM				
2011				0.71 TM				
2013				0.85 TM				

Quelle: Sortenversuch Ölkürbis "Team Versuchstätigkeit"
http://www.lako.at/de/versuche/?lang=de&a=179&a_urlname=versuche&versuche_a=1&versuche_b=5&versuche_c=13
Ölkürbis: Landwirtsschaftskammer Niederösterreich; alle am 20/11/2015 abgefragt

SUGAR BEET

Chinakohl, Kraut, Kren, Salate und Paradeis

Anbau	Ernte	Grubber	Saatbettkomb	Der Ertrag reicht von 11 - 170 t/ha:	Düngung:
-	-	-	-	Chinakohl 58 t/ha	**N**: 200-300 kg/ha
-	-	-	-	Kraut 60 t/ha	**P2O5**: 30 - 80 kg/ha
				Kren 11 t/ha	Keine Zeitangaben.
				Salate ges. 25 - 35 t/ha	
				Paradeis 130 - 170 t/ha	

(Quellen: http://www.statistik-austria.at/web_de/statistiken/wirtschaft/land_und_forstwirtschaft/agrarstruktur_flaechen_ertraege/gemuese/080121.html
und Richtlinien für die sachgerechte Düngung im Garten- und Feldgemüsebau, Lebensministerium (BMLUFW), S.11ff u 22ff)

ORCD - Apples

Steirische Äpfel

Anbau	Ernte	Grubber	Saatbettkomb	Ertrag tha	Düngung:
				ca. 24 - 35 t/h	**N**: 70 kg/ha
				<40t/ha	**P2O5**: 35 kg/ha

Die erste Düngungsteilgabe soll Ende Feb bis Anfang März erfolgen. (bei leichte Böden: Ende März bis Anfang April) Die zweite Teilgabe soll nach der Blüte erfolgen.
(Quelle: Richtlinien für die sachgerechte Düngung im Obstbau, Lebensministerium (BMLUFW), S. 24 u 26)
Ertrag: http://www.statistik-austria.at/web_de/statistiken/wirtschaft/land_und_forstwirtschaft/agrarstruktur_flaechen_ertraege/obst/index.html)

8.3 Discharge data of Mitterdorf

Monthly mean discharges at gauge 211599 Mitterdorf an der Raab (2003- 2012)

m^3/s	I	II	III	IV	V	VI	VII	VIII	IX	X	XI	XII
2003	1.16	0.88	0.71	0.54	0.48	0.78	0.51	0.39	0.52	0.64	0.90	1.03
2004	1.08	0.80	2.09	2.15	2.04	4.45	2.81	1.02	0.92	1.24	1.47	1.46
2005	1.09	0.97	1.90	1.63	1.19	0.89	2.29	6.54	3.02	2.07	1.21	1.11
2006	0.95	0.93	1.53	2.31	2.41	2.05	1.25	0.95	1.22	0.99	0.88	0.80
2007	0.88	0.77	1.19	1.06	0.78	0.92	0.68	0.93	1.85	1.25	1.12	1.20
2008	0.81	0.71	0.78	0.71	0.68	1.28	1.78	1.79	0.99	0.85	0.92	2.49
2009	1.68	1.84	2.46	2.17	2.16	2.55	4.65	4.54	4.82	2.60	2.36	2.35
2010	1.59	1.58	1.75	1.17	1.53	2.91	1.38	1.79	1.90	1.50	1.75	2.20
2011	1.53	1.10	1.73	1.02	0.86	1.95	1.11	0.96	1.13	0.99	0.81	0.68
2012	0.65	0.74	0.60	0.55	0.56	2.23	3.84	1.76	1.52	1.87	2.83	1.33

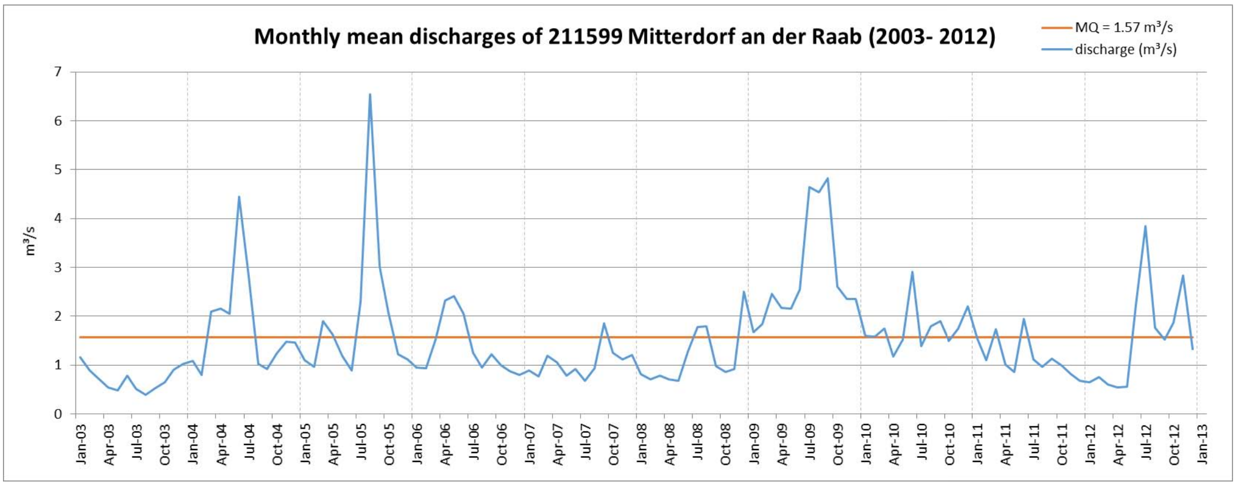

8.4 Discharge data of St. Ruprecht

Monthly mean discharges at gauge 210963 St. Ruprecht an der Raab (Weizbach) (2003- 2012)

m³/s	I	II	III	IV	V	VI	VII	VIII	IX	X	XI	XII
2003	0.71	0.52	0.46	0.42	0.38	0.37	0.33	0.30	0.46	0.48	0.49	0.39
2004	0.51	0.49	1.04	1.20	1.25	2.56	1.82	1.01	0.91	0.79	0.80	0.75
2005	0.63	0.67	0.97	0.84	0.79	0.72	1.10	3.16	1.21	1.01	0.61	0.43
2006	0.51	0.66	0.82	0.96	1.25	1.00	0.97	0.81	0.71	0.72	0.57	0.53
2007	0.61	0.58	0.74	0.72	0.68	0.88	0.77	0.83	1.18	0.88	0.81	0.81
2008	0.56	0.52	0.63	0.61	0.53	0.82	0.94	1.01	0.62	0.53	0.54	1.02
2009	0.77	1.04	1.28	1.37	1.00	1.26	2.20	2.78	2.69	1.48	1.33	1.32
2010	0.91	0.92	0.90	0.74	0.85	1.95	1.15	1.40	1.24	1.06	1.09	1.25
2011	0.96	0.89	0.94	0.72	0.76	1.77	1.07	0.95	0.81	0.61	0.60	0.63
2012	0.57	0.49	0.54	0.56	0.68	1.26	2.52	1.23	1.00	1.14	1.80	0.96

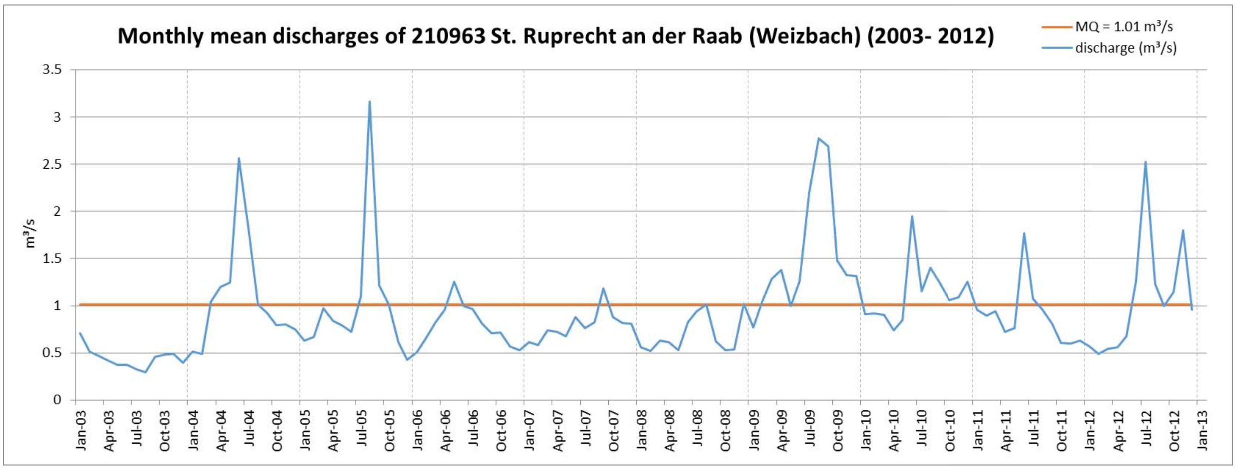

8.5 Discharge data of Feldbach

Monthly mean discharges at gauge 210989 Feldbach (2003- 2012)

m³/s	I	II	III	IV	V	VI	VII	VIII	IX	X	XI	XII
2003	3.68	2.44	2.81	2.03	1.58	1.81	1.55	1.21	1.51	2.69	2.88	2.71
2004	3.23	2.58	7.64	5.07	5.06	16.85	8.86	4.03	3.06	3.39	3.61	3.58
2005	2.76	2.17	5.70	5.09	3.39	2.26	5.12	18.44	8.64	6.19	3.55	3.86
2006	3.57	4.66	7.20	6.86	8.09	5.79	4.68	3.70	3.73	3.14	2.77	2.15
2007	2.99	2.70	5.89	3.40	2.91	3.21	1.90	2.81	7.34	4.08	3.02	4.57
2008	2.87	2.27	2.16	2.34	2.47	7.08	8.40	6.18	2.35	2.41	2.84	8.28
2009	5.23	8.55	7.15	5.06	4.90	10.96	14.39	16.29	15.17	6.70	7.16	7.59
2010	4.68	6.56	5.93	3.53	3.81	7.97	3.84	6.63	8.13	5.70	6.54	7.93
2011	5.43	3.65	5.67	3.97	3.04	8.81	3.90	4.53	4.13	3.33	2.28	2.08
2012	1.74	2.01	2.30	2.67	3.38	5.59	11.77	4.33	5.76	8.49	12.18	4.61

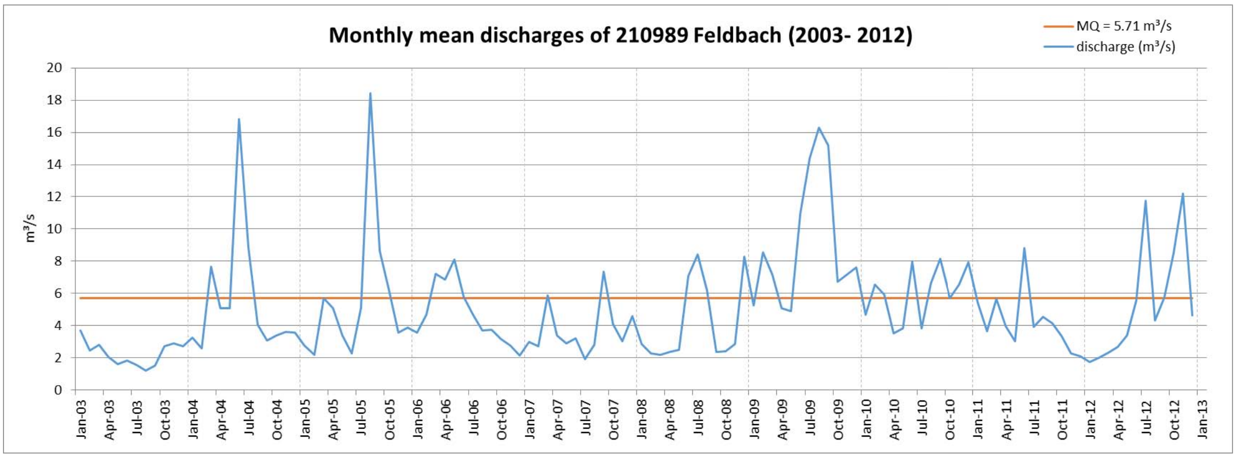

8.6 NO_3-N load calculations at gauge Takern II

Calculated NO3-N loads at gauge Takern II, based on OM Takern II data, calibration period (Sep-Dec 2009, 2011-2012), 26 data points, t/month

Date	Qmean (m^3/s)	NO_3-N mean conc. (mg/l)	NO_3-N load (t/month)	Date	Qmean (m^3/s)	NO_3-N mean conc. (mg/l)	NO_3-N load (t/month)
Sep 2009	14.19	2.35	79.54	-	-	-	-
Oct 2009	6.39	2.46	42.09	-	-	-	-
Nov 2009	6.44	2.54	42.27	-	-	-	-
Dec 2009	6.72	2.79	49.87	-	-	-	-
Jan 2011	4.13	2.99	33.02	Jan 2012	1.65	2.88	12.78
Feb 2011	2.92	2.86	20.18	Feb 2012	1.90	3.32	15.23
Mar 2011	4.80	2.78	36.49	Mar 2012	1.95	2.52	13.18
Apr 2011	3.17	2.65	21.77	Apr 2012	2.21	2.41	13.74
May 2011	2.85	2.53	19.19	May 2012	2.61	2.69	20.09
Jun 2011	7.26	2.31	41.16	Jun 2012	5.12	2.05	10.93
Jul 2011	3.55	2.50	23.64	-	-	-	
Aug 2011	3.71	2.18	21.37	-	-	-	
Sep 2011	3.71	2.24	21.29	Sep 2012	4.48	1.72	1.51
Oct 2011	3.15	2.41	20.33	Oct 2012	6.31	2.16	35.99
Nov 2011	2.24	2.85	16.54	Nov 2012	10.31	2.73	70.44
Dec 2011	2.00	2.64	14.13	Dec 2012	4.83	2.49	3.12

8.7 NO_3-N load calculations at gauge Neumarkt/Raab, monthly data

Calculated NO3-N loads at gauge Neumarkt/Raab, based on GZÜV Neumarkt/Raab data, calibration period (2003-2009), 68 data points, t/month

Date	Qd (m^3/s)	NO_3-N conc. (mg/l)	NO_3-N load (t/month)	Date	Qd (m^3/s)	NO_3-N conc. (mg/l)	NO_3-N load (t/month)
-	-	-	-	Jan 2006	5.58	4.63	69.18
Feb 2003	3.48	4.03	33.90	Feb 2006	7.66	6.44	119.29
Mar 2003	4.33	4.67	54.18	Mar 2006	10.43	7.60	212.34
Apr 2003	2.69	3.70	25.79	Apr 2006	8.86	3.60	82.66
May 2003	1.90	3.19	16.24	May 2006	12.00	7.00	225.04
Jun 2003	2.07	2.65	14.24	Jun 2006	8.78	3.65	83.02
Jul 2003	1.96	2.97	15.57	Jul 2006	4.94	3.59	47.55
Aug 2003	1.20	4.98	16.04	Aug 2006	4.44	2.96	35.23
Sep 2003	2.59	3.57	24.00	Sep 2006	4.42	3.38	38.73
Oct 2003	3.78	5.74	58.10	Oct 2006	4.14	2.92	32.37
Nov 2003	3.50	3.88	35.17	Nov 2006	3.90	2.70	27.33
Dec 2003	3.70	3.30	32.77	Dec 2006	3.05	3.36	27.42
Jan 2004	3.82	3.34	34.16	Jan 2007	3.97	3.66	38.91
Feb 2004	2.65	3.84	25.45	-	-	-	-
Mar 2004	11.77	12.47	393.00	Mar 2007	7.95	3.50	74.55
Apr 2004	7.05	3.97	72.54	Apr 2007	4.10	2.94	31.27
May 2004	6.01	5.50	88.46	May 2007	3.62	2.86	27.73
Jun 2004	21.77	6.85	386.50	Jun 2007	3.68	3.27	31.15
Jul 2004	10.15	3.32	90.23	Jul 2007	2.37	3.48	22.05
Aug 2004	4.69	3.36	42.17	Aug 2007	3.27	1.94	16.97
Sep 2004	3.70	4.01	38.46	Sep 2007	8.52	5.30	117.05
Oct 2004	4.64	3.29	40.90	Oct 2007	5.06	3.86	52.28
Nov 2004	4.71	3.22	39.27	Nov 2007	3.84	2.99	29.78
Dec 2004	4.02	3.02	32.49	Dec 2007	5.97	3.40	54.30
-	-	-	-	Jan 2008	3.40	3.12	28.41
Feb 2005	3.02	4.08	29.85	Feb 2008	2.70	3.05	20.60
Mar 2005	8.21	5.08	111.66	Mar 2008	2.75	2.38	17.50
Apr 2005	7.00	3.85	69.85	Apr 2008	2.76	2.36	16.90
May 2005	4.83	3.02	39.08	May 2008	2.81	2.25	16.92
Jun 2005	3.14	3.22	26.18	Jun 2008	7.78	4.28	86.30
Jul 2005	6.77	2.54	46.05	Jul 2008	8.54	3.30	75.53
Aug 2005	25.96	3.90	271.17	Aug 2008	7.45	2.87	57.25
Sep 2005	11.06	3.10	88.85	Sep 2008	3.97	2.63	27.09
Oct 2005	8.30	2.44	54.24	Oct 2008	3.86	2.02	20.87
Nov 2005	5.08	3.17	41.72	Nov 2008	4.23	2.08	22.76
-	-	-	-	Dec 2008	10.06	3.26	87.85

8.8 NO_3-N concentrations at the online monitoring station Takern II (2009-2012)

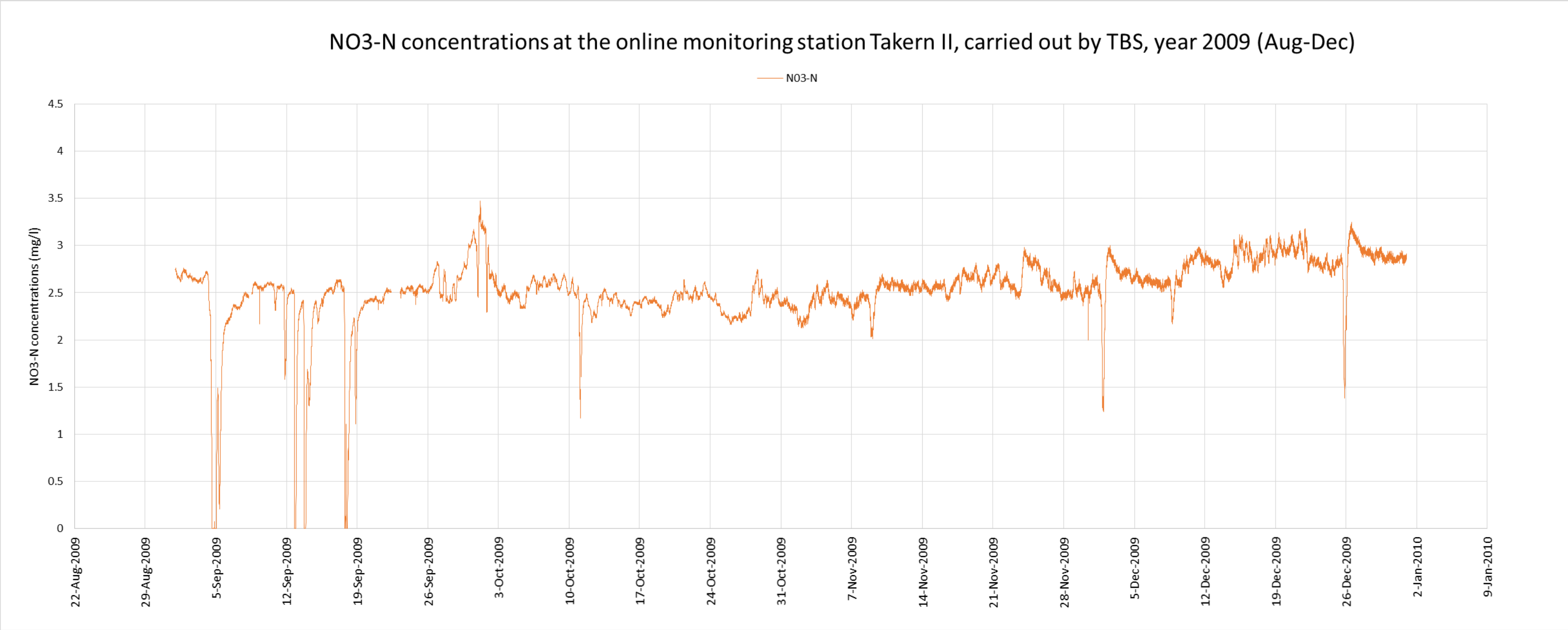

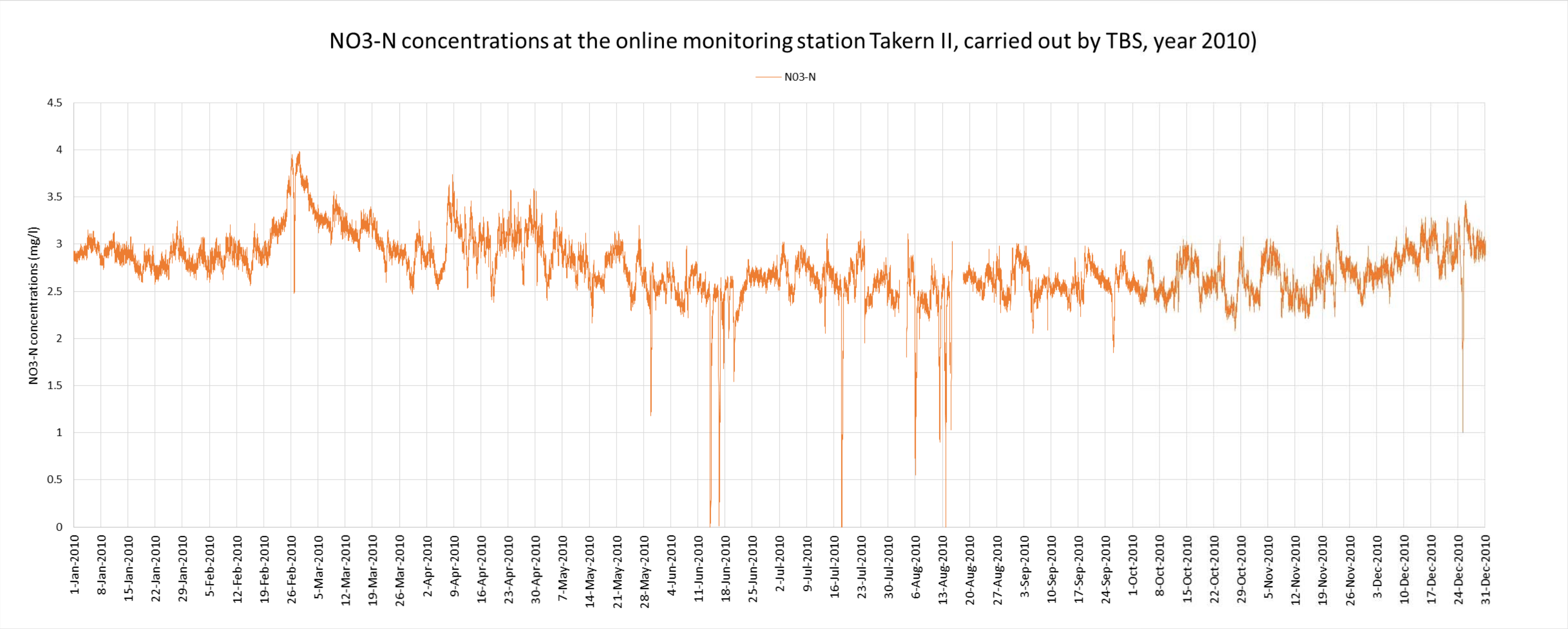
NO3-N concentrations at the online monitoring station Takern II, carried out by TBS, year 2010)
N03-N
NO3-N concentrations (mg/l)
4.5
4
3.5
3
2.5
2
1.5
1
0.5
0
1-Jan-2010
8-Jan-2010
15-Jan-2010
22-Jan-2010
29-Jan-2010
5-Feb-2010
12-Feb-2010
19-Feb-2010
26-Feb-2010
5-Mar-2010
12-Mar-2010
19-Mar-2010
26-Mar-2010
2-Apr-2010
9-Apr-2010
16-Apr-2010
23-Apr-2010
30-Apr-2010
7-May-2010
14-May-2010
21-May-2010
28-May-2010
4-Jun-2010
11-Jun-2010
18-Jun-2010
25-Jun-2010
2-Jul-2010
9-Jul-2010
16-Jul-2010
23-Jul-2010
30-Jul-2010
6-Aug-2010
13-Aug-2010
20-Aug-2010
27-Aug-2010
3-Sep-2010
10-Sep-2010
17-Sep-2010
24-Sep-2010
1-Oct-2010
8-Oct-2010
15-Oct-2010
22-Oct-2010
29-Oct-2010
5-Nov-2010
12-Nov-2010
19-Nov-2010
26-Nov-2010
3-Dec-2010
10-Dec-2010
17-Dec-2010
24-Dec-2010
31-Dec-2010

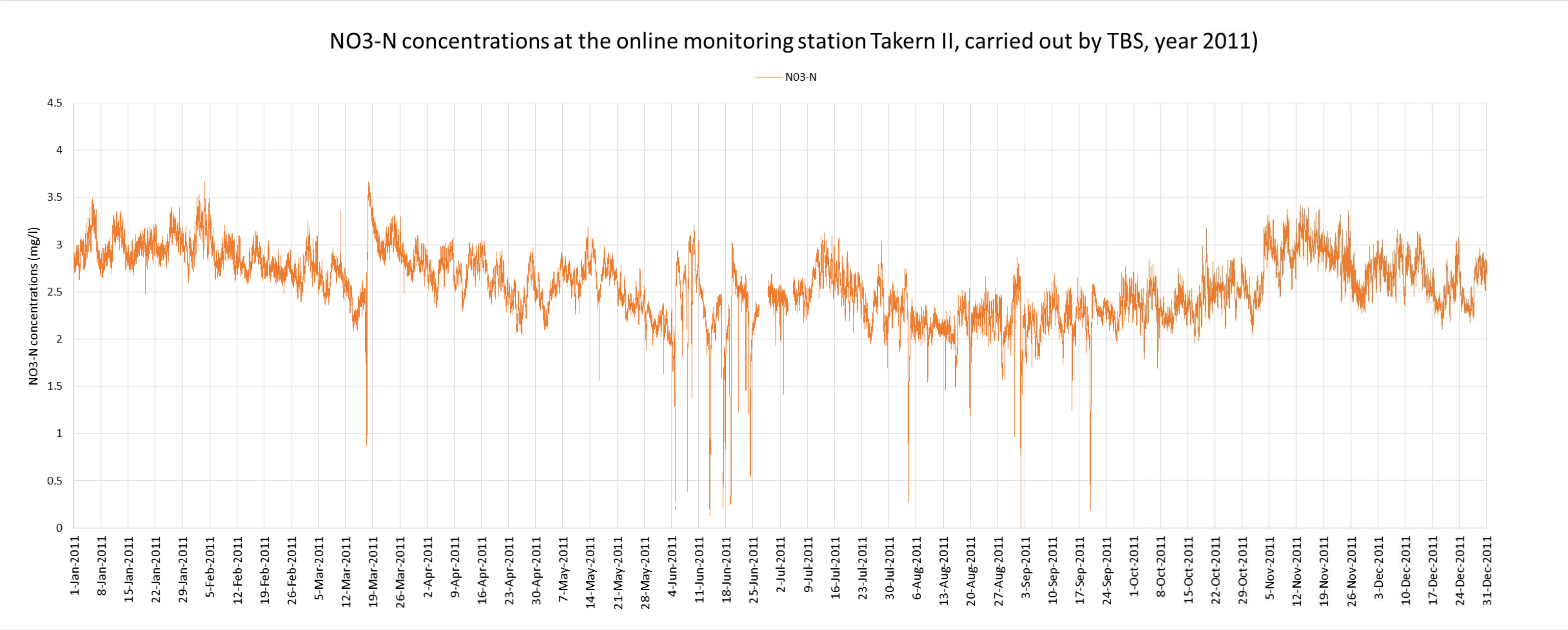
NO3-N concentrations at the online monitoring station Takern II, carried out by TBS, year 2011)
N03-N
NO3-N concentrations (mg/l)
4.5
4
3.5
3
2.5
2
1.5
1
0.5
0
1-Jan-2011
8-Jan-2011
15-Jan-2011
22-Jan-2011
29-Jan-2011
5-Feb-2011
12-Feb-2011
19-Feb-2011
26-Feb-2011
5-Mar-2011
12-Mar-2011
19-Mar-2011
26-Mar-2011
2-Apr-2011
9-Apr-2011
16-Apr-2011
23-Apr-2011
30-Apr-2011
7-May-2011
14-May-2011
21-May-2011
28-May-2011
4-Jun-2011
11-Jun-2011
18-Jun-2011
25-Jun-2011
2-Jul-2011
9-Jul-2011
16-Jul-2011
23-Jul-2011
30-Jul-2011
6-Aug-2011
13-Aug-2011
20-Aug-2011
27-Aug-2011
3-Sep-2011
10-Sep-2011
17-Sep-2011
24-Sep-2011
1-Oct-2011
8-Oct-2011
15-Oct-2011
22-Oct-2011
29-Oct-2011
5-Nov-2011
12-Nov-2011
19-Nov-2011
26-Nov-2011
3-Dec-2011
10-Dec-2011
17-Dec-2011
24-Dec-2011
31-Dec-2011

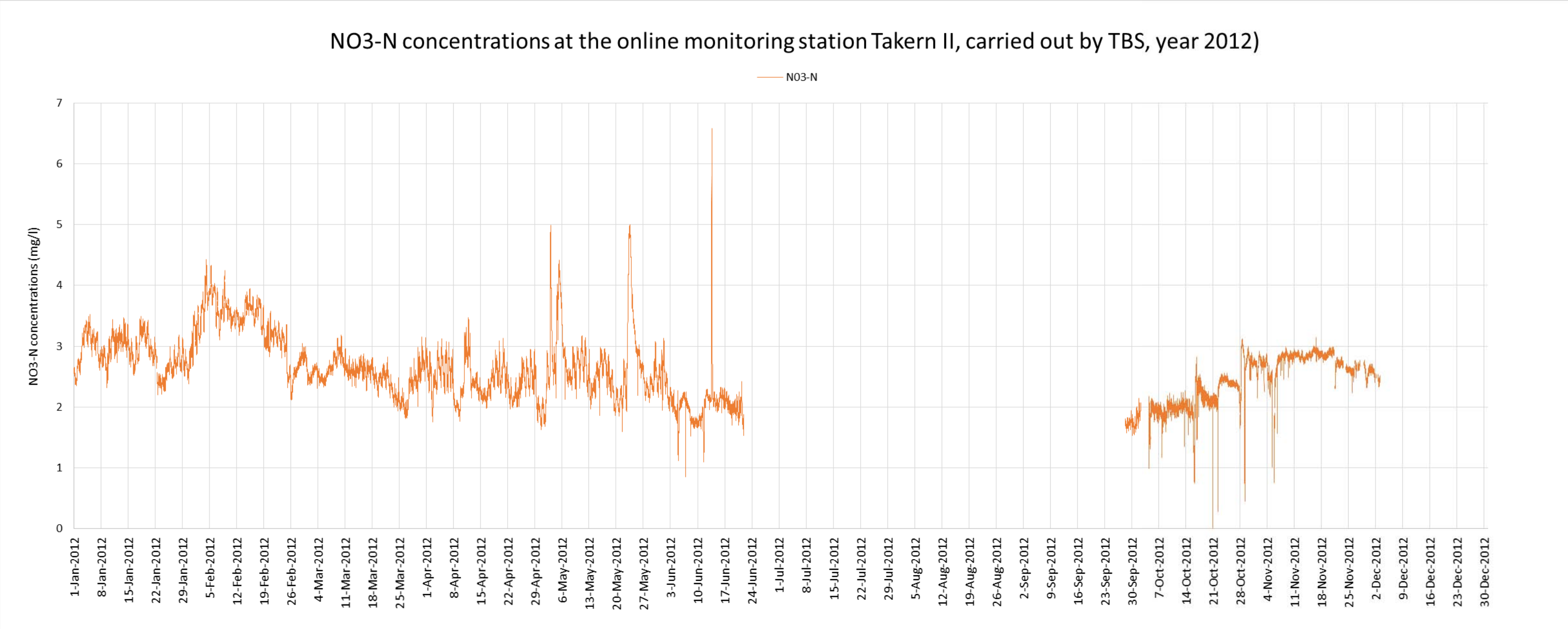
NO3-N concentrations at the online monitoring station Takern II, carried out by TBS, year 2012)
N03-N
NO3-N concentrations (mg/l)
0
1
2
3
4
5
6
7
1-Jan-2012
8-Jan-2012
15-Jan-2012
22-Jan-2012
29-Jan-2012
5-Feb-2012
12-Feb-2012
19-Feb-2012
26-Feb-2012
4-Mar-2012
11-Mar-2012
18-Mar-2012
25-Mar-2012
1-Apr-2012
8-Apr-2012
15-Apr-2012
22-Apr-2012
29-Apr-2012
6-May-2012
13-May-2012
20-May-2012
27-May-2012
3-Jun-2012
10-Jun-2012
17-Jun-2012
24-Jun-2012
1-Jul-2012
8-Jul-2012
15-Jul-2012
22-Jul-2012
29-Jul-2012
5-Aug-2012
12-Aug-2012
19-Aug-2012
26-Aug-2012
2-Sep-2012
9-Sep-2012
16-Sep-2012
23-Sep-2012
30-Sep-2012
7-Oct-2012
14-Oct-2012
21-Oct-2012
28-Oct-2012
4-Nov-2012
11-Nov-2012
18-Nov-2012
25-Nov-2012
2-Dec-2012
9-Dec-2012
16-Dec-2012
23-Dec-2012
30-Dec-2012

8.9 Online Monitoring NO_3-N Data at gauge Neumarkt/Raab (2006-2012)

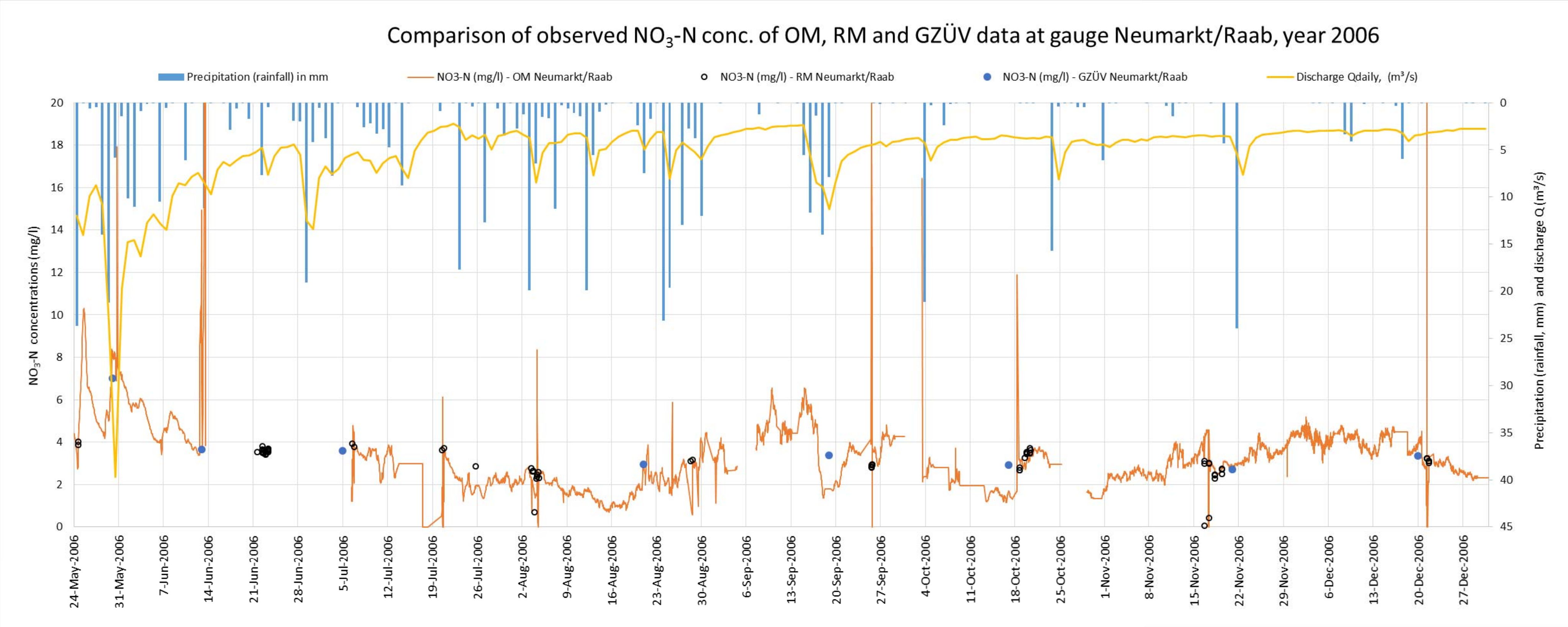

Observed NO_3-N concentrations > 20.0 mg/l are not represented in this diagram.

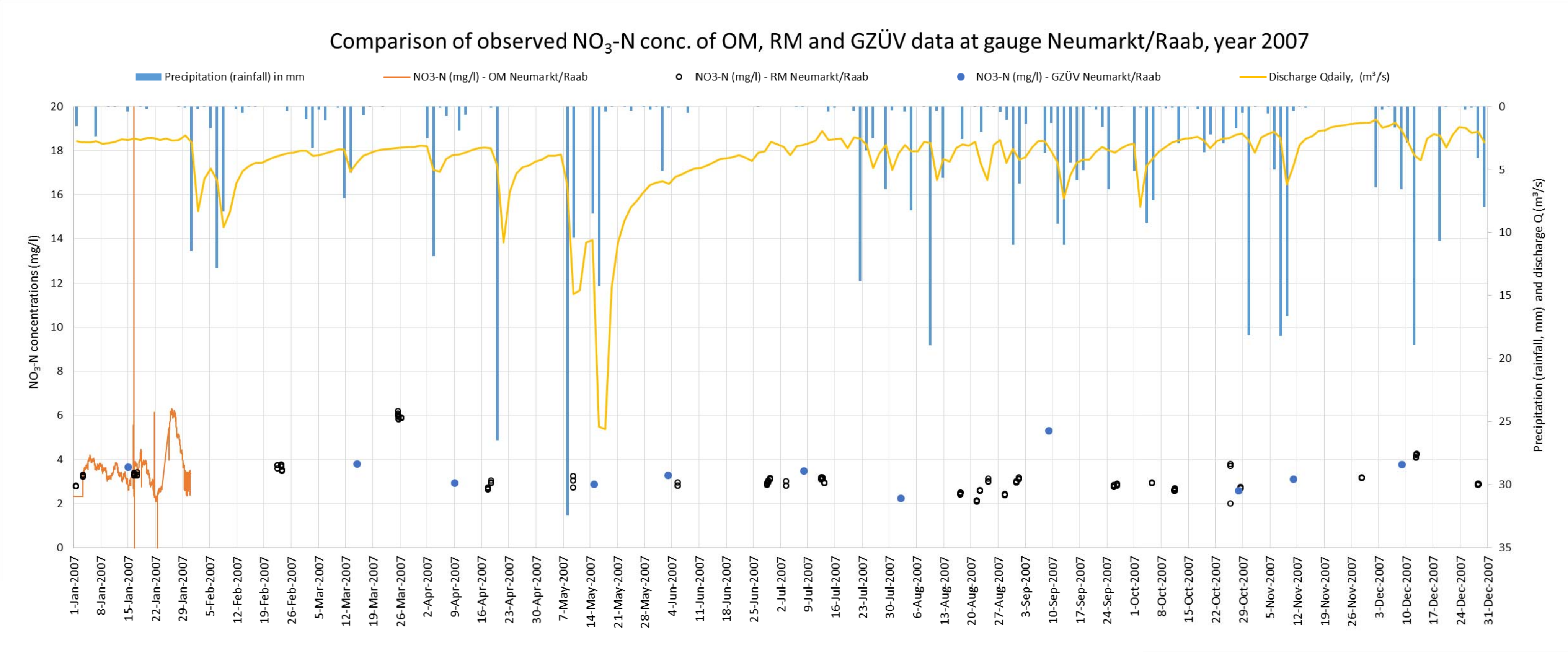

Observed NO_3-N concentrations > 20.0 mg/l are not represented in this diagram.

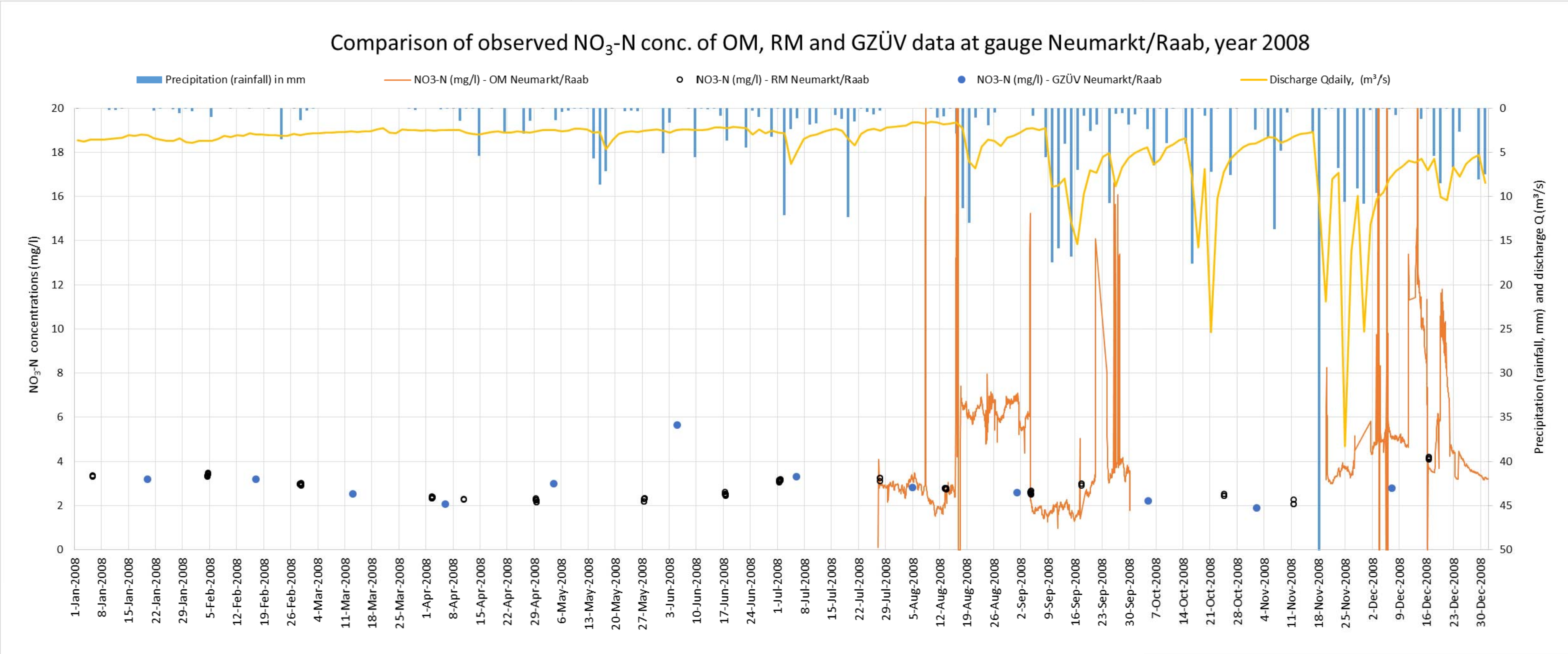

Observed NO_3-N concentrations > 20.0 mg/l are not represented in this diagram.

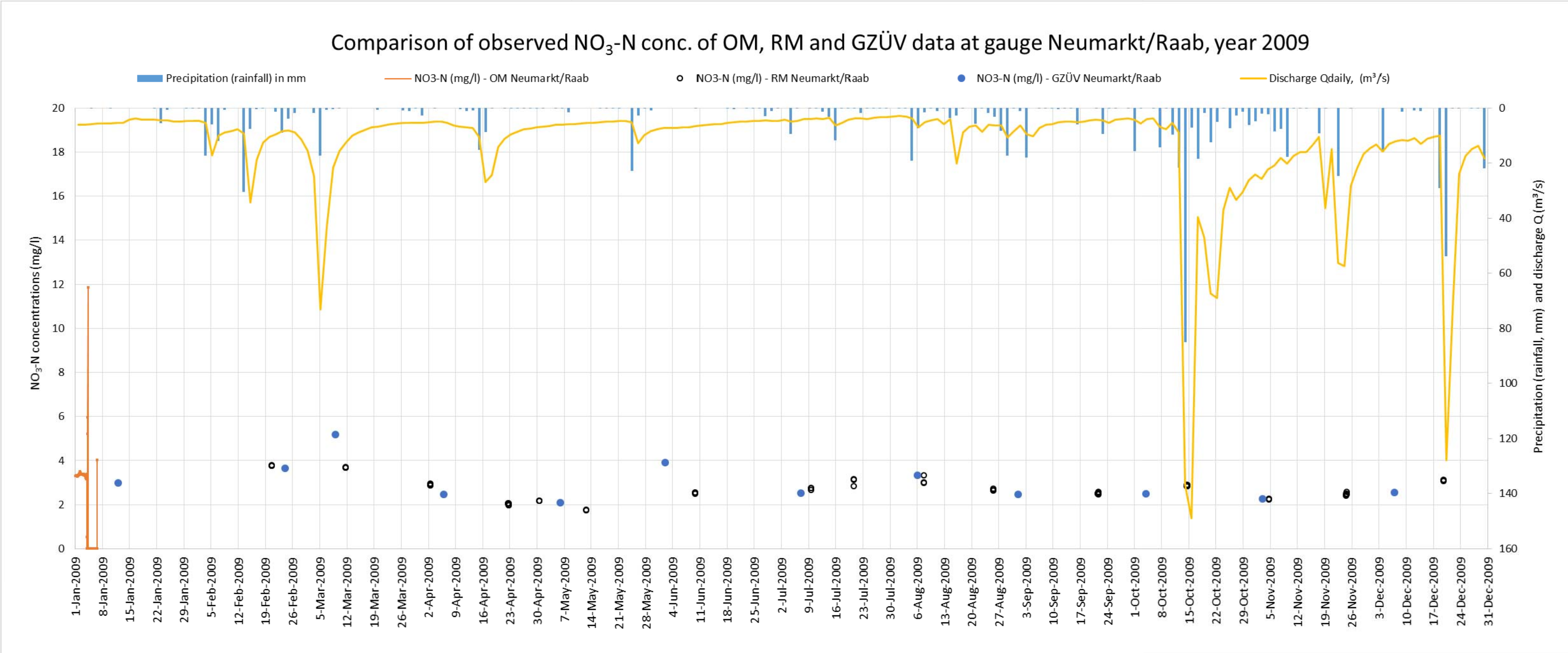

Observed NO3-N concentrations > 20.0 mg/l are not represented in this diagram.

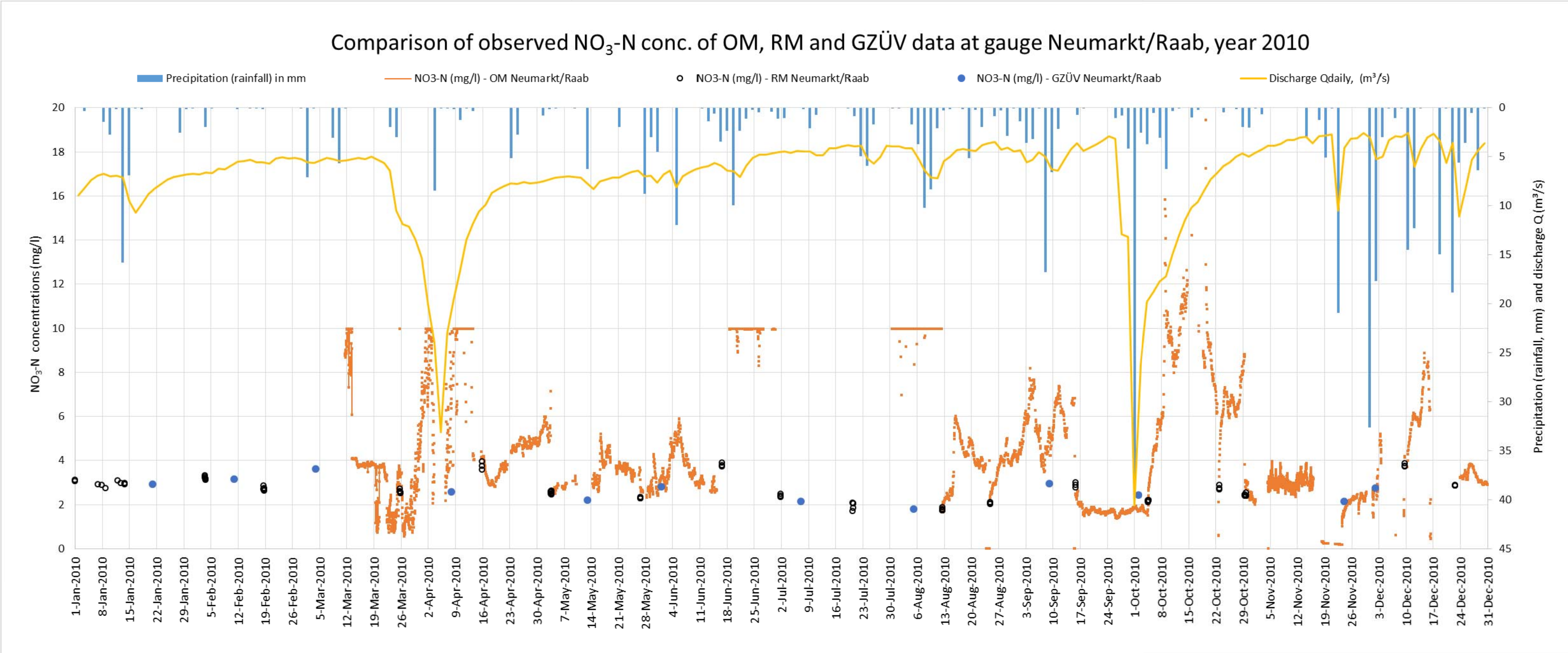

Observed NO_3-N concentrations > 20.0 mg/l are not represented in this diagram.

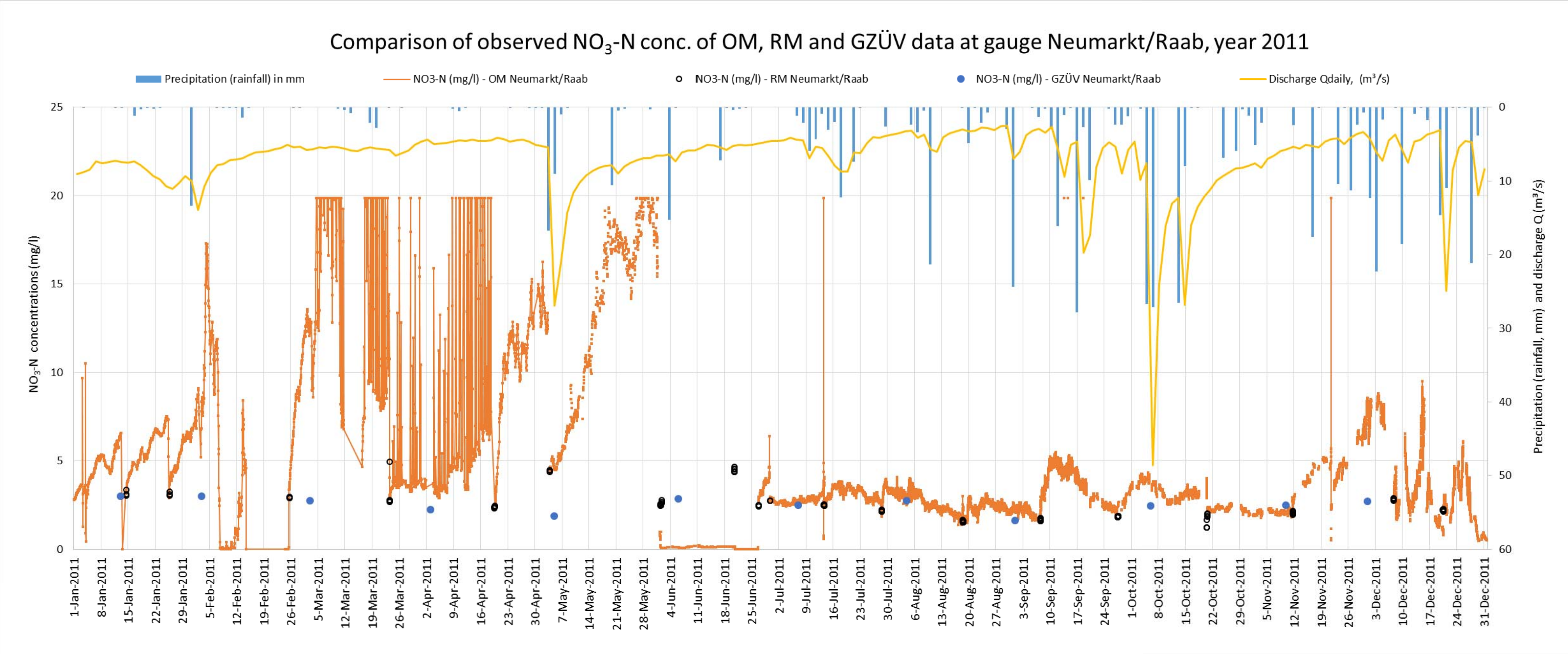

Observed NO3-N concentrations > 25.0 mg/l are not represented in this diagram.

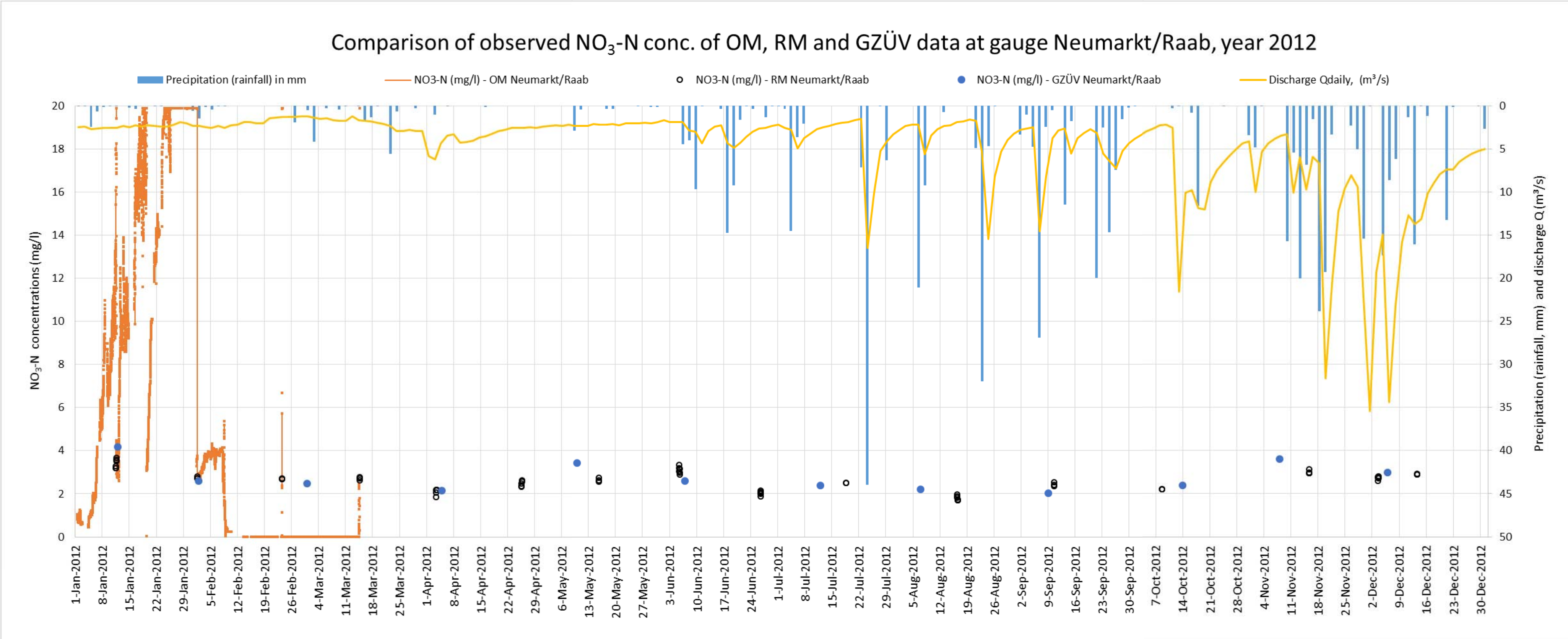

Observed NO_3-N concentrations > 20.0 mg/l are not represented in this diagram.